EFFECT OF INTERSTELLAR MEDIUM ON RADIO PULSAR SPIN-DOWN PROPERTIES

BY

UGWU CHUKWUEBUKA JUDE
(PG/M.SC/11/59540)

DEPARTMENT OF PHYSICS AND ASTRONOMY
FACULTY OF PHYSICAL SCIENCES
UNIVERSITY OF NIGERIA, NSUKKA

JANUARY, 2015

CERTIFICATION

Ugwu Chukwuebuka Jude, a postgraduate student in the Department of Physics and Astronomy, University of Nigeria, Nsukka with registration number PG/M.SC/11/59540 has satisfactorily completed the requirements for award of Masters Degree in Physics and Astronomy. The work embodied in this project report is original and has not been submitted in part or full for any other Diploma or Degree of this or any other University.

_____	_____
PROF. A.E. CHUKWUDE	**PROF. R.U. OSUJI**
SUPERVISOR	**HEAD OF DEPARTMENT**

DEDICATION

This work is specially dedicated to my dear parents for their support and encouragement throughout this programme.

ACKNOWLEDGEMENTS

This project could not have been a success if not for the numerous contributions and encouragements of many nice individuals.

In the above regard, I am most grateful to my parents, Mr and Mrs Ugwu Bartholomew for their support and tolerance. My special thanks to my supervisor, Prof. A.E. Chukwude for his fatherly love and care towards the success of this work. Thanks to my mentor, Prof. P.N. Okeke and his wife, Prof. (Mrs) F.N. Okeke for their encouragements throughout this programme. I am grateful to my lecturers, especially Prof. J.O. Urama, Dr J.A. Alhassan, Dr F.C. Odo and Okoh Daniel of Centre for Basic Space Science, Nsukka for their wonderful contributions.

I am grateful to my one and only brother, Mr Ugwu Chinonso, my sisters, Adanna, Obianujunwa, Chidimma and my cousin sister Chidimma as well as my relatives for their prayers towards the success of this project. My special thanks go to my lovely friends, Asogwa Ikechukwu, Attamah Chukwunonso, Ezeagu Sunday, Ossai Ngozichukwu Mirianrita and others too numerous to mention. May God bless you all.

TABLE OF CONTENTS

LIST OF TABLES

LIST OF FIGURES

ABSTRACT

A statistical analysis of a large sample of 668 radio pulsars was undertaken in other to investigate the possible dependence of interstellar medium (ISM) parameters [dispersion measure (*DM*) and rotation measure (*RM*)] on pulsar spin-down parameters [rotation period (*P*) and spin-down rate ($\dot{P}$)]. The existence of such relationship will have a far reaching implication on the theories of pulsar birth and evolution. A simple descriptive analysis of the data reveals that the sample is quite heterogeneous, consisting of normal and recycled millisecond pulsars. Specifically, the published values of *P*, $\dot{P}$, *DM* and *RM* for objects in the sample were found to vary over a wide range: ~ 0.002 ï 9 s, 3 × 10^{-21} ï 2 × 10^{-11} ss^{-1}, 2 ï 1100 $cm^{-3}pc$ and -3000 ï 2400 $radm^{-2}$, respectively, with the corresponding mean values of ~ 0.69 ± 0.02 s, (9.94 ± 0.05) × 10^{-14} ss^{-1}, 181 ± 7 $cm^{-3}pc$ and 157 ± 10 $radm^{-2}$. Scatter plots of *DM* and *RM* (irrespective of sign) against $\dot{P}$ reveal large amplitude (~ 3 orders of magnitude) scatter in the ISM parameters superimposed on a striking trend in which pulsars with large values of $\dot{P}$ (young pulsars), on average, are characterized by large *DM* and |*RM*| values. A simple regression analysis of the *DM*/|*RM*| ï $\dot{P}$ data yields a moderate correlation (with correlation coefficient *r* ~ 0.5). A simple interpretation of the moderate *DM*/|*RM*| – $\dot{P}$ relationship is that objects with large $\dot{P}$ (corresponding to young pulsars) are, on average, located in a region of ISM with high electron density content (in this case, the galactic plane). On the other hand, smaller values of $\dot{P}$, *DM* and |*RM*| correspond to relatively older pulsars located in regions farther away from the galactic plane (with low electron density content). The *DM*/|*RM*| – $\dot{P}$ correlation increased significantly (with correlation coefficient *r* ~ 0.95), when mean values of the parameters were employed in the analysis. The observed large scatter in the ISM data highlights the complex nature of the electron content distribution in the ISM and the large dispersion in both the magnitude and direction of pulsar space velocities. Similar analysis did show any appreciable dependence of both *DM* and *RM* on the pulsar rotation period. Our analysis also reaffirms the existence of a strong correlation (*r* ~ 0.7) between the *DM* and *RM* parameters, which are used to characterize the ISM.

CHAPTER ONE

INTRODUCTION

1.1 What are Pulsars?

A pulsar is a highly magnetized, rapidly rotating neutron star that emits beams of broad band electromagnetic radiation. This radiation can only be observed when the beam of emission sweeps across the earth, much the way a lighthouse can be seen when the light is pointed in the direction of an observer. The events leading to the formation of a pulsar begin when the core of a massive (> 10 $M_\odot$) star is collapsed into a neutron star during a supernova explosion, where $M_\odot$ is the mass of the sun which is ~ 2 × 10^{30} kg. The neutron star retains most of the angular momentum and only a tiny fraction of the size of its progenitor star. The sharp reduction in the stellar moment of inertia results in significant amplification of the rotation speed of neutron stars. Beams of radiation are emitted along the magnetic axis of the pulsar as it spins about the rotation axis of the neutron star. The magnetic axis of the pulsar determines the direction of the electromagnetic beam, with the magnetic axis not necessarily aligned with its rotation axis. This misalignment causes the beam to be modulated by the rotation of the neutron star. The beam originates from the rotational kinetic energy of the neutron star, which generates an electric field from the movement of the very strong magnetic field, resulting in the acceleration of protons and electrons on the star surface and the creation of an electromagnetic beam emanating from the poles of the magnetic field.

The rotation period (P) of most pulsars are known to increase at constant rates as the pulsars convert their rotational kinetic energy into electromagnetic radiation and particle wind according to the spin-down law (e.g. Manchester and Taylor, 1977):

$$\dot{P} = K P^{2-n}, \qquad (1.1)$$

where n is the braking index, $\dot{P}$ is the pulsar spin-down rate and K is usually assumed to be a constant. When a pulsarôs spin period slows down sufficiently, the radio pulsar mechanism is believed to turn off (the so-called ñdeath lineò). This turn-off seems to take place after about 10 - 100 million years, which means that of all the neutron stars in the 13.6 billion years age of the universe, around 99% no longer pulsate (Young *et al*., 1999). There are currently over 2000

known radio pulsars and their rotation periods are in the range of about 1.5 ms and 8.5 s (Seiradakis and Wielebinski, 2004; Manchester *et al*., 2005).

1.2 History of Discovery of Radio Pulsars

The discovery of pulsars by Professor Anthony Hewish and Jocelyn Bell Burnell in 1967 is one of the most important and dramatic advances in the history of radio astronomy (Hewish *et al*., 1968). The story began in 1965 when Hewish started the construction of an 82 MHz (3.7 m wavelength) array of 2048 $\lambda/2$ dipoles for scintillation studies of compact radio quasars. The dipoles were set horizontally several wavelengths above the ground in regular rows covering an area of 20,000 square metres. Graduate students at Cambridge University helped in the construction of the radio antenna. One of them, Jocelyn Bell from Ireland, was responsible for the network of thousands of cables (transmission lines) between the antenna and receiver. The array was physically fixed but by introducing appropriate phasing with different cable lengths, the beam could be shifted in declination. The earthôs rotation provided scanning in right ascension. Hewish had designed the antenna to investigate the compact quasar radio sources by their scintillation as produced by the irregular structure of the interplanetary medium.

In early measurements by Hey *et al*. (1946), fluctuations were observed in the radio emission from Cygnus A, which are due to inhomogeneities in the earthôs ionosphere. Hewish (1955) and Vitkevitch (1955) noted that the outer solar corona scattered radio waves, increasing the apparent diameter of radio sources. Both coronal scattering and ionospheric-induced fluctuations are similar scintillation phenomena but only differ in scale. Beginning in 1962, Hewish, Scott and Wills (1964) noted rapid fluctuations (with periods of a few seconds) in the intensity of a number of radio sources, notably 3C48, 3C119, 3C138 and 3C147, as measured at 178 MHz. Two of these sources were already known to possess very small angular diameters. It was concluded that the fluctuations were a scintillation effect produced by the interplanetary medium and is most severe for sources of angular diameter < 1 arcsec and at wavelengths of more than 1 m. The effect was found to become stronger with decreasing angular distance to the sun and the fluctuation rate faster with increasing wavelength. The belief that this scintillation effect could provide a convenient technique for estimating the angular diameter of radio sources in the range < 1 arcsec motivated the new antenna array by Hewish and his co-workers.

The plan was to survey most of the sky north of declination -08^0 once a week, keeping this region under constant surveillance. By July, 1967 construction of the array was completed and observations were begun with output recorded at short time constant with a pen-on-paper chart. Jocelyn Bell was given the responsibility of analyzing the 100 s of meters of chart paper flowing from the recorder each week in order to note times and declinations of chart deflections having a rapid fluctuation or scintillation. In October, 1967, she noted some unusual deflections lasting a minute or two which she could not readily identify as either a scintillating quasar or as interference from a terrestrial source, e.g. a gasoline engine ignition. Recalling that she had seen something like it several weeks earlier, she searched back through the records and found that it had appeared several times before and at the same declination and right ascension. This suggested that it was of celestial and not terrestrial origin, but curiously, the signals appeared conspicuously near midnight when interplanetary scintillation drops to a very low value.

Systematic investigation of these signals began in November, 1967. High speed recordings showed that they consisted of a series of pulses of about $^1/_3$ second duration with a repetition period of 1.337 s which was maintained with astonishing precision. The thought that the signal might be the beacon of an extraterrestrial civilization was entertained at one point, but lack of Doppler variation in the pulse rate from planetary motion around a star and the discovery of three more pulsing signals elsewhere in the sky seemed to rule out this possibility. Announcement of the discovering of these pulsating objects or pulsars appeared in the February 24, 1968 issue of ñNatureò with a tentative explanation offered that the sources were oscillating white dwarf or neutron stars (Hewish *et al*., 1968). The discovery of pulsars with periods less than $^1/_{10}$ second and a spin-down rate led to the identification of pulsars as rotating neutron stars.

This serendipitous discovery of pulsars was entirely unexpected but so was Karl Guthe Janskyôs discovery of radio emission from our galaxy that marked the beginning of radio astronomy, as well as Arno Penzias and Robert Wilsonôs discovering of 3 K sky background. It is remarkable that in all the three cases (pulsars, galactic radio emission and 3 K), the design of the instrument and the circumstances of its use were almost ideally suited for the discovery. Many astronomers around the world joined in further observations and studies of the pulsar and in searching for new ones, generating a vast literature on pulsars.

1.3 Classification of Pulsars

There are three generic classes of pulsars, based on the possible energy source which powers their emissions.

- **Rotation-powered pulsars** are powered by the rotational kinetic energy of the underlying neutron stars. The Electromagnetic radiation emitted can be across a large portion of the electromagnetic (EM) spectrum, generally from the x-ray region down to the radio region. Typically the radiation is seen in the radio region of the EM spectrum. As such, rotation-powered pulsars are referred to as radio pulsars. There are mainly two groups or types of rotation-powered pulsars which include the normal and the millisecond radio pulsars. The normal radio pulsars are mostly isolated, fast spinning neutron stars. More than 1000 members of this class have been discovered and they all have rotation periods in the range of ~ 0.03 to 8.5 s. The characteristic age of normal radio pulsars is of the order of 10^8 yr while their surface magnetic field is about 10^{12} G (Seiradakis and Wielebinski, 2004). More than 90 percent of the known normal radio pulsars have period derivative $\dot{P} \geq 10^{-17}$ ss^{-1}, however objects with $\dot{P} \sim 10^{-19}$ ss^{-1} also exist. Normal radio pulsars are generally expected to spin down steadily with time. However, the normal radio pulsars residing in the globular clusters (Manchester *et al*., 1985; Wolszczan *et al*., 2000) are known to be spinning up instead, presumably owing to the gravitational interaction between the pulsars and the other densely packed stars in the cluster. When these interactions result in acceleration in excess of the pulsar spin-down rate, there is a net acceleration which corresponds to spin-up of the pulsar.

Radio pulsars whose spin periods are less than 25 ms (e.g. Kaspi, 1997), and which, according to the standard evolutionary model (e.g. Bhattacharya and van den Heuvel, 1991) acquired these fast spin rates after an episode of ñspin-upò, probably through mass and angular momentum accretion from a low mass binary companion are referred to as millisecond pulsars. The fastest millisecond pulsar found to date has a period of 1.56 ms (Backer *et al*., 1982). The origin of millisecond pulsars is still unknown. The leading theory is that they begin life as longer period pulsars but are spun up or recycled through accretion (Bhattacharya, 1996; Lyne and Smith, 1998). For this reason, millisecond pulsars are sometimes called recycled pulsars. About 40 members of this class have been observed and a significant percentage of them are in binary systems with main sequence stars (Kaspi *et al*., 1994), or degenerate stars ï white dwarfs (Lyne

and Smith, 1990) or neutron stars (Taylor and Weisberg, 1982; Nice *et al*., 1996). The characteristic age of millisecond pulsars is slightly above 10^9 yr (Seiradakis and Wielebinski, 2004). Millisecond pulsars are characterized by very small spin-down rates, $\dot{P} < 10^{-17}$ ss^{-1} and relatively weak surface magnetic field, $B \sim 10^8$ ï 10^9 G. The low surface magnetic field has been associated with the accretion processes, in which the field is believed to be appreciably buried in the accreted material. However there is, as yet, no physical mechanism which plausibly explains how the magnetic field of a neutron star could significantly decay (Bhattacharya and Srinivasan, 1995).

- **X-ray pulsars** are powered by energy released during mass accretion from the binary companion and are generally classified into two: High-Mass and Low-Mass X-ray Pulsars. In High-Mass X-ray Binaries (HMXBs), the mass of the companion is greater than 10 solar masses (e.g. Joss and Rappaport, 1984). Examples of HMXBs are LMC X-4, Cen X-3 and SMC X-1. Their rotation periods range from 0.069 to 835 s, while the orbital periods have been found to lie between 0.2 and 187 days. HMXBs are characterized by high surface magnetic fields of ~ 10^{12} G (Lyne and Smith, 1998). A subclass of X-ray pulsars, in which the mass of the companion is usually less than 1 solar mass, is known as the Low-Mass X-ray Binaries (LMXBs). These objects are more difficult to study owing to the fact that only little light, if any, can be observed directly from the companion star. Orbital periods are generally less than 1 day. X-ray binaries are characterized by rapid decrease in the rotation periods (that is they spun-up with time). This observation suggests that the torque responsible for the spin-up, the accretion torque, could be orders of magnitude greater than the magnetic braking torque (Lyne and Smith, 1998).

- **Magnetars** are presumably powered by the decay of hyper-strong fields, whose decay timescale is of order ~ 10^3 ï 10^4 years (Thompson and Duncan, 1996). They are highly magnetized neutron stars in fact much more than conventional neutron stars by a factor of up to 100 or more, with magnetic fields in the order of 10^{14} G. Magnetars are capable of emitting bursts of both x-rays and gamma rays through the decay of their very strong magnetic field. The very strong magnetic field of a magnetar is thought to be inherited when the neutron star is first created during a supernova explosion (Duncan, 1998). These magnetars could manifest as soft gamma repeaters (SGR) where x-ray stars sporadically emit bright, short (0.1 s) repeating flashes of low-energy gamma rays and anomalous x-ray pulsars (AXPs) which are slowly rotating pulsars with periods of 6 ï 12 seconds (Karttunen *et al*., 2006). The Fermi space Telescope has

uncovered a subclass of rotation-powered pulsars that emits only gamma rays (Atkinson, 2008). There have been only about one hundred gamma-ray pulsars identified out of about over 2000 known pulsars (Atkinson, 2008). Although all the three classes of objects are neutron stars, their observable behaviour and the underlying physics are significantly different.

1.4 Neutron Star ï A Member of the Compact Stars

In astrophysics, those stars in which the density of matter is much larger than in ordinary stars are called compact objects, e.g. white dwarfs, neutron stars and black holes. It is believed that in compact stars, thermonuclear reactions have completely ceased in their interiors and as such, they cannot support themselves against gravity by thermal gas pressure.

In white dwarfs, gravity is restricted by the pressure of degenerate electron gas which is given (e.g. Shapiro and Teukolsky, 1983) by

$$P_e = \frac{1}{8}\left(\frac{3}{\pi}\right)^{1/3} hc\left(\frac{N}{V}\right)^{4/3}, \qquad (1.2)$$

where h is the Planckôs constant, c is the velocity of light in free space and $\frac{N}{V}$ is the electron number density. A degenerate gas is one in which all the available energy levels, up to a limiting momentum are completely filled. This limiting momentum is called Fermi momentum (P_o) and is given (e.g. Shapiro and Teukolsky, 1983) by

$$P_o = \left(\frac{3}{\pi}\right)^{1/3} \frac{h}{2}\left(\frac{N}{V}\right)^{1/3}. \qquad (1.3)$$

In neutron stars, gravity is prevented by the pressure of degenerate neutron gas (Shapiro and Teukolsky, 1983). In black holes, however, gravitational force is completely dominant and compresses the stellar material to infinite density (Karttunen *et al*., 2006).

Towards the end of the evolutionary life of a star, all its nuclear fuel is completely exhausted and core collapse then begins under gravity. If the mass of the collapsing star is not above 10 $M_\odot$, the pressure of the degenerate electron gas eventually balances gravity and the star stabilizes as a white dwarf. However, if the mass of the collapsing star is greater than 10 $M_\odot$, the star is believed to experience a sudden brightening and eventually explodes in a spectacular supernova event, leaving a remnant neutron star behind. On the other hand, if the star is too

massive ($\gg$ 10 $M_\odot$) that the core continues to collapse indefinitely, crushing matter to itself, it finally forms a black hole. The black hole has no upper mass limit. Unlike the white dwarfs and neutron stars that have very strong magnetic fields, the black holes have no magnetic fields.

1.5 The Internal Structure of a Typical Neutron Star

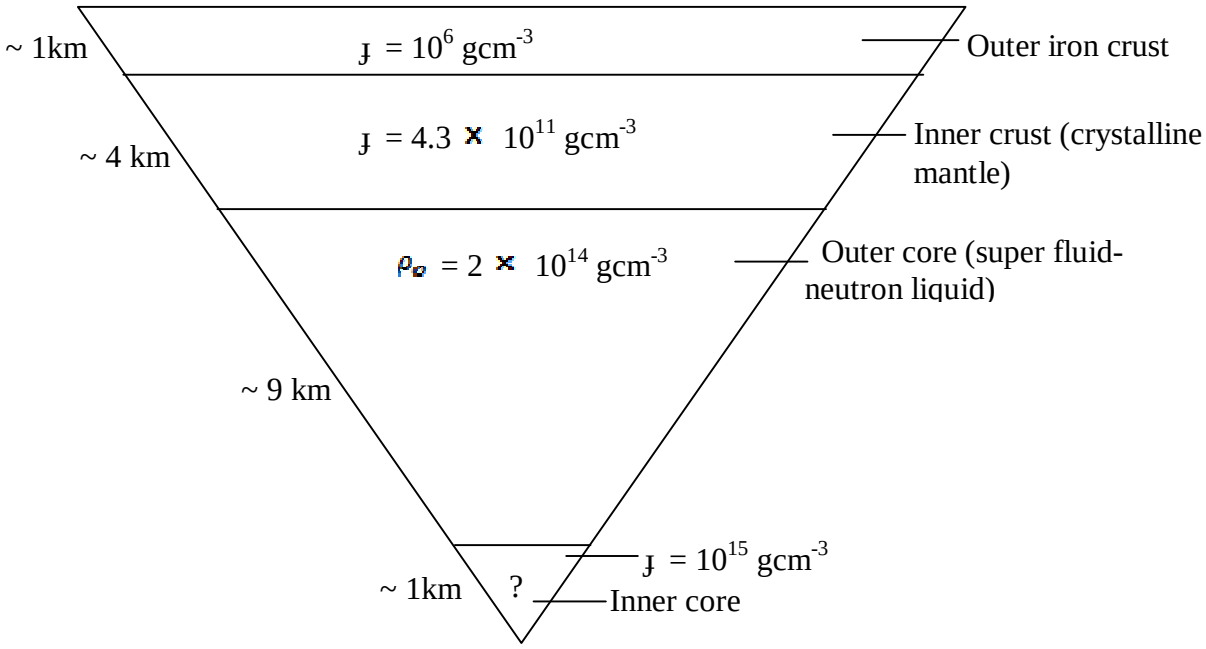

Figure 1.1: A typical structure of a neutron star interior based on soft equation of state (Oppenheimer and Volkoff, 1939).

There are different models of the neutron star. Each model depends on the equation of state used. This in turn determines the radius and mass of the neutron star. The most acceptable models show that the mass of a typical neutron star is between 0.2 and 2 $M_\odot$ (Baym, 1991; Haensel *et al*., 2007; Kiziltan, 2011). If the mass is smaller, then there will be insufficient gravitation to hold the star together in its condensed form. On the other hand, a larger mass means a more concentrated star which leads to further collapse to possibly a black hole. The diameter of a typical neutron star with mass of 1.4 $M_\odot$ is about 20 ï 30 km (Wiringa *et al*., 1988). The central density is about 3 × 10^{14} ï 3 × 10^{15} gcm^{-3} (Baym, 1991; Haensel *et al*., 2007; Kiziltan, 2011).

There are basically two broad components of the neutron starôs internal structure namely: a crystalline solid crust and a neutron liquid interior. The outer crystalline crust consists mainly of iron nuclei and has density of about 10^6 gcm^{-3} with thickness of ~ 1 km. The layer below this has density of about 10^{11} gcm^{-3} with thickness of ~ 4 km and consists mainly of protons and

electrons that fuse to form nuclei with unusual high numbers of neutrons. For example, the nucleus of ^{118}Kr has 82 neutrons and 36 protons (Lyne and Smith, 1998). The outer core is separated from the inner crust by what is called neutron drip point. The outer core with density up to 2 × 10^{14} gcm^{-3} (the density of nuclear matter, i.e. 2.8 × 10^{14} gcm^{-3}) with thickness of ~ 9 km, consists of unstable massive nuclei embedded in a super fluid called neutron fluid. This fluid contains a few percent of electrons and protons. This fluid component is important in the explanation of the pulsar glitches behaviours (Ruderman, 1976).

Furthermore, the main body of this neutron super fluid is coupled more tightly to the solid crust of the star by its magnetic field. The core which has density in excess of that of the nuclear matter has been suggested to contain exotic states of matter (Baym, 1991). Here, neutrons may be crushed into mesons or kaons which might form a solid core that could be equally useful in the explanation of glitches. The neutrons themselves would break down to quarks (ñUPò and ñDOWNò) and gluons. It has been suggested that the neutrons might even change to ñstrangeò variety of quarks (Baym, 1991).

1.6 Neutron Star Magnetosphere

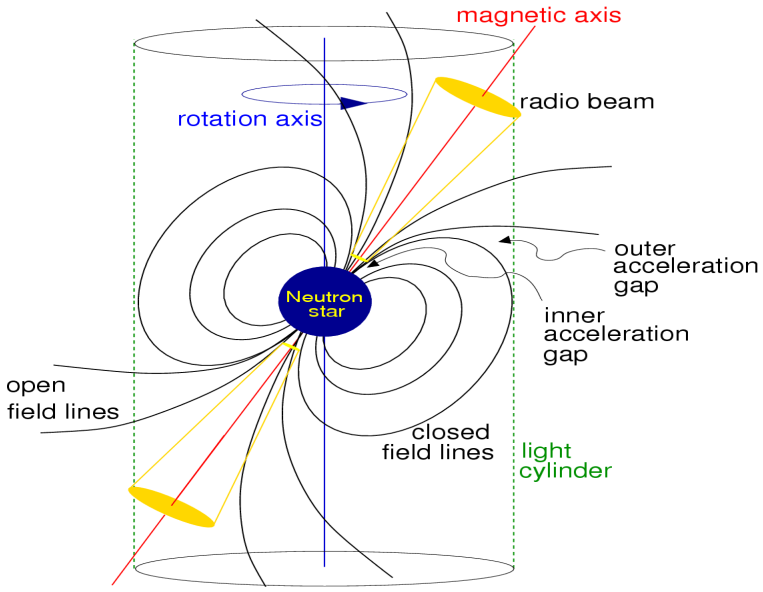

Figure 1.2: Toy model for the rotating neutron star and its magnetosphere (not drawn to scale!). From European Pulsar Network (EPN) database[1].

The pulsar magnetosphere is a region around the neutron star within which the magnetic (force) field of the star strongly dominates every other force. The magnetosphere is composed of ionized, high-energy plasma which is in rapid co-rotation with the neutron star. Within a radial distance (r_c) of the rotation axis, there is a charge-separated, co-rotating magnetosphere (Lyne and Smith, 1998). The magnetosphere consists of the area from the neutron star surface extending up to a distance, r_c from the spin axis. The radial distance (r_c), given by c/Ω (where c is the velocity of light and Ω is the angular velocity), is the ñvelocity-of-light cylinderò. The velocity-of-light cylinder is the distance at which a particle with the angular velocity of the pulsar is traveling at the speed of light. The open field line defines the polar cap region on the neutron star surface, centred on the magnetic pole. The polar caps are the radio emitting regions. The particles generated within the regions are restricted to move only along the field lines. As a result, only particles on the open field lines outside the region can flow out from the magnetosphere. The radio emitting regions are confined to these open polar cap regions (Lyne and Smith, 1998).

The external magnetic field of the neutron star is of great importance in many observable pulsar characteristics. The dipoleôs misalignment with the rotation axis generates a broad band electromagnetic radiation at the rotation frequency of the pulsar. This accounts for the observed slow down and the main loss of rotational energy of the pulsar. According to Lyne and Smith (1998), for a young pulsar, the outward energy is sufficient to provide high-energy particles in a surrounding nebula. For instance, the rotational energy of the Crab pulsar is the source of energy for the synchrotron and radiation of the surrounding Crab Nebula. The discovery of a pulsating radio source in the centre of Crab Nebula remains one of the strongest evidence that pulsars are formed during supernova explosions. The energy released as the pulsar slows down is enormous and it powers the emission of the synchrotron radiation of the Crab Nebula which has a total luminosity of about 75,000 times in excess of that of the sun (Weiler and Sramek, 1988).

[1] www.mpifr-bonn.mpg.de/div/pulsar/data

1.7 The Emitting Regions of Pulsars

The radiations from pulsars are emitted in a narrow light-house beam. According to Lyne and Smith (1998), two models have been explored extensively in the explanation of pulsar emission processes. These are the polar cap and relativistic beaming models. The polar cap model places the origin of the emission immediately above a magnetic pole and is built on the observations of beam width and polarization (Lyne and Smith, 1998). The relativistic beaming model, however, places the origin of the emission inside the magnetosphere, near the velocity-of-light cylinder and is built on the high energy radiation seen in the Crab and Vela pulsars (Lyne and Smith, 1998). The emission region of a pulsar is shown in Figure 1.3. The gamma-ray emission beam emanates from the outer acceleration gap while the radio emission beam originates from the inner acceleration gap.

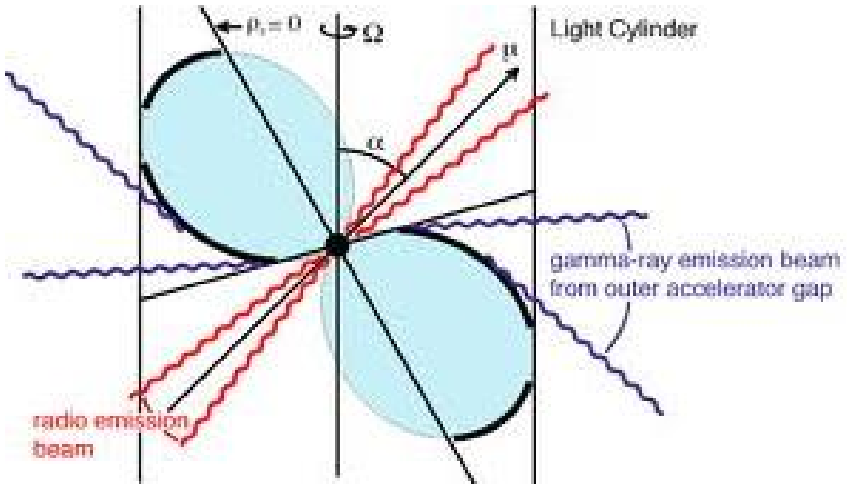

Figure 1.3: Emission region of a pulsar (Figure taken from EPN database).

1.8 Radio Pulse Characteristics

There are several observed characteristic features of the radiations from radio pulsars. Most of these features concern mainly the individual pulses, while others like polarization refer to the entire radiation. Some of these pulsar properties are discussed in this section.

1.8.1 Integrated Pulse Profile

Pulsars are weak emitters of radio signals. As a result, only individual pulses from strongest sources can be observed despite the high sensitivity of some of the current radio telescopes. Most pulsars require the coherent addition of many hundreds or even thousands of pulses together to produce an integrated pulse profile that is discernible above the background noise of the receiver (Lyne and Smith, 2012). The integrated pulse profile of a given pulsar is usually very stable and is the signature of the pulsar at the observing frequency.

1.8.2 Pulse Shapes

Pulsars have pulse shapes that vary in complexity. Some pulsars like PSR B1933+16 have single component pulse that is essentially Gaussian in form. Others like PSR B1913+16 have a double-peaked structure. Still, some other pulsars show complicated shapes with multiple components. An example of this class of pulsars is PSR B1237+25 (Lorimer and Kramer, 2005). Different pulse shapes observed in different pulsars are shown in Figure 1.4.

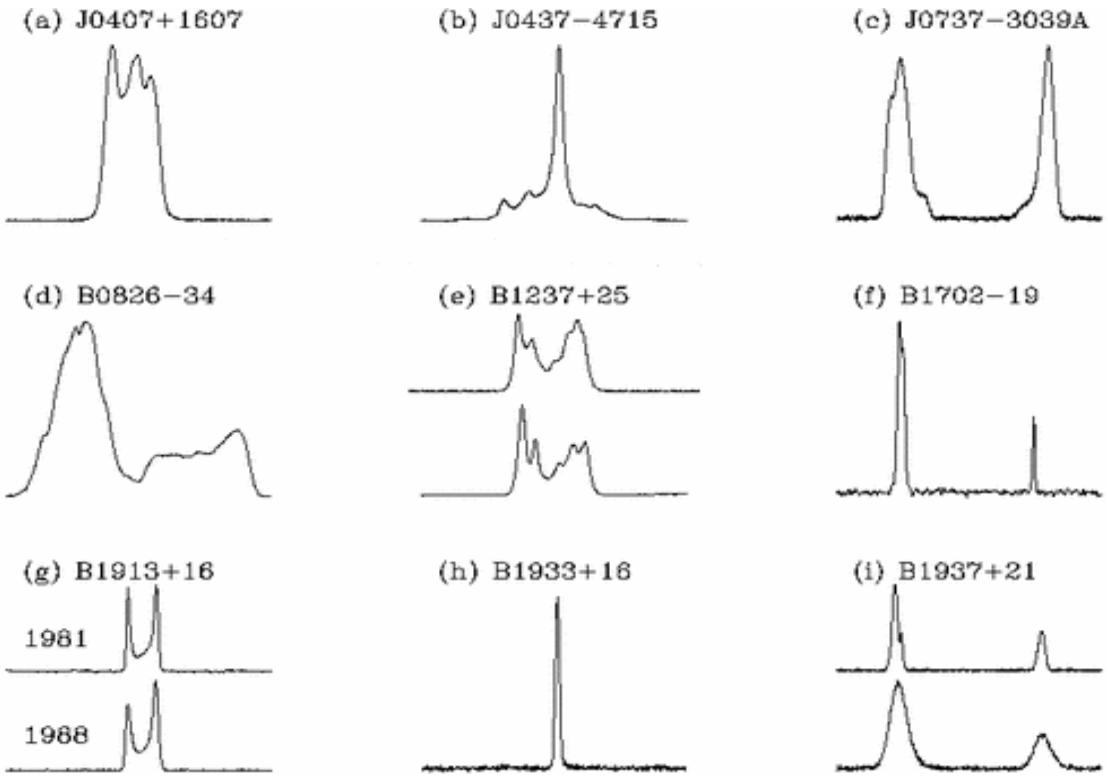

Figure 1.4: Integrated pulse profile for a sample of nine pulsars. With the exception of PSR B1237+25, each profile shows 360^0 of rotational phase (From EPN database).

It is important, however, to note that the analyses of these pulse shapes could reveal a lot about the structure of the emission beam of pulsars. Prior to the work by Kramer *et al*. (1998), the profiles of the millisecond pulsars were supposed to be far more complicated than those of the normal pulsars. Their work, however, revealed that on average, there are 3 ± 1 components for the normal pulsars and 4 ± 1 components for the millisecond pulsars.

1.8.3 Profile Evolution with Frequency

As shown in Figure 1.5 for PSRs B1133+16 and J2145-0750, there are usually changes in the pulse shape which depend on the frequency at which the pulses are observed. Normal pulsars like B1133+16 show a gradual increase in pulse width and separation of profile components when observed at lower frequencies (Komesaroff, 1970). This effect is, however, less noticeable for the millisecond pulsars. Millisecond pulsars like J2145-0750 show little change in pulse width and component separation with frequency (Kramer *et al*., 1999b). This is in agreement with the idea that the size of the emission region of millisecond pulsars is much smaller than for normal pulsars.

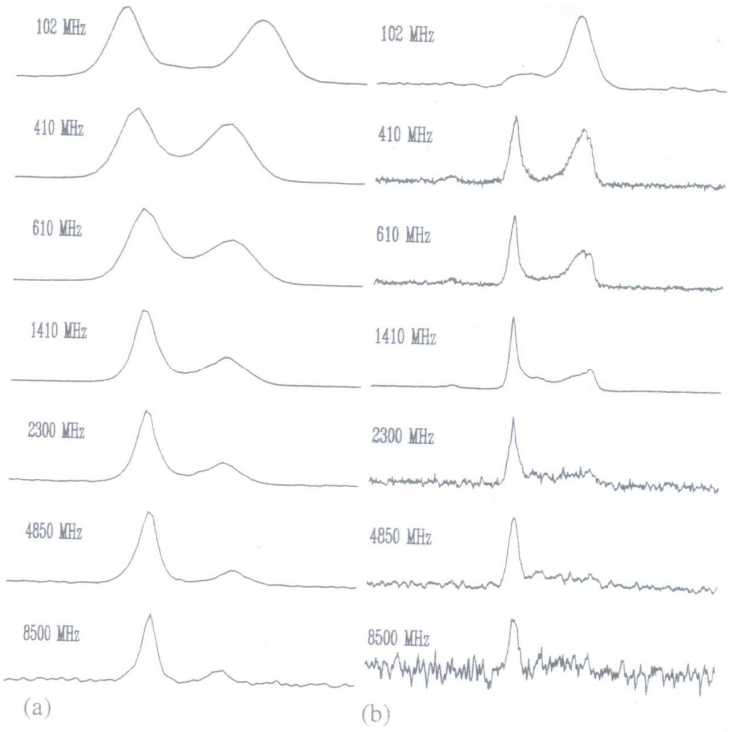

Figure 1.5: Multi-frequency pulse profiles for two pulsars: (a) 1.16 s pulsar B1133+16 and (b) 16 ms pulsar J2145-0750 (from EPN database).

1.8.4 Flux Density Spectra

Flux density is the amount of energy transferred by electromagnetic radiation through a real or virtual surface, per unit surface area and per unit wavelength. The unit of flux density measured by the telescope is the Jansky (Jy), where 1 Jy is equivalent to 10^{-26} $Wm^{-2}Hz^{-1}$. Flux density could be measured in two ways:

a. The peak flux density (the maximum intensity of a pulse profile).
b. The mean flux density (the integrated intensity of the pulse profile averaged over the pulse period).

The mean flux densities of pulsars have a strong inverse dependence on the observing frequency. For most pulsars observed above 100 MHz, the dependence has a simple power law given (e.g. Sieber, 1973) as

$$S_{mean}(f) \propto f^{\alpha}, \qquad (1.4)$$

where f is the observing frequency and Ŭis the spectral index. However, recent work by Maron *et al*. (2000) showed a more complex spectral behaviour that needs a two-component power law model. Other striking deviations from single power law behaviour are the roll over in the spectra often seen at low frequencies (Malofeev, 1996) and the tantalizing hints of spectral increase or turn-up seen for a few pulsars at millimetre wavelengths (Kramer, 1996b). For pulsar spectra that can fit the single power law satisfactorily, the range of the observed spectral indices is between -4 and 0, with the mean value of -1.8 ± 0.2 (Maron *et al*., 2000).

1.8.5 Polarization of Pulsar Radiation

Pulsars are known to be among the most polarized radio emitters. The radio signals from pulsars consist of linear and circular polarization components. Basically, there are four Stokes

parameters (I, Q, U, V) used to describe polarization, where I is the total intensity, Q and U are the linear Stokes parameters and V is the circularly polarized intensity. The linearly polarized intensity, L is given (e.g. Lyne and Smith, 1998) by

$$L = \sqrt{Q^2 + U^2}. \tag{1.5}$$

A study of 300 normal and millisecond radio pulsars at 600 and 1400 MHz (Gould and Lyne, 1998) revealed that the average degree of linear polarization, $\langle L/I \rangle$ is about 20 percent while the circularly polarized component, $\langle |V|/I \rangle$, is about 10 percent. The position angle (ψ) of linear polarization is a function of pulse phase and is given by the expression (e.g. Lorimer and Kramer, 2005):

$$\psi = \tfrac{1}{2} \tan^{-1}\left(U/Q\right). \tag{1.6}$$

The simple pattern of polarization according to Lyne and Smith (1998), suggests that the origin of the radio beam is immediately above a magnetic pole while the swing of the position angle is related to radio emitting regions whose radiation is polarized along the direction of the field lines.

1.9 Pulsars as Astrophysical Tools

Pulsars are very important astronomical objects that have a very wide range of both physical and astrophysical applications. According to Lorimer and Kramer (2005), pulsars are in many respects, a physicists dream come true. Besides testing theories of gravity, one can investigate the gravitational potential and magnetic field of the galaxy, the interstellar medium, binary systems and their evolution, solid state physics and the interiors of neutron stars. The study of the radio emission from pulsars reveals a lot about plasma physics under extreme conditions (Lyne and Smith, 1998). Some of the applications of pulsars are outlined below.

1.9.1 Pulsars as High-Precision Timing and Time Keeping Devices

Pulsars could be used as high-precision time-measuring instruments. This depends on what is called pulsar timing, which is the measurement of the pulse arrival times of photons emitted by the pulsars. The amount of useful information that could be obtained depends upon

the measurement precision of the pulse arrival time, which scales as the pulse width divided by the signal-to-noise (S/N) ratio and on the rotational stability of the objects. Since bright millisecond pulsars have short periods, hence narrow pulse width and high level of rotational stability, they are mostly used for these high precision measurements (Lyne and Smith, 1998). The current state of the art is the 5.75 ms pulsar J0437-4517, which yields a root mean square residual between measured and model arrival times of about 100 ns over an observing time of 1 yr or longer (van Straten *et al*., 2001). The stability of pulsar depends largely on its rotational kinetic energy and spin down energy loss rate. Due to the large rotational kinetic energy and relatively low spin down energy loss rate associated with millisecond pulsars, they are believed to be more stable than normal pulsars (Lorimer and Kramer, 2005). As such, millisecond pulsars give higher timing precision than normal pulsars.

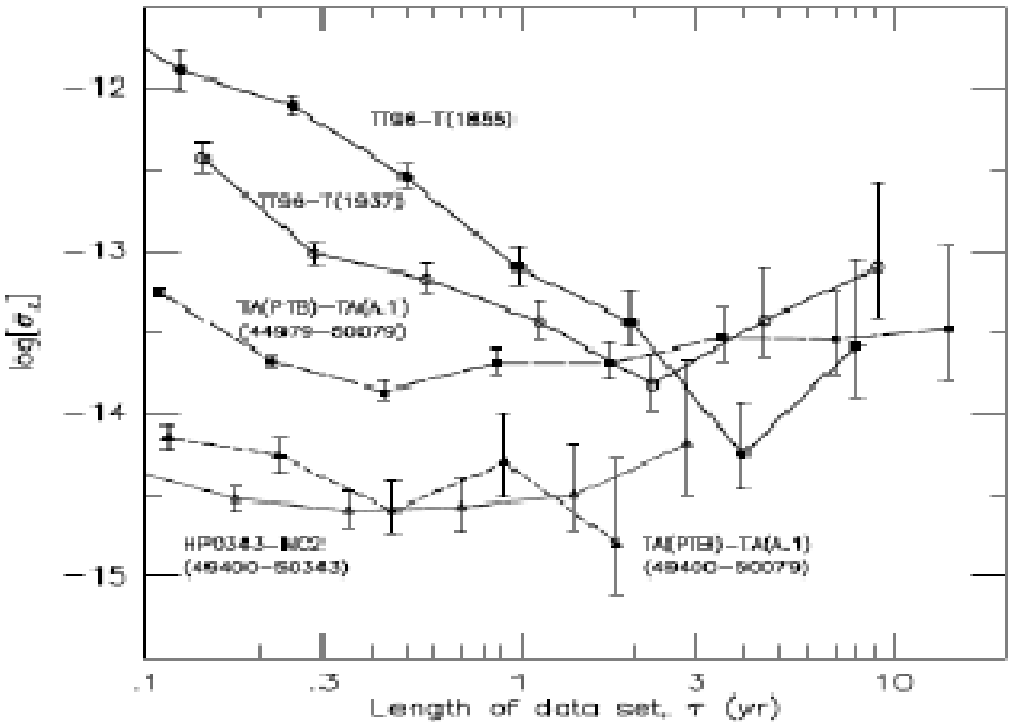

Figure 1.6: Comparing the stability of PSRs B1855+09 and B1937+21 with various atomic clock differences (Matsakis *et al*., 1997).

The performance of different clocks can be compared using their fractional stabilities (σ_z). The fractional stability (σ_z) is like the Allan variance (Matsakis *et al*., 1997) and usually decreases over a period of time during which clock behaviour is predictable. Although, the stability of millisecond pulsars are less than those of atomic clocks on short timescales, they become similar over time spans of months and years (Matsakis *et al*., 1997). Ultimately, rotational instabilities intrinsic to most pulsars known as timing noise could become important and limits the stability of the pulsar clock. This implies that timing noise limits the timing precision of pulsar clocks. The processes causing timing noise are not understood fully, but young pulsars show higher degree of timing noise than older ones (Hobbs *et al*., 2010). A trend seen among the sample of normal and millisecond pulsars indicates that the timing stability increases with smaller period derivatives and is, hence, greatest for recycled millisecond pulsars (Hobbs *et al*., 2010).

If recycled millisecond pulsars perform better than terrestrial clocks, it is possible that a time standard could be defined by timing several of most stable millisecond pulsars against each other. The problem is that each pulsar has different spin period and spin-down rates that are caused by some processes that are not yet fully understood. Similarly, unlike the current definition of the second that is based on a hyperfine transition of cesium 133, a pulsar time standard would not have a link with any reproducible physical phenomenon in any laboratory. Unless pulsars can be monitored continuously with dedicated telescopes, terrestrial clocks would still be needed to interpolate between the observations and to tie pulsar time to some terrestrial endpoint times (Lorimer and Kramer, 2005).

1.9.2 Laboratory for Testing the Predictions of General Relativity

In astrophysical experiments, the experimental set-up cannot be modified. As a result, we can only obtain information from the photons received. In probing the limits of our understanding of gravitational physics, one will be interested in extreme conditions that are not obtainable on earth. Though, solar system tests provide a number of very stringent tests of general relativity (Will, 2001), none of such tests will ever be able to test the strong-gravitational field limit. For such studies binary millisecond pulsars are the only known way to test the predictions of general relativity or competing theories of gravity in the strong-gravitational field limit.

1.9.2.1 The Use of Double Neutron Star (DNS) Binaries

Being very compact massive objects, DNS binaries are used as perfect point sources for testing theories of gravity in the strong-gravitational field limit. For all the known DNS systems, the orbital separation is much larger than the size of the compact companion. An excellent example is the original binary pulsar B1913+16 in which the orbital period is observed to decrease at a rate predicted by general relativity due to gravitational-wave damping (Taylor and Weisberg, 1989; Weisberg and Taylor, 2003, 2004). This phenomenal measurement, shown in Figure 1.7 corresponds to an orbital shrinkage of 1 cmday^{-1} and provided the first evidence for the existence of gravitational radiation as predicted by general relativity.

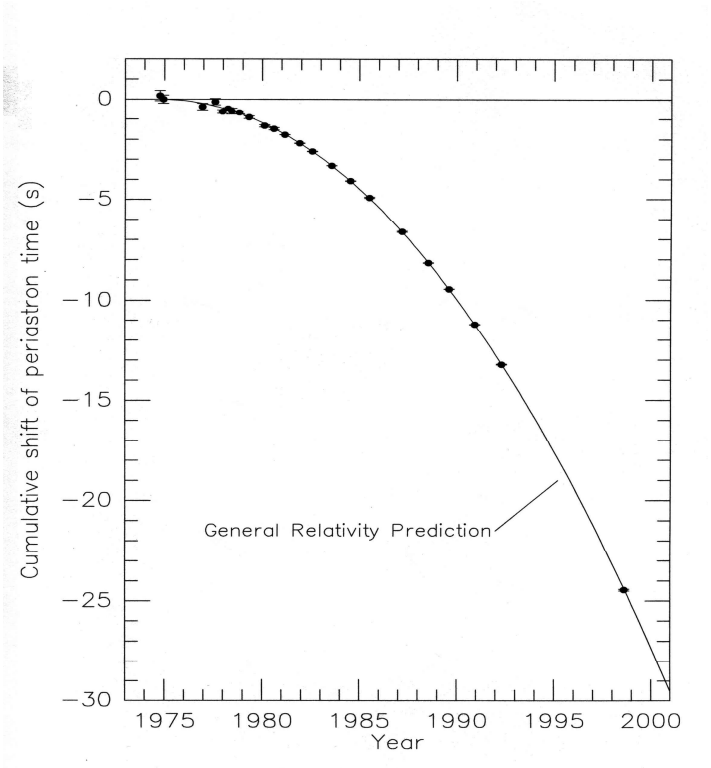

Figure 1.7: The shift in the periastron passage of the binary pulsar B1913+16 plotted as a function of time (Taylor and Weisberg, 1989).

Consequently, neither mass transfer nor tidal effects is present and the system then approximates to a pair of point masses that can be used to test the predictions of theories of gravity (Weisberg and Taylor, 2004 and references therein). For instance, the rate of advance of

periastron, $\dot{\omega}_{GR}$ due to the emission of gravitational radiation. Here the crucial factor is the ratio of gravitational potential energy and rest mass energy for pulsar B1913+16, this factor, GM/c^2r is 10^{-6}. The rate of advance of periastron, $\dot{\omega}_{GR}$ depends on the total mass of the system. If the respective mass of the pulsar and its companion is m_p and m_c, then the rate of periastron advance is given (e.g. Taylor and Weisberg, 1989) by

$$\dot{\omega}_{GR} = 2.11 \left(\frac{m_p + m_c}{M_\odot}\right)^{2/3} \text{ degree yr}^{-1}, \qquad (1.7)$$

where $M_\odot$ is the solar mass.

The original binary pulsar B1913+16 has shown a decrease in orbital period which has been measured (e.g. Taylor and Weisberg, 1989) by

$$P_b = -\frac{\dot{\nu}}{\nu^2} = (-240 \pm 0.09) \times 10^{-12}, \qquad (1.8)$$

where P_b is the orbital period, ν is the spin frequency and $\dot{\nu}$ is its first time derivative. This agrees with the predictions of the general relativity due to gravitational-wave damping. This observation provided the first evidence for the existence of gravitational radiation in accord with the predictions of general relativity (Taylor and Weisberg, 1989).

1.9.3 The Study of the Galaxy and the Interstellar Medium

The proper motions (the apparent slow movement of a star in a direction that does not change with time) of the pulsars reveal that they have very large space velocities (1000 kms^{-1}) that have carried most of them away from the vicinity of their birth places to the galactic plane (Lyne and Lorimer, 1994). In other words, pulsars should exist in any region of the galaxy. However, the nature of pulsars as galactic objects as well as the interactions between their polarized emission and the magnetized ionized interstellar medium makes it possible for pulsars to be employed in the study of the galaxy and the properties of the interstellar medium (ISM).

The measurement of the delay in arrival times of pulses as they traverse the interstellar medium gives information about the dispersion measure (*DM*), which is the integrated column density of free electrons along the line of sight to the pulsar. If the distribution of free electrons in the galaxy were known with precision, the measurement of the *DM* would give the distance to

every pulsar (Taylor and Cordes, 1993). Though uncertain, the distribution of free electrons could be estimated through the use of independently calculated pulsar distances. By this means, pulsars are used in determining the galactic distribution of free electrons (Guélin, 1973).

Pulsar signals are highly polarized as discussed in section 1.8. Consequently, the magnetized ionized interstellar medium interacts with the linearly polarized signals, thereby rotating the position angle of linear polarization, by an amount that is proportional to the galactic magnetic field component along the line of sight to the pulsar. The effect of the rotation measure (*RM*) for pulsars over a wide range of locations in the galaxy can be employed in mapping out large-scale structures of the galactic magnetic field (Smith, 1968; Taylor and Cordes, 1993; Wolleben and Reich, 2003). Earlier studies evidence of the galactic magnetic field show field-line reversals between some nearby spiral arms (Thomson and Nelson, 1980; Lyne and Smith, 1989; Rand and Lyne, 1994; Han *et al*., 2002; Noutsos *et al*., 2008).

1.9.4 The Study of Super-Dense Matter

The nature of matter inside neutron stars is said to be super dense [~ (3 ï 30) × 10^{14} gcm^{-3}]. This state of matter is not obtainable in any laboratory on earth. Application of pulsars as physical tools allows such extremely dense matter to be explored. The study of glitches, the rotational instabilities in pulsars and the subsequent post-glitch relaxation provide means of probing neutron star materials in a unique way. This is referred to as neutron star seismology (Lorimer and Kramer, 2005). Glitches are believed to occur due to variable coupling between the radio pulsar crust and its super fluid interior. Glitches are, however, rare and have been observed in a small fraction of mostly young pulsars (Lyne *et al*., 1996; Shemar and Lyne, 1996). Lyne *et al*. (1996) discovered that most young pulsars with characteristic age $\tau_c \leq 2 \times 10^3$ yr show no sign of glitch activities. The lack of glitch activities in these young pulsars is probably due to the effect of high internal temperature, which tends to reduce the effect of vortex pinning (Wang *et al*., 2000). On the other hand, Urama and Okeke (1999) found that old pulsars show high glitch activities especially those with higher spin-down rates. The excitement and expectation that followed the discovery of this glitch led to further research on pulsars and pulsar timing observations.

Glitches are classified into two ï macroglitches and microglitches (e.g. Cordes *et al*., 1988). Macroglitches (also known as glitches) are usually characterized by a sudden increase in

the pulsarôs rotation frequency, ν which is normally accompanied by an increase in the magnitude of the spin-down rate, $\dot{\nu}$ (Lyne *et al*., 1996; Urama, 2002). Macroglitches are known to originate from some form of dynamical change within the neutron star which involves a sudden and regular transfer of the angular momentum from the more rapidly rotating inner superfluid components to the slowly spinning crust (Anderson and Itoh, 1975; Ruderman, 1976). Some macroglitches have been explained as a consequence of star quakes, where sudden changes in the oblateness of the neutron star crust cause a change in the moment of inertia and, hence, the spin frequency, since angular momentum must be conserved (Baym *et al*., 1969). Macroglitches have some unique features in that the jumps in the rotation frequency ($\Delta\nu$) and the spin-down rate ($\Delta\dot{\nu}$) have a definite signature ($\Delta\nu, \Delta\dot{\nu}$) = (+, −) which corresponds to the increase in the pulsarôs spin rates and magnitude of the spin-down rates (Melatos, 2000). The jumps in the rotation frequency of pulsars are frequently accompanied by some periods of relaxation towards the undisturbed pre-glitch values that change in a wide range of time-scales (Cordes *et al*., 1988).

The microglitches consist of a class of small amplitude but resolvable jumps in both or either of the pulsar rotation frequency and its first time derivative. The study of the microglitches has received far less attention than macroglitches in the last three decades of radio pulsar timing observation (Cordes *et al*., 1988; Chukwude, 2002). This consequently has made the knowledge about this class of rotational discontinuity of the microglitches very little. Unlike the macroglitches, in which the jumps are associated with a definite signature, the amplitudes of the jumps in microglitches vary over a wide range (Cordes *et al*., 1988; Chukwude and Urama, 2010). The microglitches have a combined signs and are extraordinarily difficult to detect and understand in the framework of the available glitch theories (Chukwude, 2002). The previous information on the observations of microglitches in radio pulsars have relied fully on the visual inspection of carefully calculated residuals of pulse rotation frequency ($\Delta\nu$) and its first time derivative ($\Delta\dot{\nu}$). But observational setbacks have allowed only indirect calculation of $\Delta\nu$ and $\Delta\dot{\nu}$ through a successive numerical differentiation of phase residuals that is obtained from second-order model which fits to barycentric times of pulsar arrival data (Cordes *et al*., 1988).

The comprehensive observational description of the phenomena of microglitches and macroglitches has become indispensable in a quest for improved statistics of radio pulsar glitch activity. This will give more insight into the incidence and other features of these small

amplitude discontinuities in pulsar rotation frequency (Glampedakis and Andersson, 2009). Ultimately, a better understanding of the possible origin of the microglitches and the relationship between macroglitches and microglitches could be achieved**.**

1.9.5 The Discovery of Extra-Solar Planets

The technique of pulsar timing is extremely important in the study of pulsars and in the search for extra-solar planets/planetary systems. The first three extra-solar planets were discovered through radio pulsar precision timing technique (Wolszczan and Frail, 1992). These were detected around the 6.2 ms pulsar B1257+12. The analysis of the pulse arrival times reveals one planet of lunar mass (Planet A) and two earth-mass planets (planets B and C) with orbital periods of 25, 66 and 98 years respectively (Wolszczan and Frail, 1992). Shabanova (1995) reported evidence for a planet with at least two earth masses and a semi-major axis of 7.3 AU in orbit of a normal pulsar B0329+54. This is a very slow pulsar, which means a relatively old object (pulsation period about 0.7 s).

The unexpected discovery of this extra-solar planetary system, demonstrates the high sensitivity of pulsar timing in detecting small bodies in orbits around neutron stars. Hence, pulsar timing is now far more sensitive than optical searches for planets around main-sequence stars. It is important to note that the uncommon nature of planetary bodies orbiting the pulsars could be attributed to violent conditions in which neutron stars are born.

1.9.6 The Study of Plasma Physics under Extreme Conditions

Plasma physics is the study of charged particles and fluids interacting with self-consistent electric and magnetic fields. These conditions are believed to exist in neutron stars, and hence, they are used as laboratories for the study of such extreme physical conditions. These plasma processes occur under very high plasma densities, super-strong magnetic field and in a somewhat complex environment called the pulsar magnetosphere.

The double pulsar binary system consisting of the 22.7 ms pulsar A (Burgay *et al*., 2003) and the 2.8 s pulsar B (Lyne *et al*., 2004) serves as a suitable laboratory for understanding plasma physics. The interesting thing about pulsar A (J0737-3039) is that the mean orbital separation of the two pulsars is only about 3 light seconds (Lorimer and Kramer, 2005). At this

distance, the relativistic wind from the radiation beam of A is sufficiently energetic to penetrate into and probe the emission region of B, which is consequently distorted.

The first observation is seen as an occultation of the radiation of A by the magnetosphere of B at conjunction. The size of the region of eclipse can be found from the duration of the eclipse and the relative transverse speeds of the two stars. As they move in their orbits, the line of sight from A passes through and sweeps across the magnetosphere of B, giving the opportunity to probe the physical conditions in its magnetosphere. The determination of changes in the radio transmission properties like the dispersion and rotation measures will then allow the plasma density and magnetic field structure to be probed (Lyne and Smith, 1998).

1.10 Purpose of Study

The objectives of this study are as follows:

i. To investigate the relationship between the parameters (*DM* and *RM*) used to characterize the interstellar medium and the radio pulsar spin-down parameters (P, $\dot{P}$, τ_c and B), which characterize the intrinsic spin-down evolution of neutron stars.

ii. To investigate the relationship between the parameters (*DM* and *RM*) that probe the electron content of the interstellar medium and the radio pulsar distance from the galactic plane (Z).

iii. To determine the dependence of the pulsarsô properties on the rate of change/time derivative of DM (dDM/dt).

CHAPTER TWO

LITERATURE REVIEW

2.1 Pulsar Spin-Down Evolution

Like many things in life, the observed emission from radio pulsars does not come for free. It takes place at the expense of the rotational kinetic energy of the neutron star, which is given (e.g. Ostriker and Gunn, 1969) by

$$E = \frac{1}{2} I_n \Omega^2 , \qquad (2.1)$$

where $I_n \approx 10^{45}$ gcm^2 is the neutron star's moment of inertia and $\Omega = 2\pi/p$ is the rotational angular frequency (P is the rotation period of the pulsar). The rate of loss of rotational kinetic energy is thus (e.g. Ostriker and Gunn, 1969):

$$\dot{E} = -\frac{dE}{dt} = -I_m \Omega \dot{\Omega} , \qquad (2.2)$$

where $\dot{\Omega}$ is the rate of change of rotational angular frequency.

Pulse periods are observed to increase with time at a rate ($\dot{P} = dP/dt$). The rate of loss of rotational kinetic energy is given by this expression (e.g. Lorimer and Kramer, 2005):

$$\dot{E} = 4\pi^2 I_m \dot{P} P^{-3} . \qquad (2.3)$$

This quantity $\dot{E}$ is called the spin-down luminosity and it represents the total output power of the neutron star. A small fraction of the spin-down luminosity is converted into radio emission (Lyne and Smith, 1998; Lorimer and Kramer, 2005). The bulk of the rotational energy is converted into high-energy radiation and in particular, magnetic dipole radiation and a pulsar wind (Manchester and Taylor, 1977; Lyne and Smith, 1998).

On assumption that the dominant energy loss mechanism is the magnetic dipole radiation (i.e. the standard model), then a more general form of the spin-down law, believed to be relevant to all rotation-powered pulsars, is given (e.g. Manchester and Taylor, 1977) by

$$\dot{P} = K P^{2-n} , \qquad (2.4)$$

where K is an arbitrary positive constant which depends on the stellar magnetic field strength, moment of inertia and the angle between the magnetic axis and rotation axis, n is the braking index and is equal to 3 for the simplest case of pure magnetic dipole braking in a vacuum (Manchester and Taylor, 1977).

Equation (2.4) can be integrated, assuming a constant K and braking index $n \neq 1$, to obtain the characteristic/spin-down age of the pulsar (e.g. Lyne and Smith, 1998):

$$T = \frac{P}{(n-1)\dot{P}}\left[1-\left(\frac{P_o}{P}\right)^{n-1}\right], \qquad (2.5)$$

where P_o is the spin period at birth. On assumption that the spin period at birth is much shorter than the present value (i.e. $P_o \ll P$) and that the spin-down is due to magnetic dipole radiation (i.e. n = 3), equation (2.5) simplifies to the characteristic age, which is given (e.g. Lyne and Smith, 1998) by

$$\tau_c = \frac{P}{2\dot{P}}. \qquad (2.6)$$

Due to the assumption of a negligible initial spin period and n = 3, equation (2.6) does not necessarily provide a reliable age estimate.

Estimate of the surface magnetic field of a neutron star can also be obtained. For a canonical neutron star of diameter of 20 km and moment of inertia of 10^{45} gcm^2, the estimate of surface magnetic field is given (e.g. Lyne and Smith, 1998) by

$$B = 3.2\times10^{19}\sqrt{P\dot{P}}. \qquad (2.7)$$

As for the characteristic age, the basic observables P and $\dot{P}$ provide a handy estimate for the magnetic field strength at the pulsar surface of a rotating neutron star.

2.2 The Interstellar Medium (ISM)

The interstellar medium (ISM) is the matter that exist in space between the star systems in a galaxy. This matter includes gases in ionic, atomic and molecular form, dust and cosmic rays (Thorndike, 1930). The physics of the ISM plays a crucial role in many areas of astronomy. Galaxy formation and evolution, the formation of stars, cosmic nucleosynthesis, structure and growth of dust grains, which constitute the fundamental building blocks of planets, are intimately coupled to the physics of the ISM (Spitzer, 1978). Stars form within the densest regions of the ISM and replenish the ISM with matter and energy through planetary nebulae, stellar winds and supernova explosions. This interplay between stars and the ISM helps to determine the rate at which a galaxy depletes its gaseous content and therefore its lifespan of active star formation

(Lequeux, 2005). However, despite its importance, its structure and evolution is still poorly understood owing largely to its complexity and inaccessibility.

The ISM can be broadly classified into gas and dust components. The average density of the interstellar gas is roughly one hydrogen atom per cubic centimeter (1 cm^{-3}) which represents a density lower than can be created on earth (Lequeux, 2005). The ISM therefore represents a fascinating laboratory for studying solid state physics under extreme conditions. However, the density can vary considerably for different components of the interstellar gas. The components of the interstellar gas include cold atomic gas clouds, warm atomic gas, coronal gas, HII regions and molecular clouds. The properties of the components of the ISM of the Milky Way are shown in Table 2.1.

Table 2.1: A breakdown of the properties of the components of the ISM of the Milky Way.

Component	Fractional volume	Scale height (pc)	Temperature (K)	Density (atoms/cm^3)	State of hydrogen	Primary observational techniques
Molecular clouds	< 1%	80	10 ï 20	10^2 ï 10^6	Molecular	Radio and infrared molecular emission and absorption lines.
Cold Neutral	1 ï 5%	100 ï 300	50 ï 100	20 ï 50	Neutral	HI 21 cm line

Medium (CNM)					atomic	absorption.
Warm Neutral Medium (WNM)	10 ï 20%	300 ï 400	6000 ï 10000	0.2 ï 0.5	Neutral atomic	HI 21 cm line emission.
Warm ionized medium	20 ï 50%	1000	80000	0.2 ï 0.5	Ionized	Hα emission and pulsar dispersion.
H II regions	< 1%	70	8000	10^2 ï 10^4	Ionized	Hα emission and pulsar dispersion.
Coronal gas Hot Ionized Medium (HIM)	30 ï 70%	1000 ï 3000	10^6 ï 10^7	10^{-4} ï 10^{-2}	Ionized (metals also highly ionized)	X-ray emission; absorption lines of highly ionized metals, primarily in the ultraviolet.

The properties of the interstellar medium can be studied by examining the propagation of emissions produced by radio pulsars. Radio pulsars are point sources that have high level of linear polarization. This feature of radio pulsars makes them unique tools for probing the interstellar medium. For instance, the interactions between the polarized emission of radio pulsars and the magnetized ionized interstellar medium allow radio pulsars to be employed extensively in the study of a range of properties of the interstellar medium.

2.3 Propagation Effects in the Interstellar Medium

As radio pulses propagate through the interstellar medium, four propagation effects occur namely: pulse dispersion, scintillation, scattering and Faraday rotation.

2.3.1 Homogeneity of the ISM

The interstellar medium is a cold, ionized plasma. Electromagnetic radiation from pulsars experiences a frequency-dependent index of refraction as it propagates through the ISM (Lyne and Smith, 1990). Neglecting, small corrections due to the galactic magnetic field, the refractive index (μ) is given (e.g. Lyne and Smith, 1990) by

$$\mu = \sqrt{1 - \left(\frac{f_{\mathrm{p}}}{f} \right)^2} \ , \tag{2.8}$$

where f is the wave (observing) frequency and f_{p} is the plasma frequency. Following Guélin (1973), the plasma frequency, f_{p} is given by

$$f_{\mathrm{p}} = \sqrt{\frac{e^2 n_e}{\pi m_{\mathrm{e}}}} \ , \tag{2.9}$$

where n_e is the electron number density, while e and m_e are, respectively, the charge and mass of an electron. For the ISM, n_e ~ 0.03 cm^{-3} (Ables and Manchester, 1976), so that $f_{\mathrm{p}} \simeq$ 1.5 kHz. From equation (2.8), one notes that a wave will not propagate if $f < f_{\mathrm{p}}$. This fact is sometimes used to constrain the plasma density in a pulsar magnetosphere or the location where the radio emission leaves the magnetosphere (Ruderman and Sutherland, 1975).

2.3.2 Pulse Dispersion

The interstellar medium, with its free electrons, constitutes a dispersive medium, that is one in which the velocity of propagation of waves is a function of frequency. As the pulses propagate, they are dispersed by the ionized content of the interstellar medium between the pulsar and the earth. This causes delays in the time of arrival of pulses at two different observing frequencies. The delay in time of arrival of pulses at two different observing frequencies is directly measurable as the dispersion measure (*DM*) of the pulsar.

From equation (2.8) one notes that $\mu < 1$. It follows therefore that the group velocity of a propagating wave, $v_{\mathrm{g}} = c\mu$ is less than the speed of light, c. Consequently, the propagation of a radio signal along a path of length d from the pulsar to earth will be delayed in time with respect to a signal of infinite frequency by an amount, t given (e.g. Lyne and Smith, 1998) by

$$t = \left(\int_0^d \frac{dl}{v_g} \right) - \frac{d}{c} \ . \tag{2.10}$$

Substituting $v_{\rm g} = c\mu$ and noting that $f_{\rm p} << f$ in approximating μ, we have (e.g. Lyne and Smith, 1998)

$$t = \frac{1}{c} \int_0^d \left[1 + \frac{f_{\rm p}^{\,2}}{2 f^2} \right] dl - \frac{d}{c} = \frac{{\rm e}^2}{2\pi m_{\rm e} c} \frac{\int_0^d n_{\rm e} dl}{f^2} \equiv D \times \frac{DM}{f^2}, \tag{2.11}$$

where the dispersion measure, DM is given (e.g. Guélin, 1973) by

$$DM = \int_0^d n_{\rm e} dl \ , \tag{2.12}$$

in units of $\rm cm^{-3}pc$ and the dispersion constant, D given (e.g. Lorimer and Kramer, 2005) by

$$D \equiv \frac{e^2}{2\pi m_{\rm e} c} \ . \tag{2.13}$$

However, it has been shown that, the time delay (Δt) between pulses at two different observing frequencies, f_1 and f_2 is generally given (e.g. Lyne and Smith, 1998) by

$$\Delta t \approx 4.15 \times 10^3 \ \left(f_1^{-2} - f_2^{-2} \right) \times DM. \tag{2.14}$$

From a measurement of the pulsar arrival time at two or more different observing frequencies, the *DM* along the line of sight to the pulsar can be estimated. The *DM* then can be used to estimate the distance to a pulsar by integrating equation (2.12) for an assumed model of the galactic electron density distribution (n_e) as (e.g. Taylor and Cordes, 1993):

$$d = \frac{DM}{\langle n_e \rangle}, \tag{2.15}$$

where d is the distance to the pulsar and $\langle n_e \rangle$ is the average interstellar electron density along the line of sight.

2.3.3 Scintillation

In addition to being magnetized and ionized, the ISM is highly turbulent and inhomogeneous in electron density distribution. These irregularities in electron content produce phase modulations on the propagating pulsar signal, which cause the observed intensity to fluctuate on a variety of bandwidths and timescales (Lyne and Rickett, 1968). This phenomenon is referred to as scintillation. This effect is similar to the familiar optical ñtwinklingò of stars in visible light caused by density fluctuation in the earthôs atmosphere (Rickett, 1990). Radio scintillation can be observed due to the ionized plasma contained in the solar wind (Lyne and Smith, 2012). Radio waves also undergo scintillation as they pass through the local interstellar medium (LISM). Pulsar scintillation was recognized first as strong intensity modulations in pulsar observations by Lyne and Rickett (1968). Pulsar scintillation is usually divided into two regimes namely refractive and diffractive scintillation (Lyne and Smith, 2012). Large-scale (10^{11} - 10^{13} cm) irregularities would produce focusing and defocusing of the entire ray bundle observed as a refractive scintillation over broad frequency-band (a few GHz) and long timescales (~ weeks). Small-scale (10^{9} - 10^{11} cm) electron density irregularities in the interstellar medium would produce interference among rays in a ray bundle observed as diffractive scintillation over narrow frequency-band (~ I MHz) and short timescales (~ minutes). Rapid variability of this observable has long been interpreted as diffractive interstellar scintillation (Scheuer, 1968). Slow variability has been ascribed to an interstellar propagation process also (Sieber, 1982). Rickett *et al*. (1984) proposed that refractive interstellar scintillation could be from the same turbulence spectrum that causes diffractive scintillation. The resulting scintillation of the radio waves can be used to reconstruct information about the small scale variations in the ISM (Rickett, 1990). Due to the high velocity (up to several hundred km/s) of many pulsars, a single pulsar scans the ISM rapidly, resulting in changing scintillation patterns over timescales of a few minutes (Rickett *et al*., 1997).

The basic theory of scintillation was developed by Scheuer (1968) who modeled the turbulent ISM as a thin screen of irregularities midway between the earth and the pulsar as shown in Figure 2.1. The initially spatially coherent electromagnetic radiation from the pulsar is distorted by a thin screen of irregularities of various scales. The resulting randomly distorted waves are bent by an angle θ_s forming a scatter-broadened image of radius θ_d. Scintillation is produced as the randomly distorted wave-fronts form an interference pattern at the location of a distant observer. By considering the phase perturbations produced by such a screen, Scheuer

(1968) demonstrated that the intensity fluctuations over a characteristic scintillation bandwidth, Δf is given by

$$\Delta f \propto f^4 . \qquad (2.16)$$

The frequency and time bandwidths of pulsar intensity scintillation can be used to estimate the velocity of the pulsar itself. The different distance dependences of velocities derived from astrometric proper motion ($v \propto d$) and estimated from scintillation ($v \propto d^{1/2}$) can provide the true velocity and distance of the pulsar (Chatterjee *et al*., 2003).

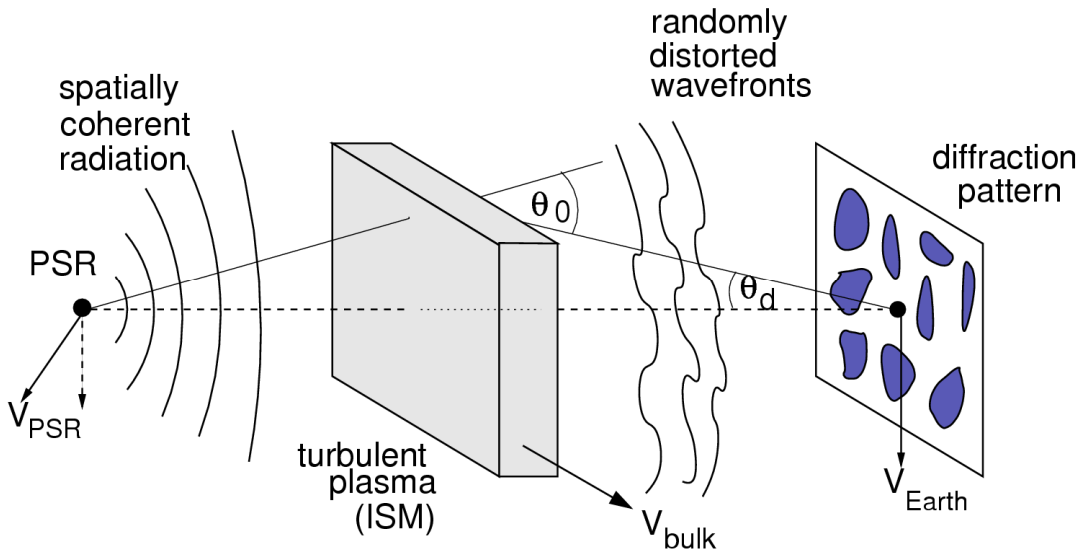

Figure 2.1: The PSRs thin screen (Scheuer, 1968).

2.3.4 Scattering

Electromagnetic radiation equally scatters as it propagates through an ionized medium. Turbulence in the interstellar gas causes density inhomogeneities in the ISM which cause scattering of the radio waves from the pulsar. Scattering effects are created by free electron inhomogeneities in the ISM (Amstrong *et al*., 1995). This effect causes the broadening of the pulse profile shape. The pulse broadening is attributed to the random refraction the waves experience while propagating through the ISM. This temporal broadening of the narrow pulsar pulses by a time Ű has been observed (Rankin *et al*., 1970; Lang, 1971; Komesaroff *et al*., 1972) and has been found to follow a f^{-4} radio frequency dependence, as predicted by several authors (Scheuer, 1968; Salpeter, 1969). In the thin-screen model, this effect can be related directly to the variable path lengths and, hence, arrival times of the pulses as they are scattered by irregularities in the ISM. As a result, there is a delayed arrival of the scattered rays that combine to broaden an otherwise intrinsically narrow pulse shape. This effect introduces significant uncertainty in measurement of pulse times of arrival.

The random density variation in the ISM causes the signals to travel many different paths as they are refracted. When a signal takes a bent path, it travels a longer distance to the telescope and thus the signal will arrive latter. Averaging over all paths taken as the approximate effect of convolving the intrinsic pulse with an exponential decay of scattering time-scale (Ű) predicts the pulse broadening (Lyne and Smith, 1998). The value of Ű depends on the radio frequency and the statistical properties of the medium through which the signal traveled. Bhat *et al*. (2004) showed that measurements of τ for a large sample of pulsars correlated strongly with *DM* as shown in Figure 2.2. More distant pulsars with larger *DM* s are in general, more likely to be scattered (Lorimer and Kramer, 2005). When searching for pulsars, this effect is highly undesirable since the scattering effectively stretches the true narrow pulse shape which result in a reduction in the signal to noise ratio.

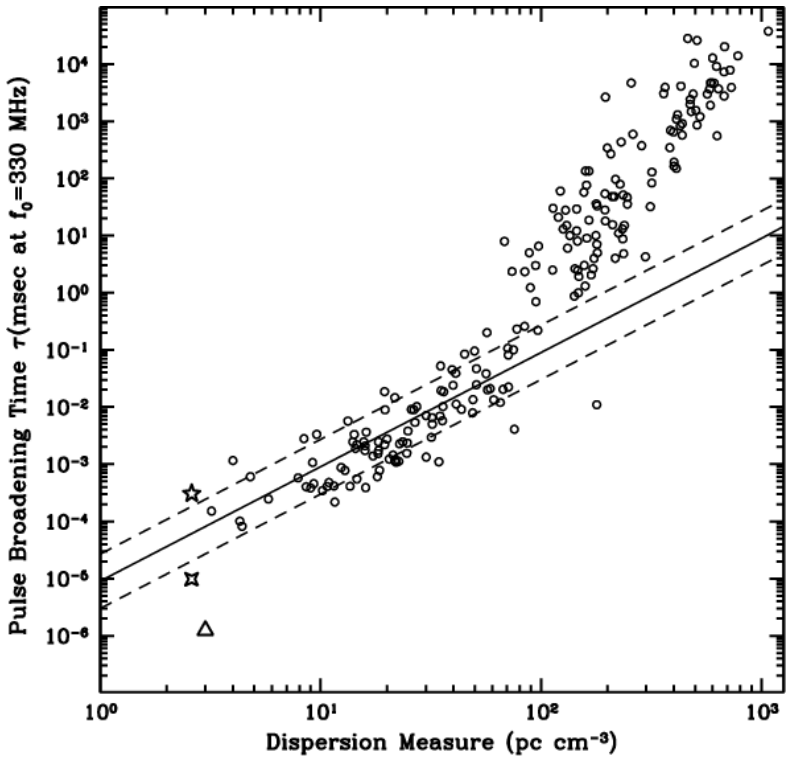

Figure 2.2: Pulsar scatter-broadening times as a function of dispersion measure (Bhat *et al*., 2004).

)03), the pulsar is a distance *d* from the observer. A ray emerging from the pulsar at an angle θ_o intersects the screen (i.e. a distance d_s from the pulsar) and is scattered by some mechanism through an angle θ_{scatt} towards the telescope. The observed angle is $\theta = \theta_{scatt} - \theta_o$.

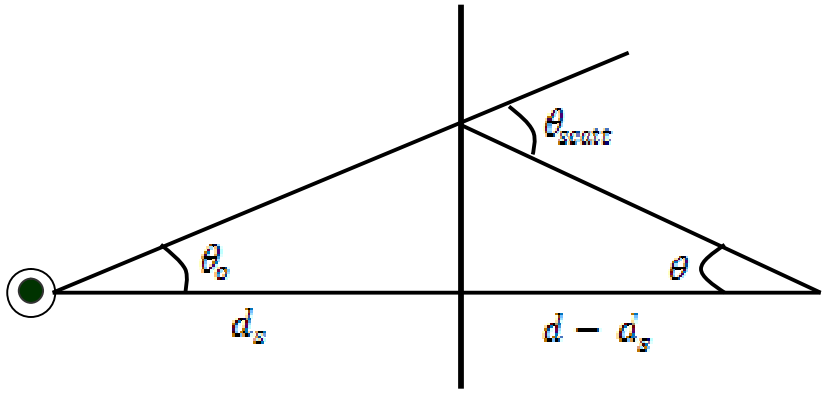

Figure 2.3: The geometry of scattering (Hill *et al*., 2003).

2.3.5 Faraday Rotation

The presence of a magnetic field together with free electrons in the ISM causes Faraday rotation which changes the orientation of the electric fieldôs polarization vector (Han *et al*., 2006). Faraday rotation is the rotation of the plane of polarization of linearly polarized signal as it passes through the ionized and magnetized plasma. The frequency-dependent delay of the signal can be expressed in terms of phase rotations. Compared to a pulse observed at infinite frequency, the pulse phase at a frequency f, is observed to lag in phase by an amount given (e.g. Lorimer and Kramer, 2005) by

$$\Delta\psi = -kd \ , \tag{2.17}$$

where $k = 2\pi/\lambda$ is the wave number and λ is the wavelength. For a cold magnetized plasma, the wave number as a function of frequency is given (e.g. Lyne and Smith, 1990) by

$$k(f) = \frac{2\pi}{c}\mu f = \frac{2\pi f}{c}\sqrt{1 - \frac{f_p^2}{f_p} \mp \frac{f_p^2 f_B}{f^3}} \ , \tag{2.18}$$

where f_p is the plasma frequency, f is the observing frequency, μ is the refractive index and f_B is the cyclotron frequency, which is given (e.g. Lyne and Smith, 1990) by

$$f_B = \frac{eB_{\|}}{2\pi m_e c} \ , \tag{2.19}$$

where $B_{\|}$ is the galactic magnetic field along the line of sight, e and m_e are the charge and mass of an electron, respectively. The galactic magnetic field along the line of sight, $B_{\|}$ can be computed from the cyclotron frequency. On assumption that, $B_{\|} \sim 1$ εG, one expects $f_B \sim 3$ Hz for the ISM.

The last term in equation (2.18) reflects the different propagation speeds for the left (upper ñ− õô sign) and right (lower ñ+ò sign) circularly polarized waves in a magnetized medium. The time corrections to the group velocity for an unmagnetized medium are Ò1 ns and, hence, negligible. However, this minute difference in propagation speeds is the cause of Faraday rotation. The differential phase rotation between left and right circular polarizations is given (e.g. Lyne and Smith, 1998) by

$$\Delta\psi_{\text{Faraday}} = \int_0^d \left(K_{\text{R}} - K_{\text{L}}\right) dl\,, \tag{2.20}$$

where K_{L} and K_{R} are the wave number of the left and right circularly polarized wave respectively. Since $f >> f_{\text{p}}$ and $f >> f_{\text{B}}$, then, it can be shown (e.g. Lyne and Smith, 1998) that

$$\Delta\psi_{\text{Faraday}} = \frac{\text{e}^3}{\pi \text{m}_{\text{e}}^2 c^2 f^2} \int_0^d n_e B_{\parallel} dl\,. \tag{2.21}$$

In addition, as the polarization position angle (PPA) is periodic on ´ rather than 2´, the change in PPA can be expressed (e.g. Noutsos *et al*., 2008) as

$$\Delta\psi_{\text{PPA}} = \psi_{\text{Faraday}} / 2 \equiv \lambda^2 \times RM\,, \tag{2.22}$$

where *RM* (expressed in radm^{-2}) is the rotation measure given (e.g. Noutsos *et al*., 2008) by

$$RM = \frac{e^3}{2\pi m_{\text{e}}^2 c^4} \int_0^d n_{\text{e}} B_{\parallel} dl\,. \tag{2.23}$$

An observable property of the above magneto-optical interaction is that for a particular pulsar, the higher the wavelength, the greater the effect of Faraday rotation, with infinitely waves of small wavelength being unaffected. The measurement of both *RM* and *DM* gives the average magnetic field strength along the line of sight weighted by electron density $\langle B_{\parallel} \rangle$, which is expressed (e.g. Lorimer and Kramer, 2005) as

$$\langle B_{\parallel} \rangle \equiv \frac{\int_0^d n_e B_{\parallel} dl}{\int_0^d n_{\text{e}} dl} = 1.23 \varepsilon \text{G} \left(\frac{RM}{\text{radm}^{-2}}\right)\left(\frac{DM}{cm^{-3} pc}\right)^{-1}. \tag{2.24}$$

The electron density, n_e is not homogenous throughout the galaxy. Regions of enhanced electron density (e.g. HII regions along the line of sight) produce an unequal weighting and can contribute significantly to the measurement of $\langle B_{\parallel} \rangle$. Also, if the direction of the magnetic field changes, the average value, $\langle B_{\parallel} \rangle$ is a poor reflection of the true situation. Due to paucity of data for the scintillation and scattering effect, we shall concentrate mainly on dispersion measure and rotation measure for our study.

2.4 Dispersion Measures

Radio waves produced by a pulsar interact with the free electrons in the ISM causing the waves to travel at frequency dependent velocities. Because of the dispersive nature of the interstellar plasma, lower frequency radio waves travel through the medium slower than higher frequency radio waves. In this case, the delay in pulse arrival times is inversely proportional to the observing frequency. The resulting delay in the arrival of pulses at a range of frequencies is directly measurable as the dispersion measure of the pulsar. By measuring the variation with time in the delay, the electron - density variations in the interstellar medium can be measured. Most pulsar distances are estimated from their dispersion measures by assuming a value for the average interstellar electron density (Hewish *et al*., 1968, Lyne and Rickett, 1968; Taylor and Cordes, 1993). The general assumption of a uniform medium with an electron density of 0.1 cm^{-3} has been criticized (Habing and Pottasch, 1968; Shutter *et al*., 1968) as being too high. Manchester *et al*. (1969) showed that the assumption of a uniform interstellar medium is not realistic and that a multi-component medium is more appropriate when interpreting pulsar observations. Davidson and Terzian (1969a) and Terzian (1972b) concluded from statistical studies of dispersion measures that the average electron density in the interstellar medium is ~ 0.03 to 0.04 cm^{-3}.

Precise model-independent measurements of distances to pulsars are rare, yet they are invaluable resources with which to study the interstellar medium. Knowledge of accurate distances and dispersion measures provides valuable information on the mean electron density in interstellar medium (Guélin, 1973). Independent pulsar distance measurements can be achieved through HI absorption or parallax measurements. For CP 0328 and NP 0531 distances of 0.8 kpc and 2.0 kpc, both correspond to about 0.03 electrons per cm^3 (Guelin *et al*., 1968; Gordon *et al*., 1969; DeJager *et al*., 1969, Trimble, 1968). Manchester *et al*. (1969) have redetermined the dispersion measure for PSR 0833-45 and found it to be ~ 69 cm^{-3}pc, some what higher than that suggested by previous measurements (Radhakrishnan *et al*., 1969). For a distance of 500 pc, the electron density would be 0.14 cm^{-3} for a uniform medium. However, the line of sight to PSR 0833-45 passes through the Gum Nebula, the largest known nebula in our galaxy. Encrenaz and Guélin (1970) computed a lower limit to the mean electron density (n_e) in the direction of the pulsar to be < 0.015 cm^{-3}. This is significantly smaller than a value of ~ 0.03 cm^{-3} usually

assumed for the interstellar medium. From the study of pulsarsô dispersion measure and the mean and mean-squared interstellar electron density, Gould (1971) found that the electron density in the galactic plane is ~ 0.12 cm^{-3}, which is considered to be too high when compared to a value of ~ 0.03 cm^{-3} usually assumed for the interstellar medium.

From the study of ISM using pulsars, Guélin (1973) found that pulse polarization and time of arrival measurements indicate a relatively uniform magnetic field of about 3 µG, whereas new distance measurements through 21-cm line absorption indicate an electron density of about 0.03 cm^{-3}, which is uniform when averaged over large distances (Ó kiloparsec). Gordon and Gordon (1973) studied measurements of neutral-hydrogen absorption in the spectra of eight pulsars and found a value for the mean ISM electron concentration $\langle n_e \rangle \approx 0.04$ cm^{-3}. This estimate is based on distances of one-half the upper limit, or the arithmetic mean of upper and lower limits (and arbitrarily d = 9 kpc for PSR 1933+16). The inclusion of three pulsars (PSR 0736-40, 0740-28, and 0833-45) inside or behind the Gum Nebula, a local giant Hll region, only increased the estimate to $\langle n_e \rangle \approx$ 0.05 cm^{-3}.

Gómez-Gonzàlez and Guélin (1974) showed that the electron density averaged over any path longer than 1.5 kpc in the solar neigbourhood is very close to 0.03 cm^{-3}. Distant pulsars are scattered over a large range of galactic longitude, $\langle n_e \rangle$ towards these sources was found to be in the range of ~ 0.015 and 0.06 cm^{-3}. The large-scale averaged electron density in the solar neighbourhood thus appears to be roughly uniform and of the order of 0.03 cm^{-3} even in the distant parts of our galaxy. Terzian and Davidson (1976) found from the study of pulsarsô observational parameters and dispersion measures that the range of the electron densities in the diffuse ISM is 0.01 $cm^{-3} \leq n_e <$ 0.1 cm^{-3} and $\langle n_e \rangle \cong$ 0.03 cm^{-3}.

For a measured distance of 1.2 kpc from annual trigonometric parallax and a DM of 27.31 cm^{-3}pc (Philips and Wolszczan, 1992), the derived mean electron density toward B0919+06 is 0.023 cm^{-3}. This line of sight is along the same galactic longitude as the supper bubble proposed by Heiles (1998), as well as clouds of ionized gas in the local neighbourhood (Dupin and Gry, 1998), though at a higher galactic latitude. Annual trigonometric parallax measurement of PSR J1744-1134 yielded a mean electron density in the path to the pulsar, n_e = 0.0088 ± 0.0009 cm^{-3} which is the lowest for any disk pulsar close to the galactic equator (Toscano *et al*., 1999). Their result showed that the ionized regions are associated with

interaction at the boundary between the Local Hot Bubble (LHB) and the more distant superbubble.

Other methods have been used to estimate n_e in the ISM. Gordon and Gottesman (1971) obtained a mean rms electron density of approximately 0.15 cm^{-3} in the interstellar medium from recombination lines of hydrogen at 18 cm in the galactic plane. This density is considerably larger than those permitted by the theoretical model of Field *et al*. (1969) based upon ionization by soft cosmic rays. The density is not inconsistent with observations of pulsars within 2 kpc of the sun (Hjellming *et al*., 1969) nor with the 10 MHz absorption of radio sources (Bridle, 1969) because the velocity extent of the recombination lines implies that the ionization is low in these regions. Gordon and Gottesman (1971) observations show that the experimental parameters used for these theoretical models may be different in the inner region of the galaxy and hence these models may not be valid there. Additional observations are required to explore the extent of the ionization with galactic longitude and latitude.

The ratio of the magnesium ionization stage column densities N(MgII)/N(MgI) has been used to compute an electron density of $n_e \approx 0.2$ ï 0.4 cm^{-3} toward Sirius, for an assumed LISM temperature of 7000 K (Frisch *et al*., 1990; Lallement *et al*., 1994; Frisch, 1994; Lallement and Ferlet, 1997). Larger MgII/MgI ratios have been measured toward ‘ CMa and ŭ Cas, suggesting densities of $n_e = 0.09^{+0.23}_{-0.07}$ cm^{-3} and n_e = 0.11 ï 0.50 cm^{-3} respectively (Gry *et al*., 1995; Lallement *et al*., 1996). However, this technique suffers from the requirement of ionization equilibrium and a strong temperature dependence unlike the ratio of the collisionally excited carbon line column density to the resonance line column density which can provide n_e estimates without the need for ionization equilibrium and has a very weak temperature dependence. However, due to the weakness of the excited carbon II (CII*) absorption and saturation of the only available UV ground state carbon II (CII) resonance line, few local interstellar medium (LISM) lines have been analyzed using this technique. The excited absorption along other LISM sight lines has been measured at moderate resolution (R ~ 20,000) with Copernicus (York and Kinahan, 1979) and the Far Ultraviolet Spectroscopic Explorer (FUSE; Lehner *et al*., 2003), although typically individual absorbers are not resolved, so the estimates are of average measurements.

Lallement *et al*. (1993) found n_p å n_e = 0.06 ï 0.10 cm^{-3} from the observed 5 ï 6 kms^{-1} decrease in velocity of HI atoms at the heliospheric interface, where n_p is the number of proton

density. This result however is dependent on the accuracy of heliospheric models. Wood and Linsky (1997) used high spectra resolution spectra of nearby star system capella to calculate n_e = $0.11^{+0.12}_{-0.06}$ cm^{-3} along the line of sight from the ratio of CII*/CII (where CII* is the excited carbon II and CII is the ground state carbon II) and demonstrated that the relatively simple absorption profiles through the LISM provide an excellent opportunity to make precise measurement of the electron density. Holbery *et al*. (1999) estimated the number of electron density, (n_e = $0.11^{+0.07}_{-0.06}$ cm^{-3}) from the population ratio of the excited to ground state fine-structure levels in CII using high resolution spectra of the hot DA (where DA is hydrogen-dominated atmosphere) white dwarf REJ 1032+532. Redfield and Falcon (2008) found that the distribution of measured LISM electron densities using the CII*-to-CII ratio is consistent with a lognormal profile, with an unweighted mean value of n_e (CII_{SII}) = $0.11^{+0.10}_{-0.05}$ cm^{-3}. The distribution of electron densities based on using silicon II (SII) as a proxy for CII is similar to the distribution based on carbon alone, while significantly tighter and proves to be a more promising technique to avoid grossly overestimating the CII column density based on the saturated line profile. This is a strong endorsement for using SII as a proxy for CII, in order to make more accurate electron density measurement. All electron densities derived using SII as a proxy range from 0.07 to 0.80 cm^{-3}.

2.5 Rotation Measures

Rotation measure is an important tool for the investigation of magnetic field strength of the ISM using radio pulsars. Measurement of accurate values of rotation measure provides reliable estimates of the galactic magnetic field. Extragalactic sources give data for the global magneto-ionic medium while pulsars trace the medium within a few kpc from the sun. Pulsars have no intrinsic rotation measures while that of extragalactic sources can be quite dominant. Prior to the discovery of pulsars, only the Zeeman splitting effect seen in HI absorption lines was able to give quantitative values for the magnetic field strength of the interstellar medium. These observations have been successful in several radio sources having deep absorption lines (Verschuur, 1969a), but they give the magnetic field strength in the absorbing HI cloud rather than in the general interstellar medium (Verschuur, 1969b). Measurements of the polarization of starlight give the direction of the field component perpendicular to the line of sight. This gives a poor reflection of the true situation as a result of change in the direction of the magnetic field.

By combining the deduced rotation measures and dispersion measures, several observers have estimated the longitudinal component of magnetic field in pulsar lines of sight (Smith, 1968; Ekers *et al*., 1969; Radhakrishnan *et al*., 1969; Staelin and Reifenstein, 1969). Large *et al*. (1968), Ekers *et al*. (1969) and Radhakrishnan *et al*. (1969) estimated an interstellar magnetic field of ~ 0.8 μG using data on Vela pulsar (PSR B0833-45). This represents a mean value for the field component weighted by the electron concentration along the line of sight to the pulsar. If the field is not well ordered, typical values of the interstellar field may be much large. Verschuur (1969a) obtained field strength of the order of 10 μG in dense HI clouds and suggested that such large values could be a consequence of field amplification as the HI clouds contract. For PSR B0833-45, there is no dense HI cloud in the path and so the values of 0.8 μG might represent, to first order, the unamplified local field in the direction of the pulsar concerned. The absence of absorption feature in the spectrum of PSR B0833-45 suggests that the measured magnetic field of 0.8 μG represents the order of the unamplified local galactic field (Manchester *et al*., 1969).

The Faraday rotation measurements for the pulsar CP 0950 at a frequency, з = 151 MHz yields a remarkably small value of ɣ, which corresponds to a field $\bar{H} < 0.2$ εG (Smith, 1968). This result has been interpreted as a peculiar value for the magnetic field in the direction of the pulsar concerned. From a statistical study of Faraday rotation in pulsars, Staelin and Reifenstein (1969) found 36 ± 5 and 63 ± 5 radm^{-2} as the magnitudes of the rotation measures for pulsars NP 0527 and CP 0328, respectively. These correspond to mean longitudinal galactic magnetic field of 0.9 μG and 2.8 μG, respectively. The indicated uncertainty is dominated by the uncertainty in the ionospheric contributions. The average density of thermal electrons in the galactic plane is about 0.03 cm^{-3} and the average of the regular magnetic field along the line of sight is about 1 to 2 μG (Taylor and Cordes, 1993; Goméz *et al*., 2001). Wolleben and Reich (2003) found that further observational constraints from Hα observations limit the thermal electron density to less than 0.8 cm^{-3} and concluded that the regular magnetic field strength parallel to the line of sight exceeds 20 μG to account for the observed intrinsic rotation measure.

CHAPTER THREE

MATERIALS AND METHODS

3.1 Source of Data

A total of 667 pulsars with known rotation measure and dispersion measure values were selected from the Australia Telescope National Facility (ATNF) pulsar catalogue[2] (Manchester *et al*., 2005). Most of the pulsars in the catalogue have known dispersion measure values while few are associated with rotation measure values. The rotation measure values of 104 pulsars from the ATNF pulsar catalogue were replaced with the new and more accurate values published by Noutsos *et al*. (2008). One pulsar (J1507ï 6604) with a new rotation measure value in Noutsos *et al*. (2008) sample was included in our sample, increasing the sample to 668 pulsars. The dispersion measure (*DM*), rotation measure (*RM*), pulsarsô rotation period (P), period derivative ($\dot{P}$), characteristic age (τ_c), surface magnetic field (B) and the radio pulsar distance from the galactic plane (Z) for the 668 pulsars were taken from the ATNF pulsar catalogue. The sample is heterogeneous, consisting of 39 recycled millisecond pulsars and 629 normal pulsars. All objects have positive *DM* values, while 358 and 310 pulsars have positive and negative *RM* values, respectively. The absolute values of pulsarsô rotation measure were used since we are interested in the magnitude of the rotation measure.

To investigate for any relationship between the time rate of change/time derivative of *DM* (dDM/dt) and interstellar medium parameters (*DM* and *RM*) as well as the spin-down parameters (P , $\dot{P}$, τ_c and B) of radio pulsars, a total of 349 pulsars with known time rate of change of *DM* (dDM/dt) and dispersion measure (*DM*) values were selected from Hobbs *et al*. (2004) sample. The sample of 349 pulsarsô rotation period, period derivative, characteristic age and surface magnetic field were taken from the ATNF pulsar catalogue. Pulsars with positive time rate of change of *DM* were separated from those with negative time rate of change of *DM*. A total of 175 pulsars have positive time rate of change of *DM* while 174 pulsars are associated with negative time rate of change of *DM*. The logarithm of a negative value does not exist and as such, the absolute values of pulsarsô time rate of change of *DM* were used, since we are interested in the logarithmic values due to the wide spread (~ 3 orders of magnitude) in the

[2] www.atnf.csiro.au/research/Pulsar/Psrcat

parameters values. Not all the 349 pulsars with known time rate of change of *DM* have measured rotation measure values. Therefore, all the pulsars with measured values of time derivative of *DM* and rotation measure were sorted out from both samples (i.e. sample of 349 pulsars and sample of 668 pulsars). A total of 266 pulsars have known time rate of change of *DM* and rotation measure values from the literature.

3.2 Data Analysis and Results

The statistical analysis technique employed in the analysis of current data involves the simple descriptive and regression methods. Simple descriptive method is used to describe the distribution of parameters in a sample of data. It is used for frequencies, averages, modes, ranges and other statistical calculations. This method cannot describe what caused a situation and as such cannot be used to as the basis of a relationship, where one variable affects another. In other words, simple descriptive method can be said to have a low requirement for internal validity. Simple regression method is a statistical process for estimating the relationships between variables. This method is widely used for prediction and forecasting. It is also used to understand which among the independent variables are related to the dependent variable and to explore the forms of their relationships. This method enables one calculate the correlation coefficient *r,* which provides the strength of correlation between parameters. The input data used in data analysis and results are the dispersion measure (*DM*), rotation measure (*RM*), pulsarsô rotation period (P), period derivative ($\dot{P}$), characteristic age (τ_c), surface magnetic field (B) and the radio pulsar distance from the galactic plane (Z). In view of wide spread (~ 3 orders of magnitude) in the parameters values, only the logarithm of the parameters was considered.

3.2.1 Simple Descriptive Analysis

This involves the plotting of the parameters (both ISM and pulsar spin-down parameters) on the parameter plane in other to appreciate their distribution.

The distribution of the measured dispersion measure (*DM*) of the 668 radio pulsars is shown in Figure 3.1 (a). Evidently, the spread in the parameter is ~ 2 orders of magnitude (~ 2 ï 1100 $cm^{-3}pc$) with a mean value of ~ 181 $\pm$ 7 $cm^{-3}pc$. Apparently, the distribution is skewed towards the lower values with ~ 440 (~ 66 %) of the objects having *DM* value below the mean value. The distribution is unimodal and follows a lognormal distribution.

Similarly, the distribution of the magnitude of rotation measure ($|RM|$) of the 668 radio pulsars is shown in Figure 3.1 (b). The rotation measure ranges from ~ -3000 ï 2400 radm^{-2}. This is a wide spread (~ 2 orders of magnitude) with a mean value of ~ 157 ± 10 radm^{-2}. The distribution of *RM* (irrespective of sign) is skewed towards the left side of the mean value (i.e the lower values of the parameter) with ~ 484 (~ 70%) of the objects having $|RM|$ value below the mean value. The distribution is unimodal and follows a lognormal distribution.

The distribution of the 665 radio pulsarsô distance from the galactic plane (Z) is shown in Figure 3.2. Due to selection effect, three pulsars (J0045-7319, J0529-6652, J1543+0929 with Z values = -43.19, -29.06, 4.23 kpc, respectively) with extreme values of Z were excluded from the sample of 668 pulsars in other to appreciate the distribution. The distance of pulsars from the galactic plane ranges from ~ -2 ï 2 kpc with a mean value of ~ 0.43 ± 0.02 kpc. The distribution is multimodal and symmetric about the mean value. Evidently, about ~ 350 (> 50%) of the pulsars in the sample are found between -0.3 Ò Z Ò 0.3 kpc. These pulsars are believed to be young pulsars and are concentrated within the galactic plane (Z = 0), which is the birth place of pulsars. Again there is bunching of pulsars (~ 56 number of them) farther away from the galactic plane (i.e at $|Z|$ ~ 2 kpc). These pulsars have characteristic age between the range of about 10^5 and 10^8 yr and are believed to be middle-aged pulsars (normal pulsars). Pulsars are born within the galactic plane and as they get old, they tend to move farther away from the galactic plane (Terzian and Davidson, 1976).

Figure 3.3 is the distribution of the period derivative ($\dot{P}$) of the 668 radio pulsars. Evidently, the spread in the parameter is ~ 3 orders of magnitude (~ 3 × 10^{-21} ï 2 × 10^{-11} ss^{-1}) with a mean value of ~ (9.94 ± 0.05) × 10^{-14} ss^{-1}. Evidently, about ~ 450 (~ 67%) of the pulsars in the sample are found between 10^{-16} Ò $\dot{P}$ Ò 10^{-14} ss^{-1}. This modal range is within the spin-down rate of normal pulsars, implying that most of the pulsars in the sample are fast rotating pulsars. The distribution is bimodal, which corresponds to the existence of the two classes of objects in the sample ï normal and recycled millisecond pulsars.

Again the distribution of the characteristic age (τ_c) of the 668 radio pulsars is shown in Figure 3.4. The characteristic age is ranging from ~ 1 × 10^3 ï 5 × 10^{11} yr. This is a wide spread (~ 2 orders of magnitude) with a mean value of ~ (4.31 ± 0.09) × 10^8 yr. The characteristic age distribution has a tail at the lower value with ~ 620 (~ 93%) of the pulsars

having characteristic age below the mean value. This shows that most of the pulsars in the sample are young pulsars, which are believed to be normal pulsars. The distribution shows the expected bimodal distribution of the spin-down age, which corresponds to the existence of young and old pulsars in the sample.

Figure 3.5 is the distribution of the surface magnetic field (B) of the 668 radio pulsars. The surface magnetic field ranges from ~ 8 × 10^7 ï 3 × 10^{14} G. The parameter is characterized by a wide spread (~ 2 orders of magnitude) with a mean value of ~ (3.09 ± 0.06) × 10^{12} G. Notably, about ~ 450 (~ 67%) of the pulsars have surface magnetic field, B ~ 10^{11} ï 10^{12} G. This modal range is of the order of 10^{12} G of surface magnetic field of normal pulsars given by Lorimer and Kramer (2005). This result reveals that most of the pulsars in the sample are normal pulsars. As expected, the distribution shows a bimodal distribution.

Finally, The distribution of the rotation period (P) of the 668 radio pulsars is shown in Figure 3.6. Clearly, the spread in the parameter is ~ 2 orders of magnitude (~ 0.002 ï 9 s) with a mean value of ~ 0.69 ± 0.02 s. The rotation period distribution has a tail at the upper value with ~ 436 (~ 65%) of the pulsars having rotation period above the mean value. This implies that our sample of 668 radio pulsars is dominated with fast rotating pulsars. These pulsars are believed to be normal pulsars and they dominate the galactic population of pulsars (Lyne and Smith, 2012). It is apparent that the distribution shows the expected bimodal distribution of the rotation period, which corresponds to the existence of normal and recycled millisecond pulsars in the sample.

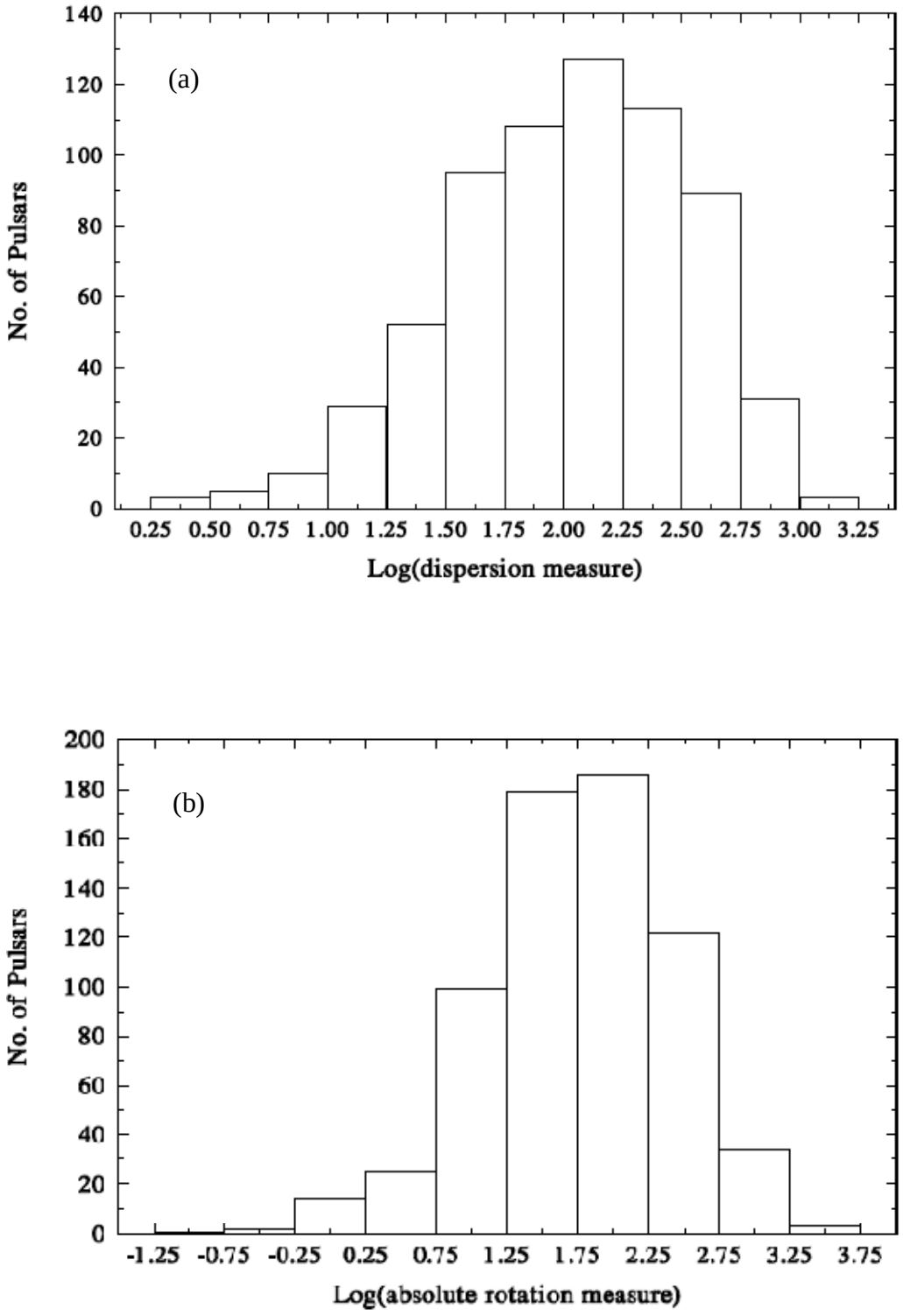

Figure 3.1: Histogram of the distribution of the dispersion measure (a) and rotation measure (b) of the 668 radio pulsars on logarithmic scales.

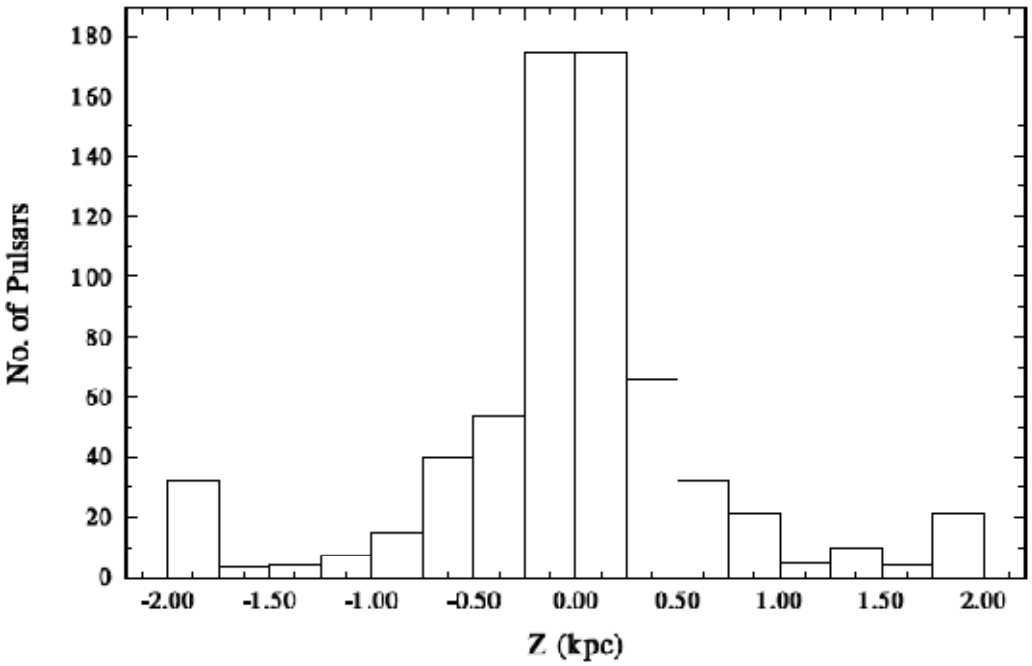

Figure 3.2: Histogram of Z – height of 665 radio pulsars from the galactic plane.

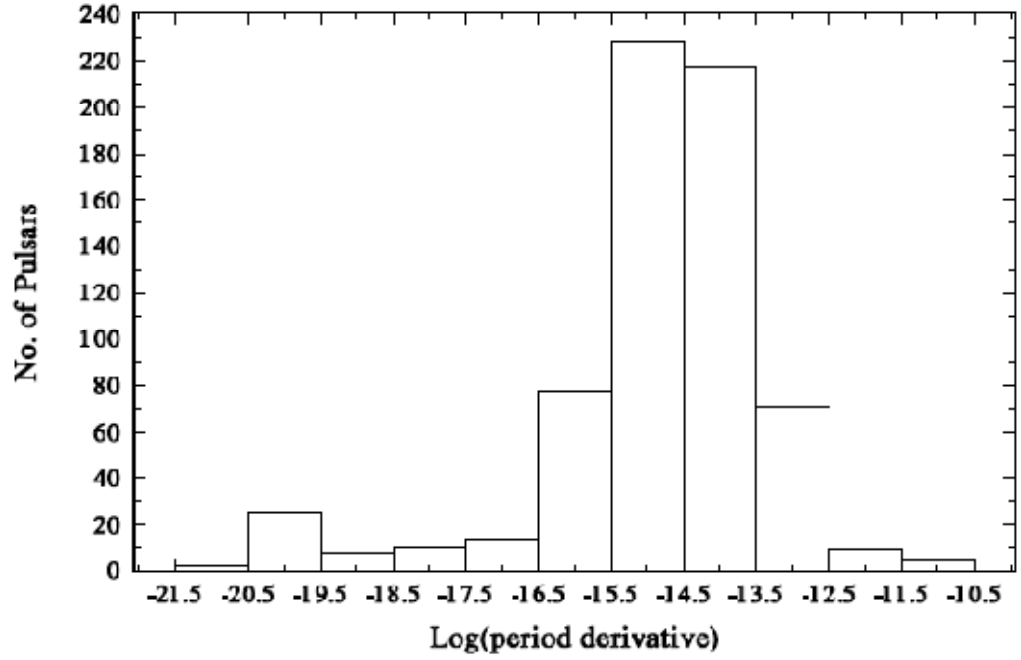

Figure 3.3: Histogram of 668 radio pulsars' period derivative on logarithmic scale.

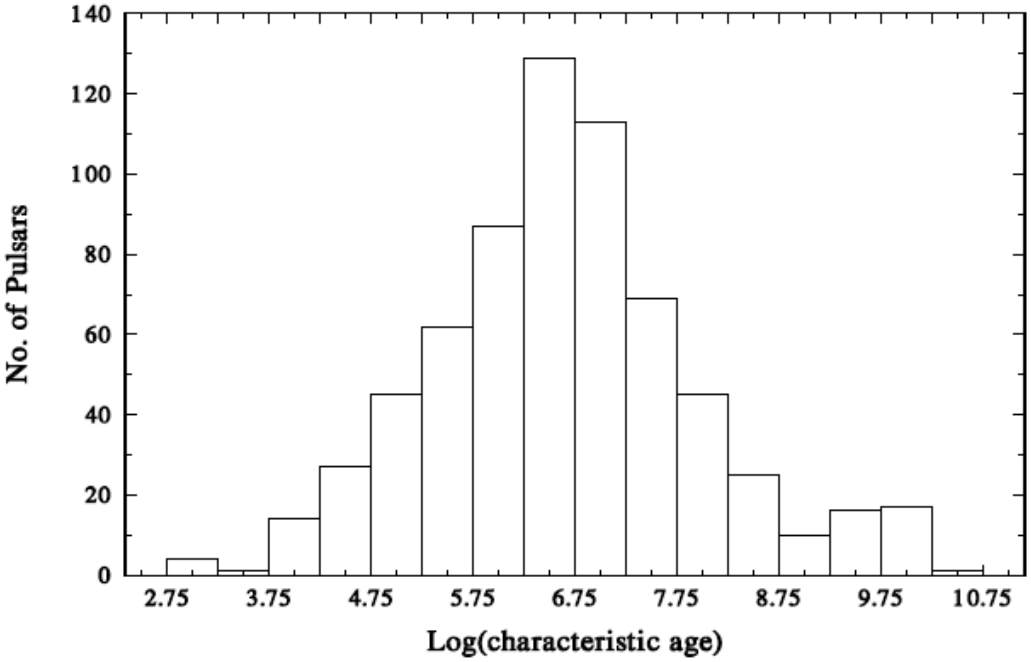

Figure 3.4: Histogram of 668 radio pulsars' characteristic age on logarithmic scale.

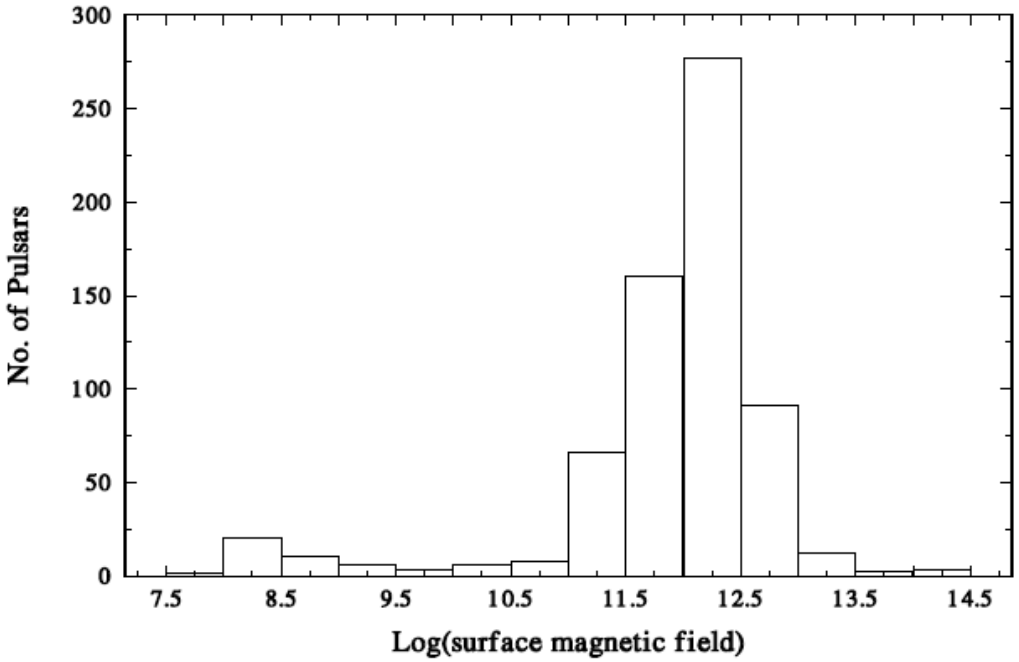

Figure 3.5: Histogram of 668 radio pulsars' surface magnetic field on logarithmic scale.

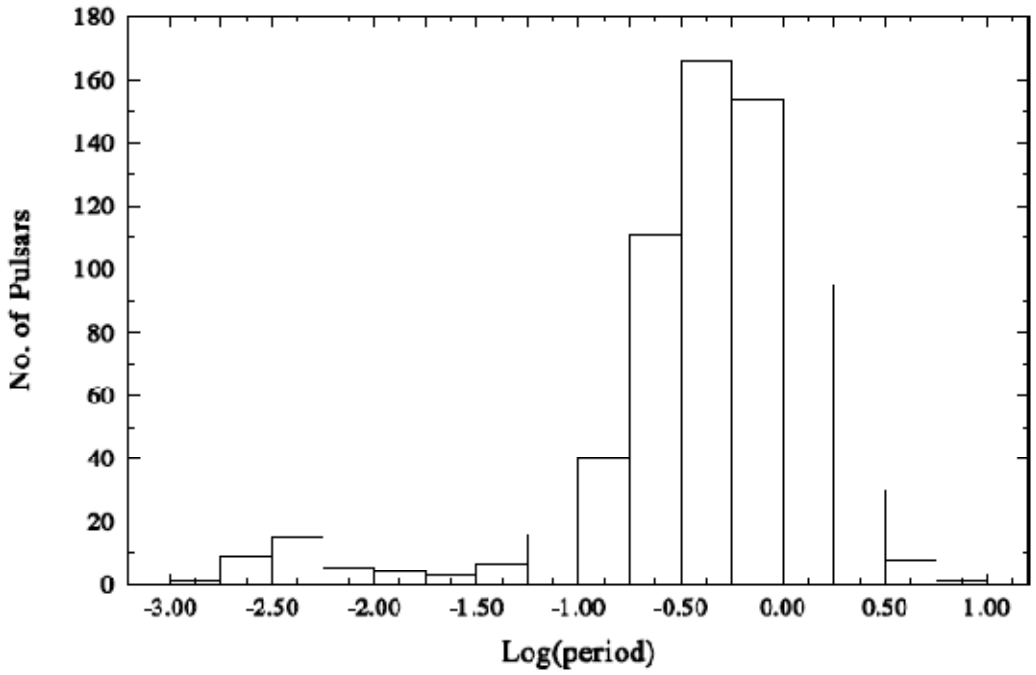

Figure 3.6: Histogram of 668 radio pulsars' rotation period on logarithmic scale.

3.2.2 Simple Regression Analysis

In this section, our analysis involves the scatter plots of the ISM parameters (*DM* and *RM*) against the pulsar spin-down parameters (P, $\dot{P}$, τ_c and B). The objective is to determine the level of dependence (if any) between these two sets of parameters, which probe different phenomena.

The scatter plot of the magnitude of *RM* against *DM* for the 668 radio pulsars on logarithmic scales is shown in Figure 3.7. A simple linear regression analysis of the data shows that they are strongly correlated (with correlation coefficient $r > 0.7$). However, the plot reveals significant scatter in the values of both parameters. In particular at lower *RM* values, the scatter in *DM* data could be up to 3 orders of magnitude. This appears to decrease as |*RM*| increases and less than an order of magnitude at $|RM| > 100$ radm^{-2}.

The scatter plots of logDM and log|RM| against the pulsarsô height from the galactic plane (Z) for the 665 radio pulsars are shown in Figures 3.8 and 3.9, respectively. It is shown that most of the pulsars in our sample are within the height of Z = ± 1. The scatter in the DM data for any given Z is quite large and could be up to 3 orders of magnitude at the galactic plane (Z = 0). However, it is striking to observe that both DM and RM (irrespective of sign) appear, on average, to increase towards the galactic plane.

Similarly, the scatter plots on logarithmic scales of DM and |RM| against radio pulsar period derivative ($\dot{P}$) for the 668 radio pulsars are shown in Figures 3.10 and 3.11, respectively. Evidently, Figures 3.10 and 3.11 are characterized by large amplitude (~ up to 3 orders of magnitude) scatter in dispersion measure and rotation measure data. However, superimposed on this scatter is a trend which suggests a relationship between the parameters, in which pulsars with large spin-down rate, on average, have large DM and |RM|. A simple linear regression analysis of the data shows that both DM and the magnitude of RM are ~ 50% correlated with the radio pulsar spin-down rate.

The scatter plots on logarithmic scales of the DM and |RM| against radio pulsar characteristic age (τ_c) for the 668 radio pulsars are shown in Figures 3.12 and 3.13, respectively. Again the Figures are characterized by a weak trend, which superimposed on large amplitude (~ up to 3 orders of magnitude) scatter in both dispersion measure and rotation measure data. It is apparent that the ISM parameters (DM and RM) are, on average, anti-correlated (with correlation coefficient r ~ -0.5) with pulsar spin-down age.

Similarly, the scatter plots on logarithmic scales of the DM and |RM| against radio pulsar surface magnetic field (B) for the 668 radio pulsars are shown in Figures 3.14 and 3.15, respectively. Evidently, Figures 3.14 and 3.15 are characterized by large amplitude (~ up to 3 orders of magnitude) scatter in dispersion measure and rotation measure data. However, superimposed on this scatter is a trend which suggests that pulsars with large surface magnetic field, on average, have large dispersion measure and rotation measure. A simple linear regression analysis of the data shows that both DM and the magnitude of RM are ~ 50% correlated with the radio pulsar surface magnetic field.

No trend was apparent in the DM ï P and |RM| ï P scatter plots of the current sample as shown in Figure 3.16 and 3.17, respectively. As expected, a simple linear regression analysis of

the DM ï P and $|RM|$ ï P data yields $r \sim 0.1$ as the correlation coefficient in each case. Table 3.1 shows the summary of correlation coefficient results.

Table 3.1: A summary of correlation coefficient, *r* results.

Parameters	Correlation coefficient, *r*	Strength of correlation
DM ï $\|RM\|$	0.7	strong
$DM/\|RM\|$ ï $\dot{P}$	0.5	moderate
$DM/\|RM\|$ ï τ_c	-0.5	moderate
$DM/\|RM\|$ ï B	0.5	moderate
$DM/\|RM\|$ ï P	0.1	weak

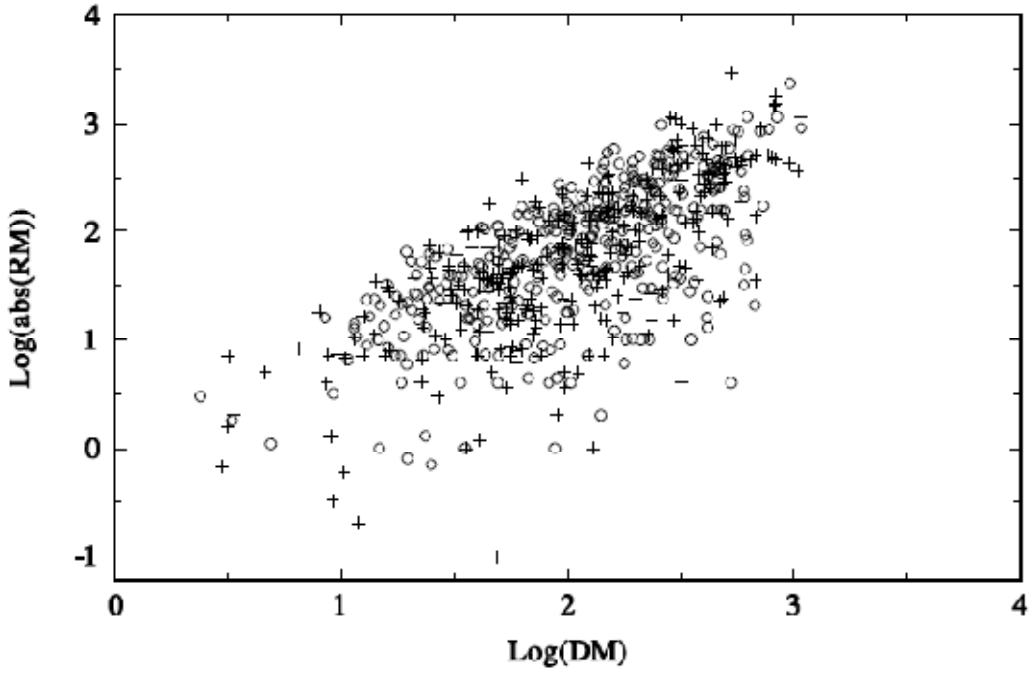

Figure 3.7: Scatter plot of the absolute values of the rotation measure (*RM*) against the dispersion measure (*DM*) on logarithmic scales for the 668 radio pulsars. Key: ○ = pulsars with +ve *RM*; + = pulsars with -ve *RM*.

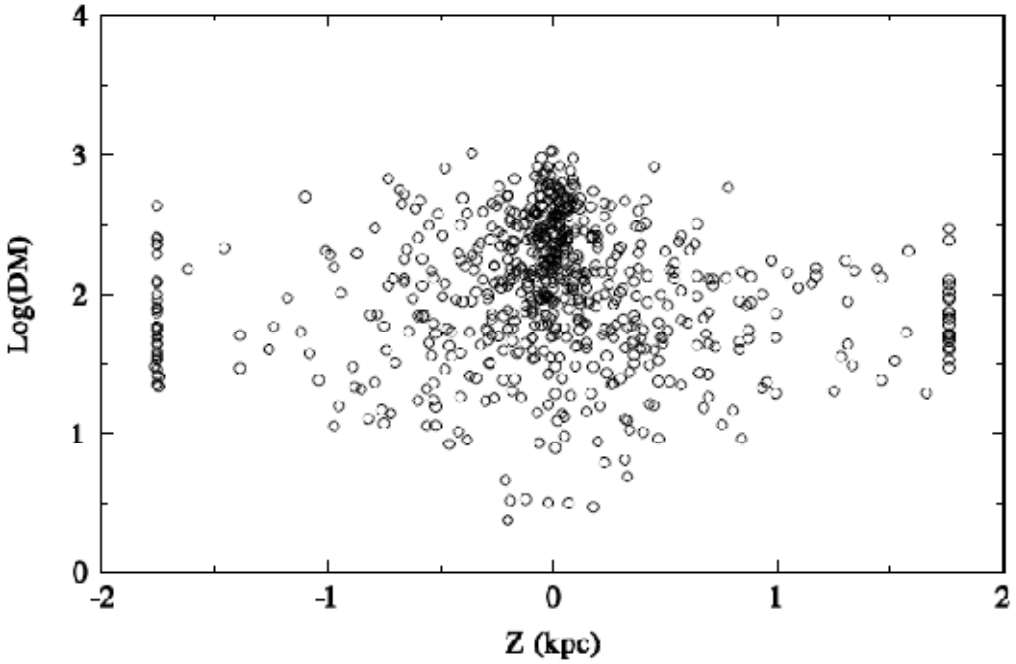

Figure 3.8: Scatter plot on Logarithmic scale of the dispersion measure (*DM*) against pulsars' distance from the galactic plane (*Z*) for the 665 radio pulsars.

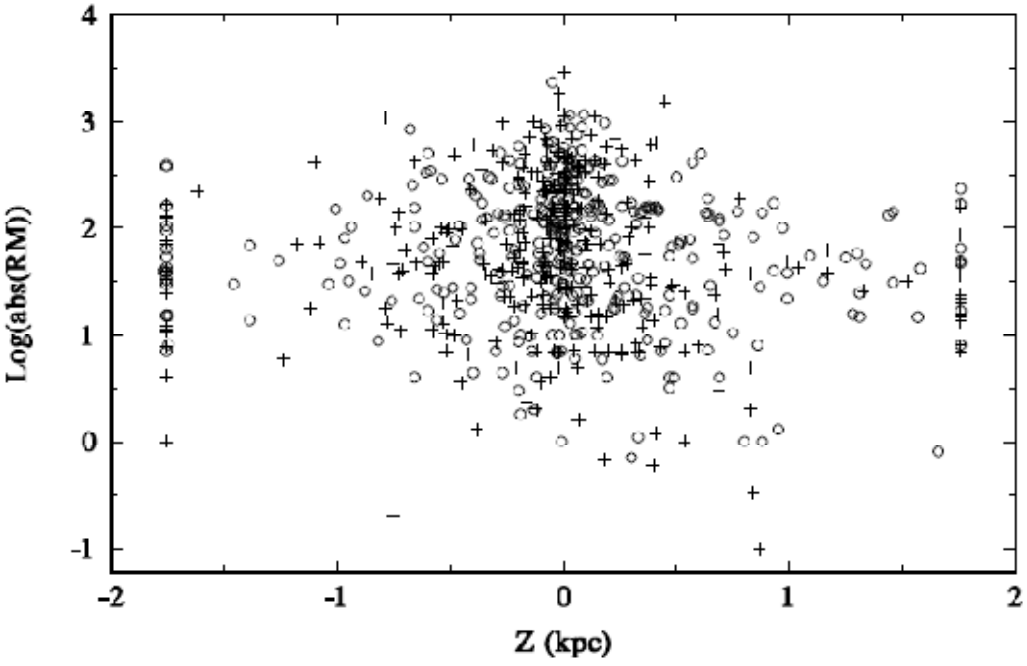

Figure 3.9: Scatter plot on Logarithmic scale of absolute values of rotation measure against pulsars' distance from the galactic plane (*Z*) for the 665 radio pulsars.
Key: ○ = pulsars with +ve *RM*; + = pulsars with -ve *RM*.

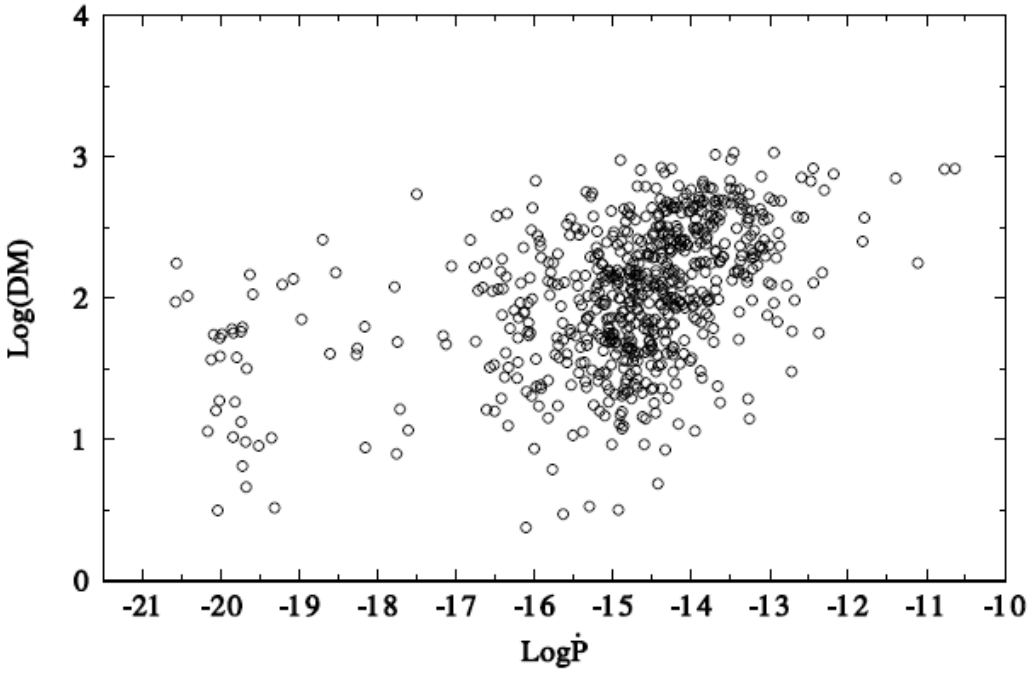

Figure 3.10: Scatter plot of the dispersion measure (*DM*) against period derivative ($\dot{P}$) on Logarithmic scales for the 668 radio pulsars.

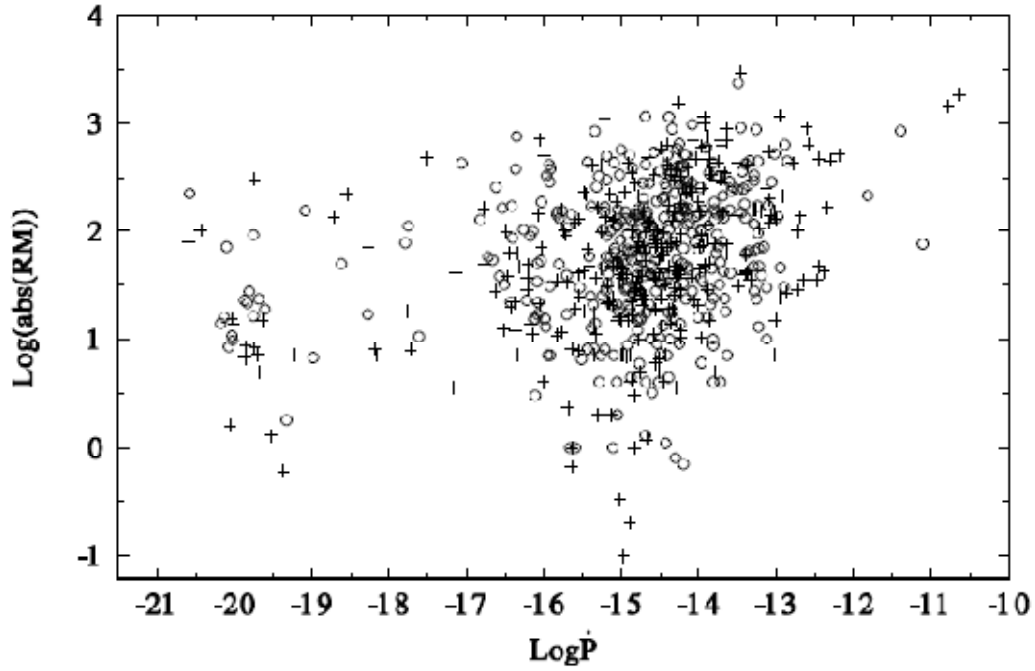

Figure 3.11: A scatter plot of logarithm of absolute values of rotation measure against logarithm of period derivative for the 668 radio pulsars. Key: ○ = pulsars with positive *RM*; + = pulsars with negative *RM*.

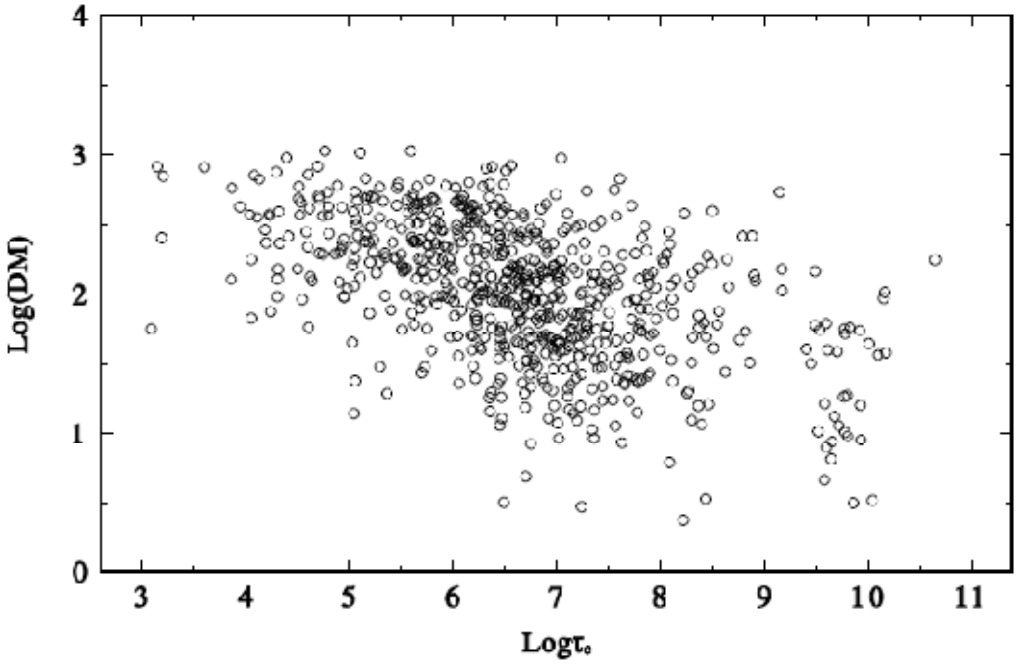

Figure 3.12: Scatter plot of the dispersion measure (*DM*) against characteristic age (τ_c) on logarithmic scales for the 668 radio pulsars.

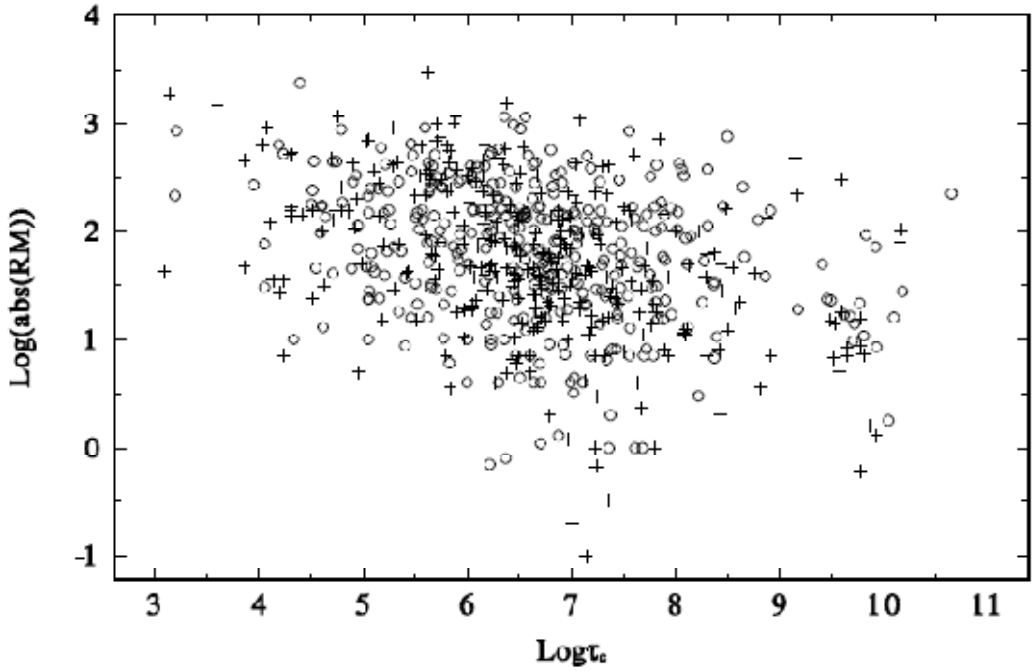

Figure 3.13: A scatter plot of logarithm of absolute values of rotation measure against logarithm of characteristic age for the 668 radio pulsars. Key: ○ = pulsars with positive *RM*; + = pulsars with negative *RM*.

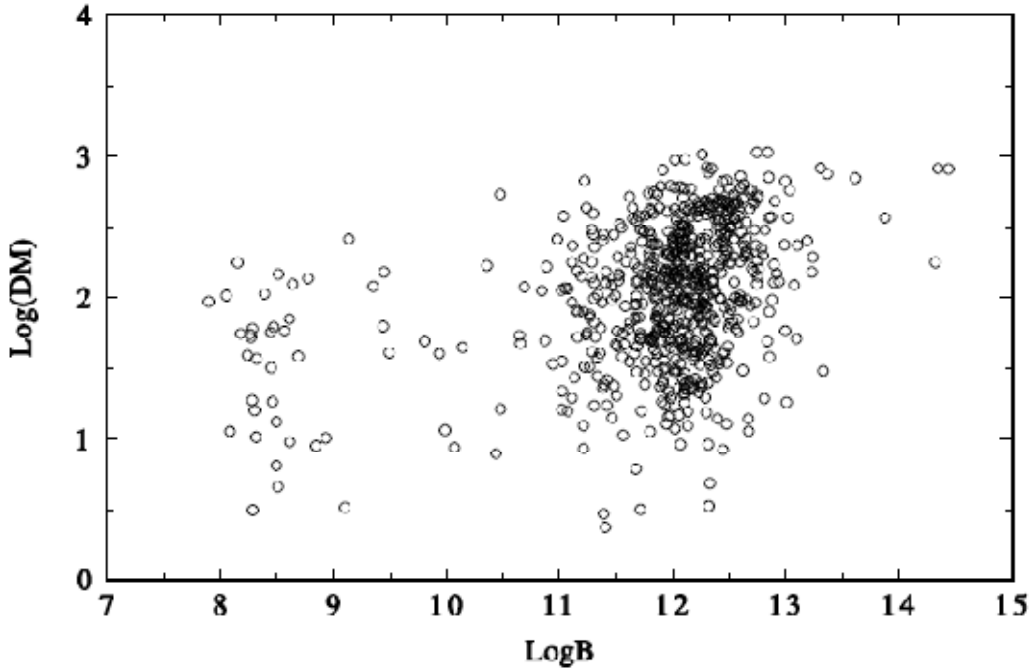

Figure 3.14: Scatter plot of dispersion measure (*DM*) against surface magnetic field (*B*) on logarithmic scales for the 668 radio pulsars.

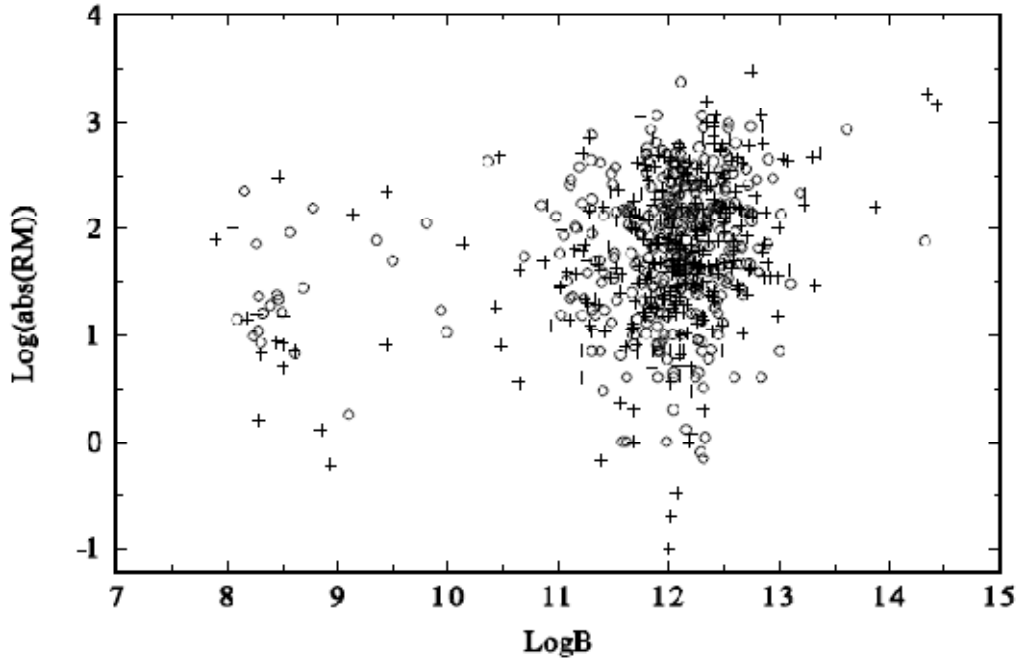

Figure 3:15: Scatter plot of absolute values of rotation measure against surface magnetic field on logarithmic scales for the 668 radio pulsars. Key: ○ = pulsars with +ve *RM*; + = pulsars with -ve *RM*.

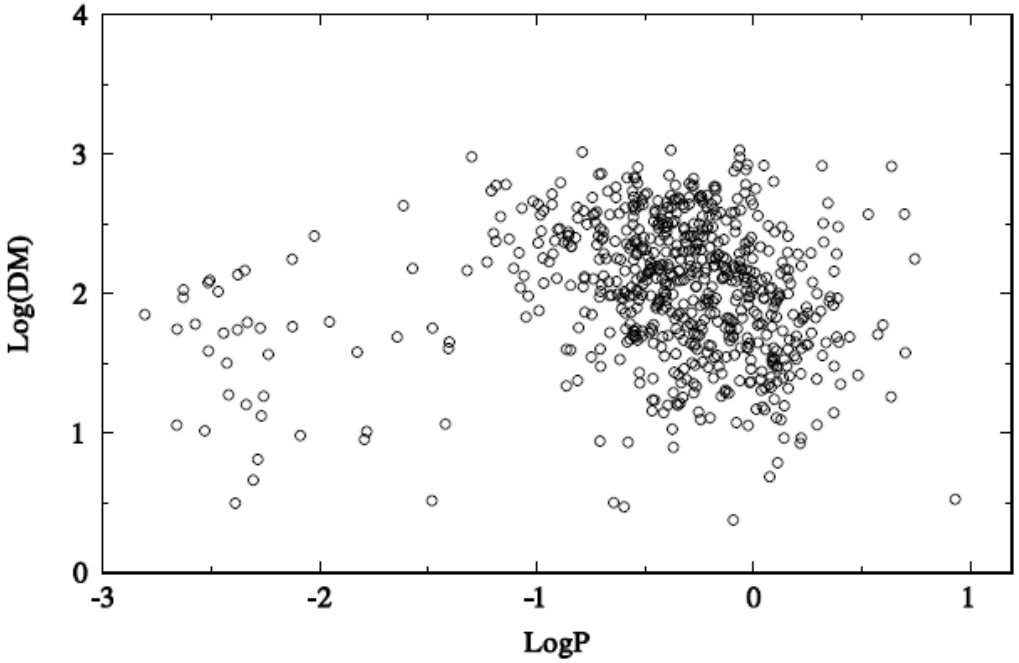

Figure 3.16: Scatter plot of logarithmic dispersion measure against logarithm of rotation period for the 668 radio pulsars.

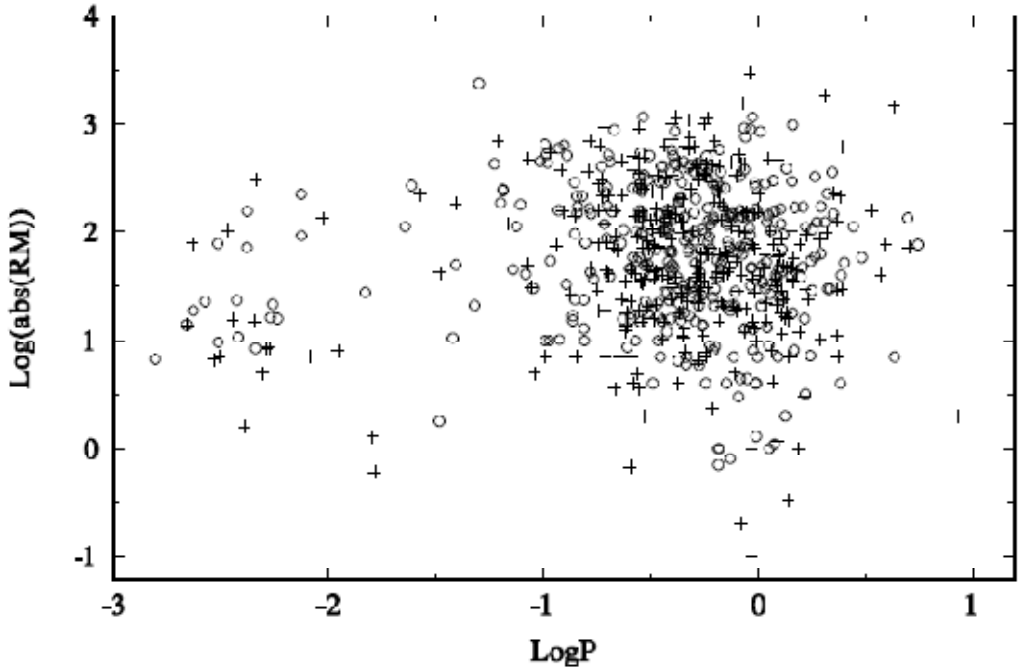

Figure 3.17: Scatter plot of logarithm of absolute values of rotation measure against logarithm of rotation period for the 668 radio pulsars. Key: ƹ = pulsars with positive *RM*; + = pulsars with negative *RM*.

3.3 Analysis of Time Rate of Change of DM (dDM/dt) of a Sample of Radio Pulsars

Our sample of 349 pulsars consists of 30 recycled millisecond pulsars and 319 normal pulsars. The time rate of change of dispersion measure ranges between ~ -10 and 10 $cm^{-3}pcyr^{-1}$. The parameter is characterized by a wide spread (~ 2 orders of magnitude) with a mean value of ~ 0.48 ± 0.08 $cm^{-3}pcyr^{-1}$.

Figures 3.18 and 3.19 are the scatter plots of the magnitude of dispersion measure derivative ($|dDM/dt|$) against dispersion measure (DM) and absolute values of rotation measure ($|RM|$) on logarithmic scales, respectively. A simple linear regression analysis of the data shows that both dispersion measure and rotation measure are poorly correlated (with correlation coefficient r ~ 0.3) with the time rate of change of dispersion measure. The plots nonetheless suggest some form of linear relationship between the parameters.

The scatter plots on logarithmic scales of the magnitude of dispersion measure derivative against radio pulsarsô spin-down rate, characteristic age, surface magnetic field and rotation period are shown in Figures 3.20, 3.21, 3.22 and 3.23, respectively. A simple linear regression analysis of the $|dDM/dt|$ ï $\dot{P}$, $|dDM/dt|$ ï τ_c, $|dDM/dt|$ ï B, and $|dDM/dt|$ ï P data yields r ~ 0.3, -0.3, 0.2 and 0.04, respectively as the correlation coefficients. However, the $|dDM/dt|$ ï $\dot{P}$ and $|dDM/dt|$ ï B correlation suggests a positive relationship between them while the $|dDM/dt|$ ï τ_c correlation suggests a negative relationship between them. There is no apparent relationship between the time rate of change of DM and rotation period as seen from the very weak correlation between them.

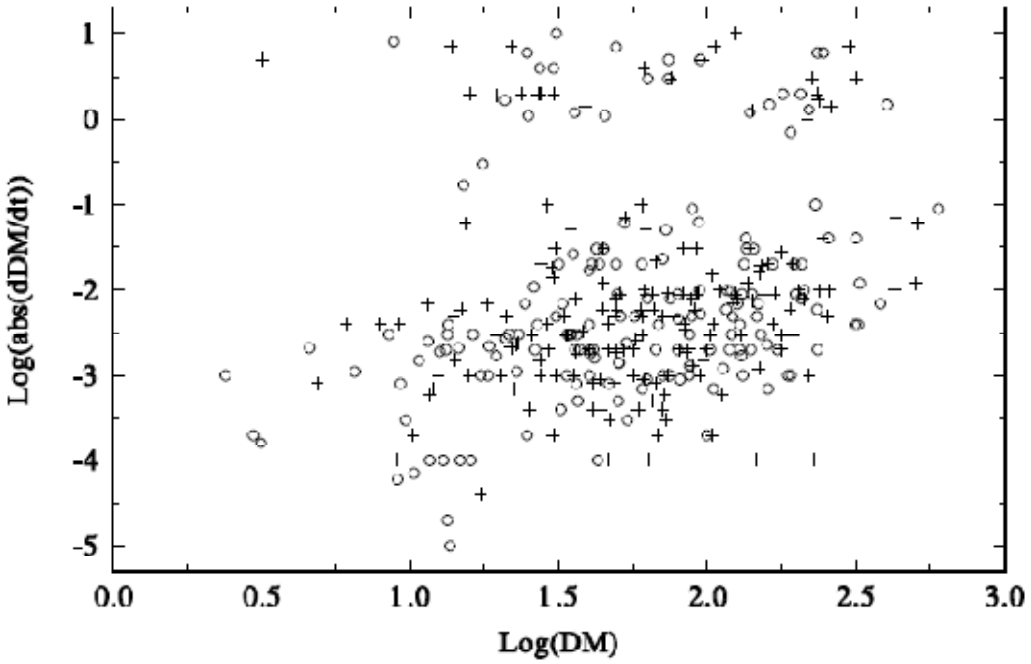

Figure 3.18: Scatter plot of absolute values of dispersion measure derivative against dispersion measure on logarithmic scales for the 349 pulsars. Key: ʒ = pulsars with +ve *dDM/dt*; + = pulsars with -ve *dDM/dt*.

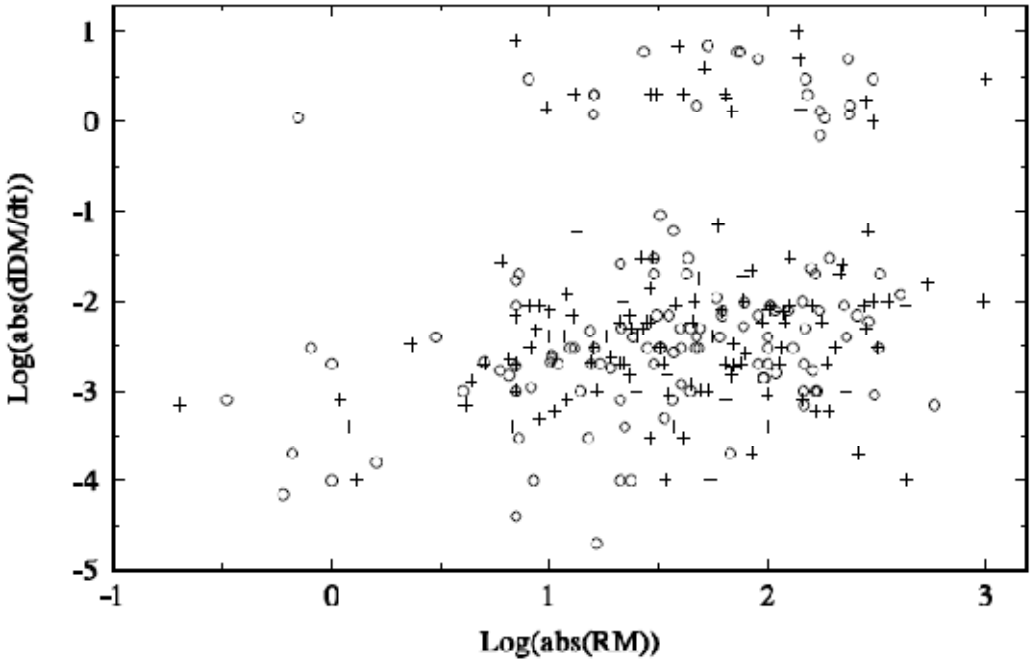

Figure 3.19: Scatter plot of absolute values of dispersion measure derivative against absolute values of rotation measure on logarithmic scales for the 266 pulsars. Key: ʒ = pulsars with +ve *dDM/dt*; + = pulsars with -ve *dDM/dt*.

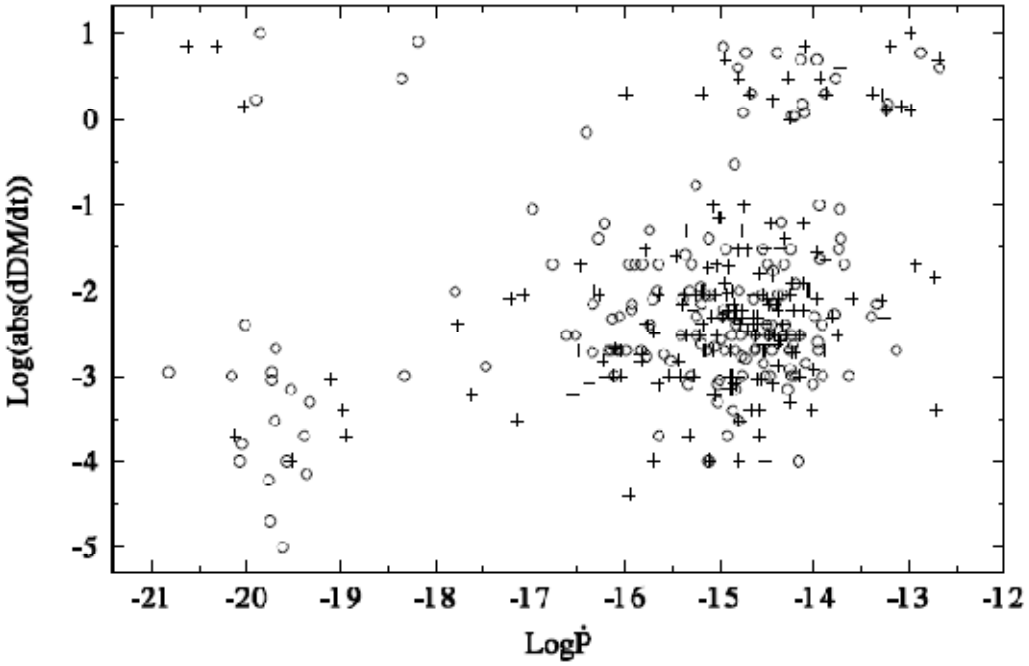

Figure 3.20: Scatter plot of absolute values of dispersion measure derivative against period derivative on logarithmic scales for the 349 pulsars. Key: ƹ = pulsars with +ve *dDM/dt*; + = pulsars with -ve *dDM/dt*.

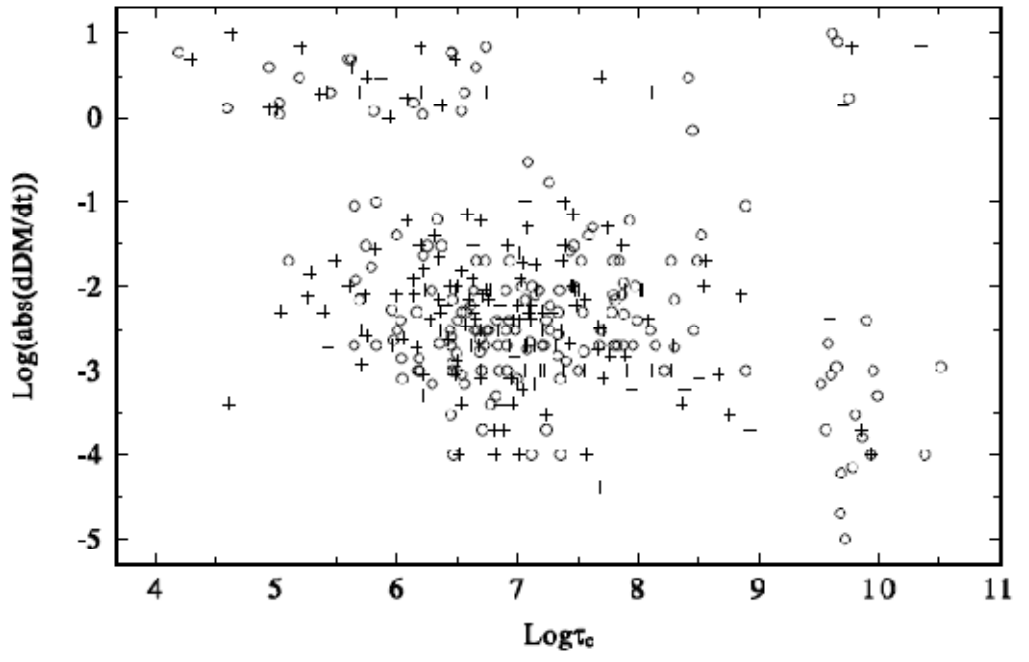

Figure 3.21: Scatter plot of absolute values of dispersion measure derivative against characteristic age on logarithmic scales for the 349 pulsars. Key: ƹ = pulsars with +ve *dDM/dt*; + = pulsars with -ve *dDM/dt*.

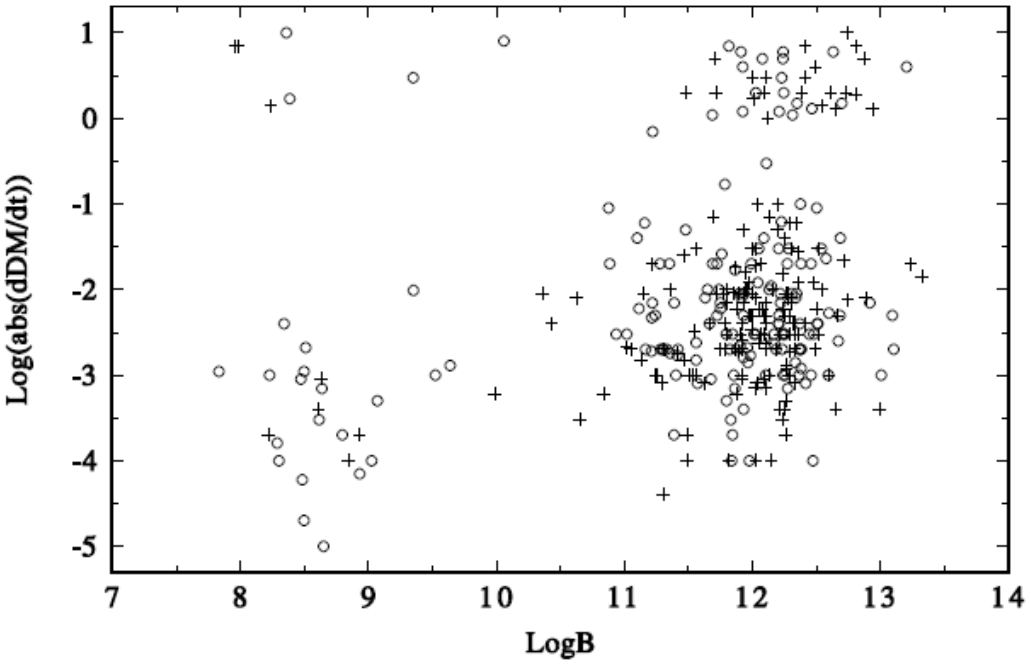

Figure 3.22: Scatter plot of absolute values of dispersion measure derivative against surface magnetic field on logarithmic scales for the 349 pulsars. Key: ʒ = pulsars with +ve *dDM/dt*; + = pulsars with -ve *dDM/dt*.

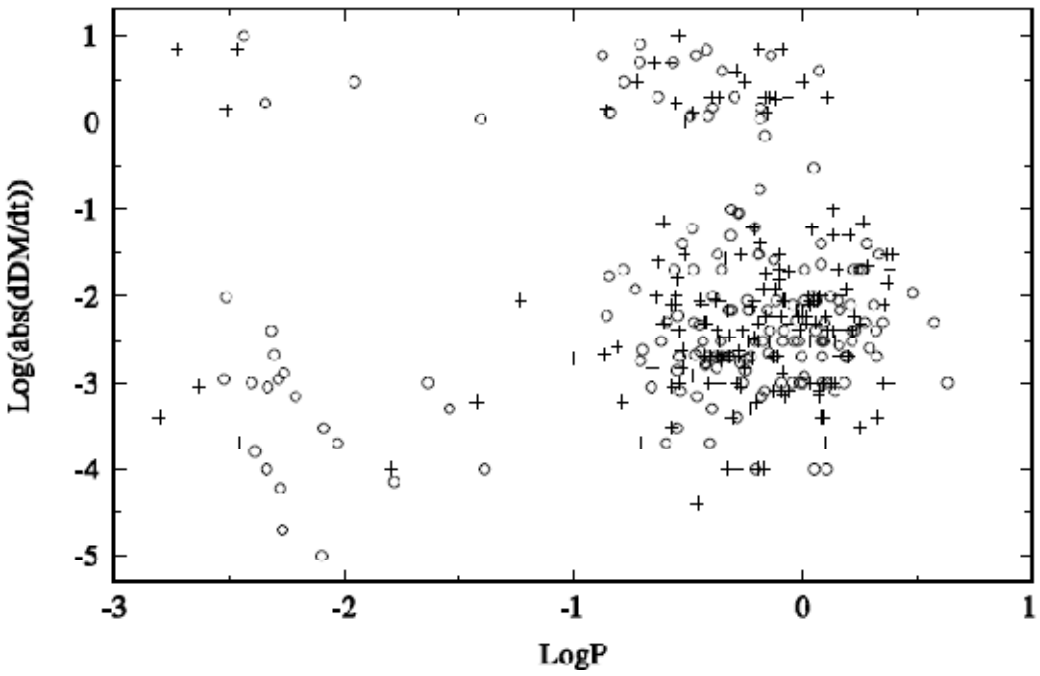

Figure 3.23: Scatter plot of absolute values of dispersion measure derivative against rotation period on logarithmic scales for the 349 pulsars. Key: ʒ = pulsars with +ve *dDM/dt*; + = pulsars with -ve *dDM/dt*.

3.3.1 Features of some Peculiar Pulsars

The properties of eight peculiar pulsars found at the upper left region of Figures 3.20, 3.22 and 3.23 are summarized in Table 3.2. The pulsar J1952+3252g is not among the seven pulsars in Figures 3.20 and 3.22, but in Figure 3.23 while the pulsar J0700+6418 is not inclusive of the seven pulsars in Figure 3.23, but in Figures 3.20 and 3.22. It is worthy of note that six of the pulsars (J0034-0534, J0613-0200, J1623-2631, J1911-1114, J2051-0827 and J2317+1439) are millisecond pulsars in binary system. The pulsar J0700+6418 is a normal pulsar but is believed to be in binary system (Manchester *et al*., 2005) while PSR J1952+3252g is a gamma ray pulsar (Thompson, 2008). Perhaps, the peculiar features observed among these pulsars could have arisen due to the fact that they belong to a different class of pulsars.

Table 3.2: Properties of the peculiar pulsars.

PSR	*P* (s)	$\dot{P}$ (ss^{-1})	*DM* ($cm^{-3}pc$)	*RM* ($radm^{-2}$)	τ_c (yr)	*B* (G)	*d(DM)/dt* ($cm^{-3}pcyr^{-1}$)
J0034-0534	0.001877	4.96E-21	13.7632	-	5.99E+09	9.76E+07	-7
J0613-0200	0.003062	9.54E-21	38.785	9.7	5.06E+09	1.73E+08	-1.4
J0700+6418	0.195671	6.51E-19	8.771	-7	4.52E+09	1.14E+10	8
J1623-2631	0.011076	4.41E-19	62.8647	-8	2.62E+08	2.24E+09	3
J1911-1114	0.003626	1.40E-20	30.962	-	4.06E+09	2.28E+08	10
J1952+3252g	0.039531	5.84E-15	45.006	-182	1.07E+05	4.86E+11	1.1
J2051-0827	0.004509	1.27E-20	20.75	-	5.61E+09	2.42E+08	1.7
J2317+1439	0.003445	2.37E-21	21.905	-	2.26E+10	9.15E+07	-7

3.4 Further Analysis of *DM* and *RM* Dependence on Radio Pulsar Spin-Down Parameters

The scatter plots of the ISM parameters (*DM* and *RM*) against the spin-down parameters ($\dot{P}$, τ_c and B) are characterized by moderate correlations ($|r| \sim 0.5$) which superimposed on intrinsic scatters of large (~ 3 orders of magnitude) amplitudes. These observations suggest that other unknown factors might be playing significant roles in the relationship between these parameters. This result might not be unexpected in view of complex and largely poorly

understood interstellar medium. Moreover, it is widely believed that the distribution of electron density in the ISM is very inhomogeneous (Backer *et al*., 1993; Hobbs *et al*., 2004; Lorimer and Kramer, 2005).

To further investigate the relationship between these ISM parameters and the spin-down parameters, we average the *DM* and *RM* over a given range/bin of $\log \dot{P}$, $\log \tau_c$ and $\log B$. This method is capable of dealing with the effects of the unknown factors by averaging them out.

For the characteristic age, the binning is done over the logarithm of the τ_c and are as follows: $\log \tau_c$ Ò5; 5 < $\log \tau_c$ Ò6; 6 < $\log \tau_c$ Ò7; 7 < $\log \tau_c$ Ò8; 8 < $\log \tau_c$ Ò9; $\log \tau_c$ > 9 for both *DM* and |*RM*|. The average logarithmic values of the *DM* and |*RM*| are calculated for each bin. The standard errors of the mean values of these parameters (*DM* and *RM*) were also calculated. The average logarithmic values for each bin of the τ_c were employed in the analysis. The scatter plots of the average values of log*DM* and log|*RM*| against the average logarithmic values of the pulsar characteristic age are shown in Figures 3.24 and 3.25, respectively. A simple linear regression analysis of the data shows a very strong anti-correlation (*r* ~ -0.98) between the parameters.

Similarly, for the pulsar spin-down rate ($\dot{P}$), the binning is done over the logarithm of the $\dot{P}$ and are as follows: $\log \dot{P}$ Ò-18; -18 < $\log \dot{P}$ Ò-17; -17 < $\log \dot{P}$ Ò-16; -16 < $\log \dot{P}$ Ò-15; -15 < $\log \dot{P}$ Ò-14; $\log \dot{P}$ > -14 for both *DM* and |*RM*|. The average logarithmic values of the *DM* and |*RM*| are calculated for each bin. The standard errors of the mean values of these parameters (*DM* and *RM*) were also calculated. The average logarithmic values for each bin of the $\dot{P}$ were employed in the analysis. The scatter plots of the average values of log*DM* and log|*RM*| against the average logarithmic values of the pulsar spin-down rate are shown in Figures 3.26 and 3.27, respectively. A simple linear regression analysis of the data shows a very strong correlation (*r* ~ 0.95) between the parameters.

Finally for the pulsar surface magnetic field, the binning is done over the logarithm of the B and are as follows: $\log B$ Ò9; 9 < $\log B$ Ò10; 10 < $\log B$ Ò11; 11 < $\log B$ Ò12; 12 < $\log B$ Ò 13; $\log B$ > 13 for both *DM* and |*RM*|. The average logarithmic values of the *DM* and |*RM*| are calculated for each bin. The standard errors of the mean values of these parameters (*DM* and *RM*) were also calculated. The average logarithmic values for each bin of the B were employed

in the analysis. The scatter plots of the average values of log*DM* and log|*RM*| against the average logarithmic values of the pulsar surface magnetic field are shown in Figures 3.28 and 3.29, respectively. A simple linear regression analysis of the data shows a very strong correlation ($r \sim 0.98$) between the parameters. The correlations are statistically significant at 98% confidence.

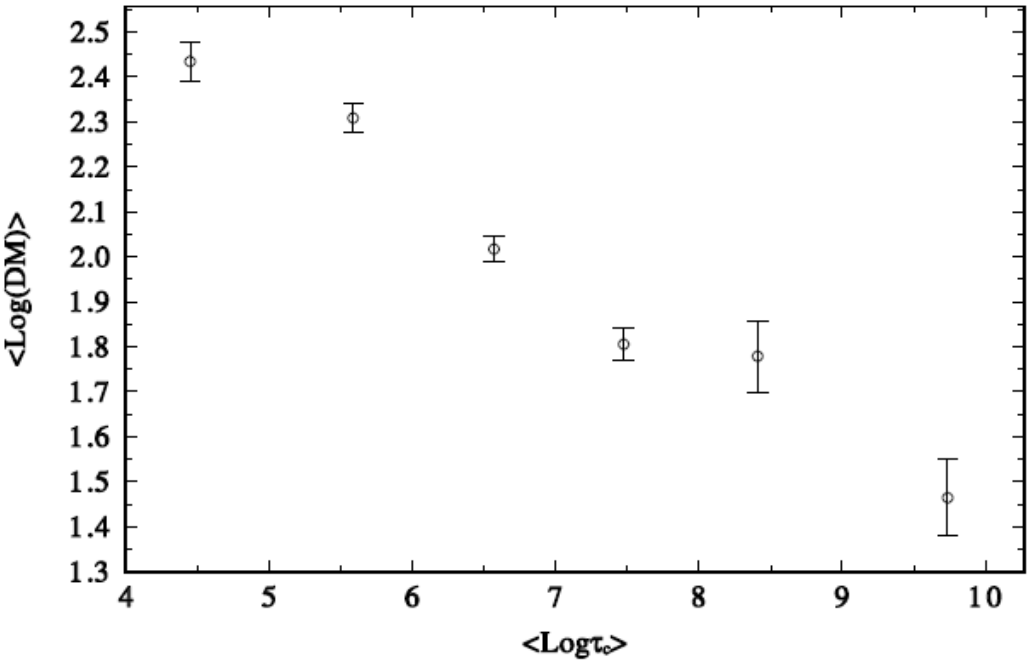

Figure 3.24: Plot of the mean values of logarithmic dispersion measure against mean values of logarithmic characteristic age.

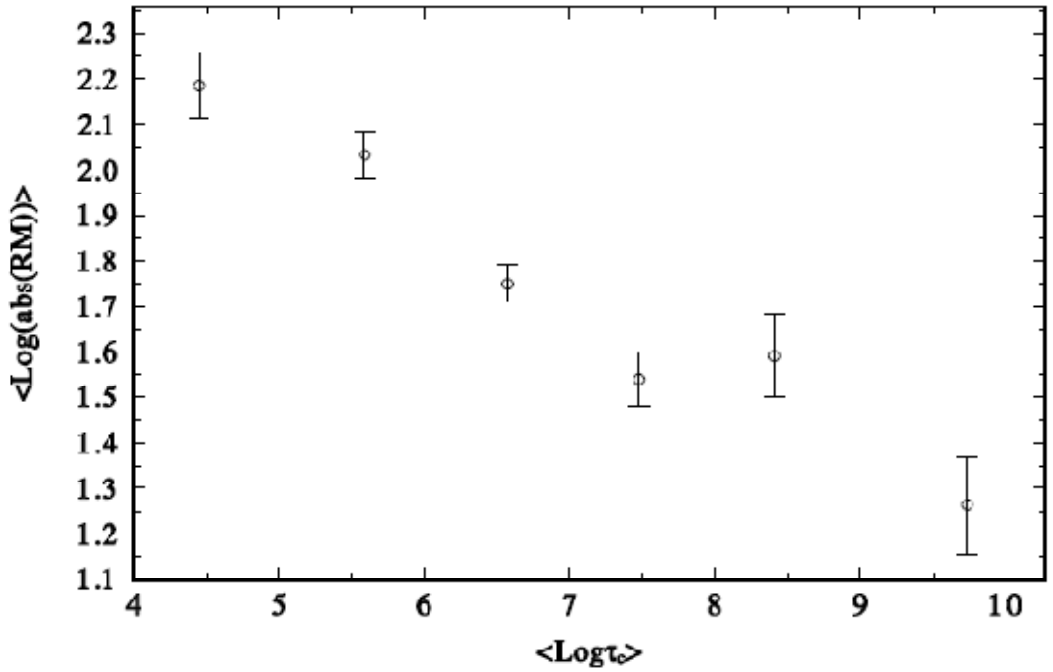

Figure 3.25: Plot of the mean values of logarithmic absolute values of rotation measure against mean values of logarithmic characteristic age.

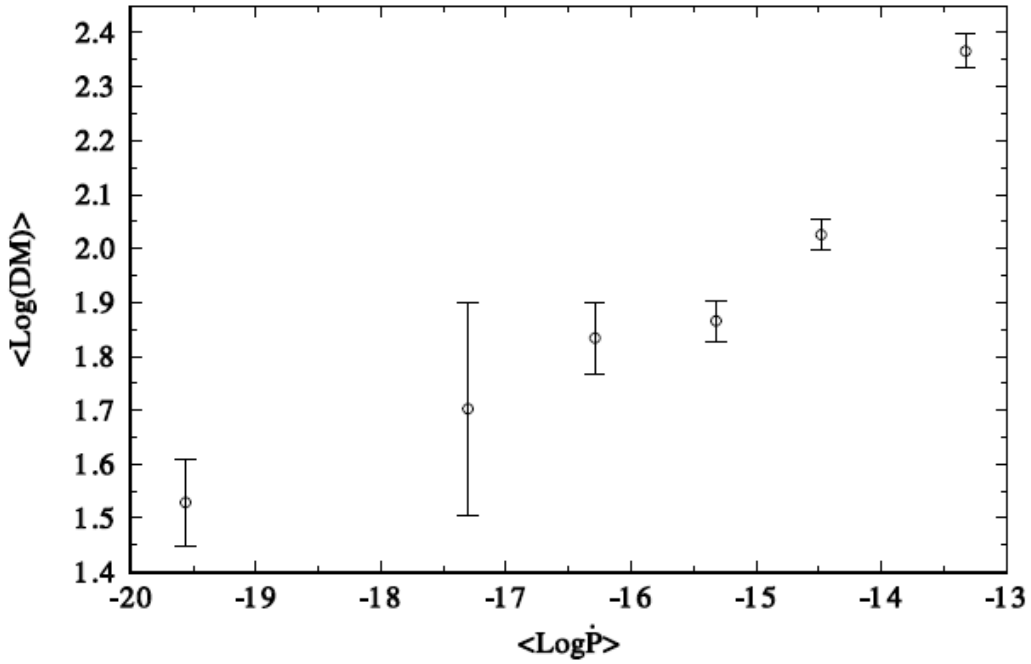

Figure 3.26: Plot of the mean values of logarithmic dispersion measure against mean values of logarithmic period derivative.

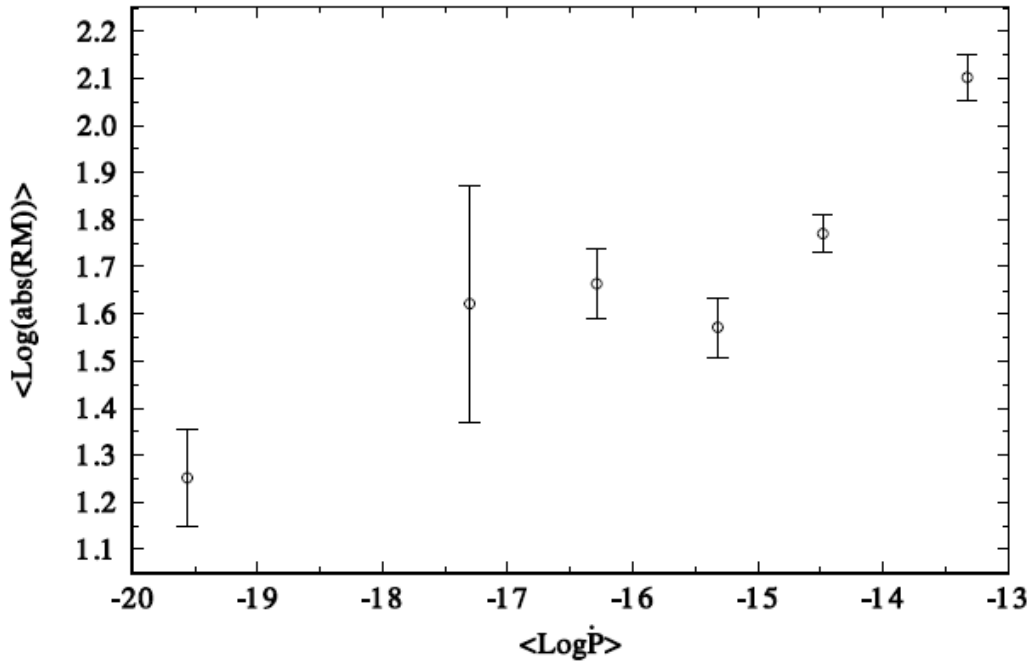

Figure 3.27: Plot of the mean values of logarithmic absolute values of rotation measure against mean values of logarithmic period derivative.

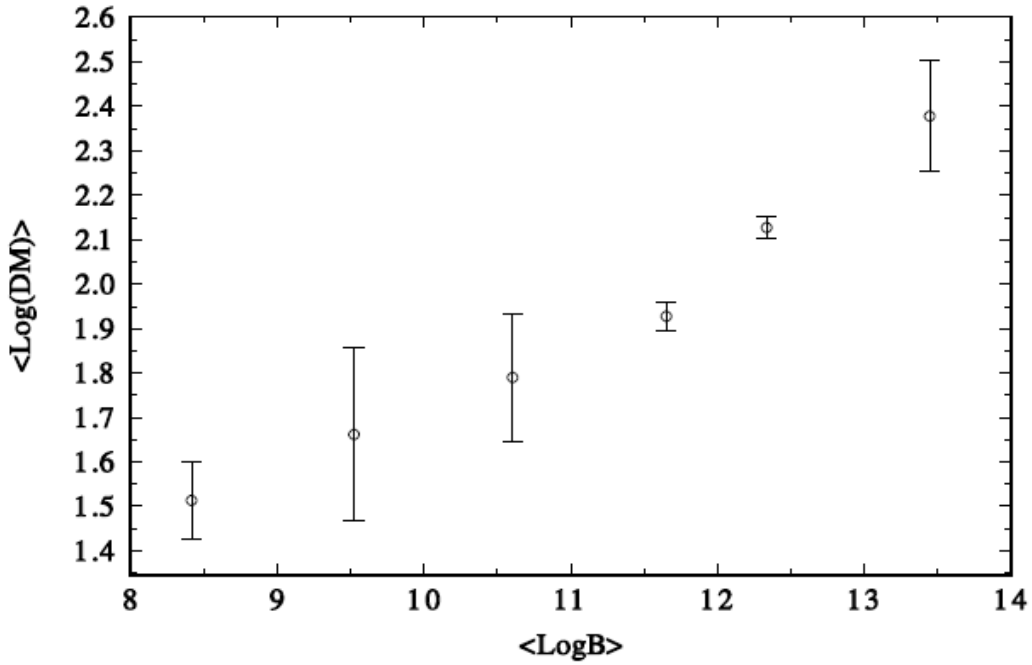

Figure 3.28: Plot of the mean values of logarithmic dispersion measure against mean values of logarithmic surface magnetic field.

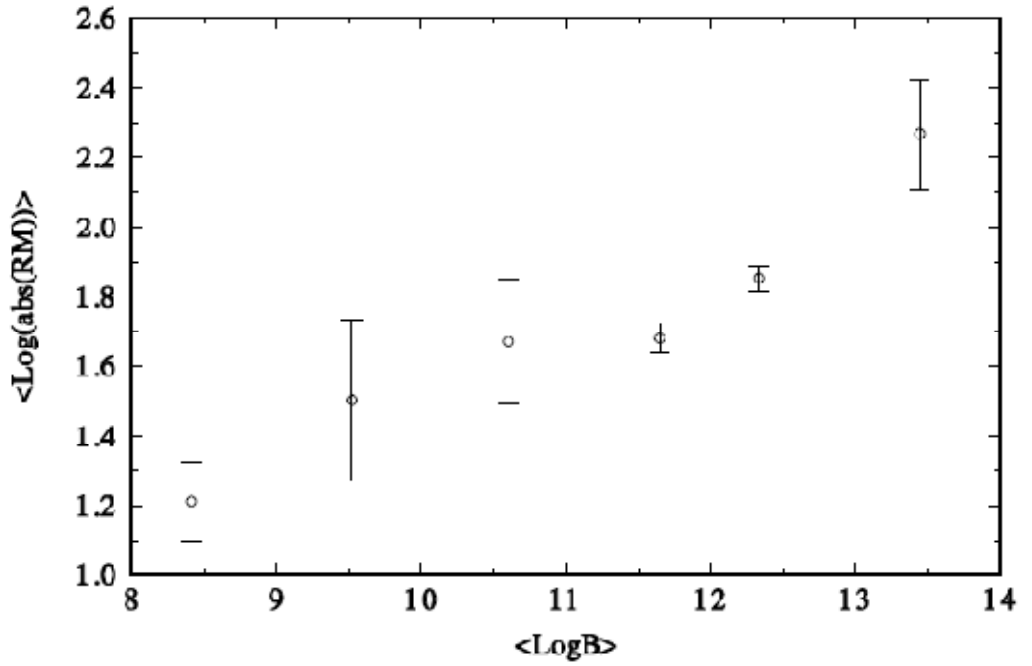

Figure 3.29: Plot of the mean values of logarithmic absolute values of rotation measure against mean values of logarithmic surface magnetic field.

CHAPTER FOUR

DISCUSSION AND CONCLUSION

4.1 Discussion

The dispersion measures and the rotation measures are believed to be caused by similar effect, which is the effect of electron content of the interstellar medium on propagation of radio pulses. Therefore, strong correlation between the rotation measure and the dispersion measure is as expected, since the rotation measure is directly related to the dispersion measure (e.g. Guélin, 1973; Noutsos *et al*., 2008; Lyne and Smith, 2012). Pulsars that are located where the electron content along the line of sight to the pulsars is high or low will be invariably associated with large or small dispersion measure and rotation measure, respectively (e.g. Guélin, 1973; Noutsos *et al*., 2008; Lyne and Smith, 2012).

Pulsars are believed to be born from massive O and B stars (i.e. population I stars) that are concentrated strongly along the galactic plane. This observation is consistent with the standard theory of the birth of neutron stars in the core collapse supernova explosion of massive stars (Kaspi and Helfand, 2002). From the violent condition associated with the birth of pulsars during supernova explosions, it is not surprising to know that pulsars are high velocity objects. Pulsars are born within the galactic plane with high kick velocities that are largely asymmetric (Shklovskii, 1970) and large spin-down rate (Ostriker and Gunn, 1969). The origin of these kicks is not yet clear, but may lie in small asymmetries in the supernova explosions (Lyne and Lorimer, 1994). The random velocities of massive stars (O and B stars) from which pulsars are believed to be born during supernova explosions are within the range of ~ 5000 ï 7000 kms^{-1} (Shklovskii, 1966). Pulsars are associated with large space velocities that could carry most of them generally away from the vicinity of their birth places (Lyne and Lorimer, 1994). They are characterized by random space velocities distribution. The space velocities estimated from interpretation of vertical distribution of pulsars with different ages are ~ 100 kms^{-1} (Gunn and Ostriker, 1970). The rms space velocities extracted from measurement of proper motion are ~ 210 kms^{-1} (Lyne *et al*., 1982). The rms space velocities estimated from interstellar scintillations are ~ 160 kms^{-1} (Cordes, 1986). Space velocities of ~ 690 kms^{-1} were estimated from pulsar

supernova remnant association (Caraveo, 1993). The mean pulsar birth velocity is ~ 450 kms^{-1} (Lyne and Lorimer, 1994).

The trend observed in the relationship between the interstellar medium parameters (*DM* and *RM*) and the radio pulsar spin-down parameters ($\dot{P}$, τ_c and B) is remarkable. This is because the interstellar medium is not expected to significantly affect the intrinsic spin-down of radio pulsars on pulsar rotation. The significance of the relationship is that it strongly supports the widely accepted theory for pulsar birth and evolution, in which pulsars are believed to be born near the galactic plane with asymmetric kick velocities. Consequently, pulsars move progressively away from the galactic plane (hence steadily into regions of average lower electron density content) as they age. Young pulsars are believed to be associated with large spin-down rate and surface magnetic field and are found close to the galactic plane, where every line of sight will, on average, contain higher electron density which corresponds to higher dispersion measure/rotation measure. As pulsars get old, their initial velocity carries them farther away from the galactic plane and hence steadily into regions of average lower electron density content which corresponds to lower dispersion measure/rotation measure. This region, whether above or below the galactic plane will be populated by relatively older pulsars that are characterized by smaller spin-down rate and surface magnetic field.

On the other hand, the electron density is considerably higher in HII regions, supernova remnants and nebulae (Davidson and Terzian, 1969b; Prentice and Ter Haar, 1969). If a pulsar (whether young or old) is located behind the nebula or associated with H II region or supernova remnant, it will invariably be associated with higher dispersion measure/rotation measure, irrespective of the pulsar being near the galactic plane or farther away from the plane. This could account for the large scatter observed in both *DM* and *RM* data.

Again a pulsar may be young and probably associated with very high space velocity, which might be able to move it farther away from the galactic plane and hence into a region of lower electron density content which corresponds to lower dispersion measure as well as rotation measure. Similarly, some older pulsars might have been associated with very low space velocities that were not able to carry them farther away from the galactic plane. As such, they are believed to be still lying within the galactic plane, where every line of sight, on average, is

characterized by higher electron density content which corresponds to higher *DM*/*RM*. This interpretation might possibly explain the large scatter seen in both *DM* and *RM* data.

Furthermore, it is expected that pulsars move in different directions but generally away from the galactic plane. If the direction of a pulsar (whether young or old) is at longitude 0^o. The pulsar is thought to be lying near the galactic plane, where the electron density content is very high, resulting to high dispersion measure/rotation measure. Similarly, if the direction of a pulsar is at longitude 90^o, it is believed to be above or below the galactic plane. This region below or above the galactic plane is characterized by relatively lower electron density content which corresponds to lower *DM*/*RM*.

It is widely known that most activities of radio pulsars such as timing noise, glitches etc do not depend significantly on the pulsar rotation period. In fact, it has been shown that most of the pulsar parameters (like second time derivative of the spin frequency, stability parameter, timing residual etc), which characterize radio pulsar timing noise revealed no appreciable dependence on pulsar rotation period (e.g. Hobbs *et al*., 2010). As such, the existence of no appreciable dependence of both *DM* and *RM* on the rotation period of pulsars is not unexpected. Most activities of radio pulsars depend strongly on the pulsar spin-down rate. Although, most of the derived parameters of pulsar such as spin-down age, surface magnetic field, spin-down energy loss rate etc depend on the rotation period of pulsar. Pulsars are born with different rotation period. Some pulsars are millisecond and young pulsars while some are millisecond and old recycled pulsars.

It is believed that irregularities in the electron density distribution in the galaxy are responsible for *DM* variation of pulsars (e.g. Backer *et al*., 1993; Hobbs *et al*., 2004; Lorimer and Kramer, 2005). Other factors such as turbulent spatial variations which drift across the line of sight between the earth and the pulsar (You *et al*., 2007) and ionospheric effect as well as solar wind contributions such as coronal mass ejection (McComas *et al*., 2000; Schwenn, 2006) can cause *DM* variation. The existence of a linear relationship between the time rate of change of *DM* and the *DM*/*RM* is as expected as proposed by Backer *et al*. (1993) and Hobbs *et al*. (2004). Very young pulsars with large spin-down rate and surface magnetic field are thought to be associated with large time rate of change of *DM* due to their location in the galaxy, where the electron density irregularity is large while very old pulsars with small spin-down rate and surface

magnetic field are thought to be associated with small time rate of change of *DM* due to their location in the galaxy, where the electron density irregularity is small.

The time rate of change of *DM* is not expected to have any dependence on pulsar rotation and as such, there is no appreciable relationship between the time rate of change of *DM* and the pulsarsô rotation period, which depend on pulsar rotation. It is also noteworthy that the peculiar pulsars are in binary system and are associated with large dDM/dt, which is thought to be as a result of contribution from the ionized envelope of the companion object (Freire *et al*., 2003).

4.2 Conclusion

The observed parameters of 668 radio pulsars have been extensively studied for any relationship between those that are intrinsic to the pulsars and those that characterize the interstellar medium. There is an existence of a positive relationship between the parameters (dispersion measure and rotation measure) that characterize the interstellar medium and the radio pulsar spin-down rate and surface magnetic field, which characterize the intrinsic spin-down evolution of neutron stars. On the other hand, a negative relationship between the parameters (dispersion measure and rotation measure) that depend on the electron content of the interstellar medium and the radio pulsar characteristic age, which depends on the spin-down rate of radio pulsars, was observed. There is also some form of striking negative relationship between the dispersion measure and rotation measure and the radio pulsar distance from the galactic plane. The significance of the relationship is that it strongly supports the widely accepted theory for pulsars birth and evolution, in which pulsars are believed to be born near the galactic plane with asymmetric kick velocities. The observed large scatter in both *DM* and *RM* data highlights the complex nature of the electron content distribution in the ISM and the large dispersion in both the magnitude and direction of pulsar space velocities. Variation in dispersion measure is pronounced and has been attributed to the electron density irregularities along the line of sight to pulsars.

REFERENCES

Ables, J.G. and Manchester, R.N., 1976, Hydrogen-line Absorption Observations of Distant Pulsars, A&A, 50, 177.

Anderson, P.W. and Itoh, N., 1975, Pulsar Glitches and Restlessness as a Hard Superfluidity Phenomenon, Nature, 256, 25.

Armstrong, J.W., Rickett, B.J. and Spangler, S.R., 1995, Electron Density Power Spectrum in the Local Interstellar Medium, ApJ, 443, 209.

Atkinson, N., 2008, Fermi Telescope Makes First Big Discovery: Gamma Ray Pulsar, Universe Today.

Backer, D.C., Hama, S. and Van Hooks, S., 1993, Temporal Variations of Pulsar Dispersion Measures, ApJ, 404, 636.

Backer, D.C., Kulkarni, S.R., Heiles, C., Davies, M.M. and Goss, W.M., 1982, A Millisecond Pulsar, Nature, 300, 615.

Baym, G., 1991, The High Density Interiors of Neutron Star, Ventura, J. and Pines, D., eds, 21, Kluwer, Dordrecht.

Baym, G., Pethick, C., Pines, D. and Ruderman, M., 1969, Superfluidity in Neutron Stars, Nature, 224, 872.

Bhat, N.D.R., Cordes, J.M., Camilo, F., Nice, D.J. and Lorimer, D.R., 2004, Multi Frequency Observation of Radio Pulse Broadening, ApJ, 605, 759.

Bhattacharya, D., 1996, The Origin of Millisecond Pulsars, ASPC, 105, 547.

Bhattacharya, D. and Srinivasan, G., 1995, in Lewin, W.H.G., van Paradijs, J. and van den Heuvel, E.P.J., eds, X-ray Binaries, Cambridge University Press.

Bhattacharya, D. and van den Heuvel, E.P.J., 1991, Formation and Evolution of Binary and Millisecond Radio Pulsars, Physics Reports, 203, 1.

Bridle, A.H., 1969, Distribution and Temperature of Interstellar Electron Gas, Nature, 221, 648.

Burgay, M., DôAmico, N., Possenti, A., Manchester, R.N., Lyne, A.G., Joshi, B.C., McLaughlin, M., Kramer, M., Sarkissian, J.M., Camilo, F., Kalogera, V., Kim, C. and Lorimer, D.R., 2003, The Double Pulsar System in its 8th Anniversary, Nature, 426, 531.

Caraveo, P.A., 1993, The Crab Pulsar Proper Motion, ApJ, 415, 111.

Chatterjee, S., Cordes, J.M. and Lazio, T.J.W., 2003, Probing the Galaxy with Pulsar Parallaxes and Proper Motions, ASP Conference Series, 302.

Chukwude, A.E., 2002, PhD thesis, University of Nigeria, Nsukka.

Chukwude, A.E. and Urama, J.O., 2010, Observations of Microglitches in Hartebeesthoek Radio Astronomy Observatory Radio Pulsars, MNRAS, 406, 1907.

Cordes, J.M., 1986, Space Velocities of Radio Pulsars from Interstellar Scintillations,

ApJ, 311, 183.

Cordes, J.M., Downs, G.S. and Krauss-Polstorff, J., 1988, A Statistical Analysis of Radio Pulsar Timing Noise, ApJ, 330, 847.

Davidson, K. and Terzian, Y., 1969a, Observation of Interstellar Scintillations of Pulsar Signals at 2388 MHz, AJ. 74, 849.

Davidson, K. and Terzian, Y., 1969b, Dispersion Measures of Pulsars, Nature, 221, 729.

DeJager, G., Lyne, A.G. and Pointon, L., 1969, Distance Estimate for Pulsars, Private Communication.

Duncan, R.C. 1998, Magnetar Models for Soft Gamma Repeaters and Anomalous x-ray Pulsars, AAS, 193, 5640.

Dupin, O. and Gry, C., 1998, Local Cloud: Ionization, Temperature, Electron Densities and Interfaces from GHRS and IMAPS Spectra of Canis Majoris, A&A, 335, 661.

Ekers, R.D., Lecqueux, J., Moffet, A.T. and Seielstad, G.A., 1969, A Measurement of the Galactic Magnetic Field using the Pulsating Radio Source PSR 0833-45. ApJ, 156, 21.

Encrenaz, P. and Guélin, M., 1970, Pulsar AP 2015: 21cm Line Absorption Profile, Nature, 227, 476.

Field, G.B., Goldsmith, D.W. and Habing, H.J., 1969, Cosmic-Ray Heating of the Interstellar Gas, ApJ (Letters), 155, 149.

Freire, P.C., Camilo, F., Kramer, M., Lorimer, D.R., Lyne, A.G., Manchester, R.N. and DôAmico, N., 2003, Further Results from the Timing of the Millisecond Pulsars in 47 Tucanae, MNRAS, 340, 1359.

Frisch, P.C., 1994, The Heliosphere in the Local Interstellar Medium, Science, 265, 1423.

Frisch, P.C., Welty, D.E., York, D.G. and Fowler, J.R., 1990, Diffuse Ionized Gas Toward Beta Canis Majoris, ApJ, 357, 514.

Glampedakis, K. and Andersson, N., 2009, Superfluid Signatures in Magnetar Seismologyphys. Rev. Lett., 102, 1101.

Goméz, G. C., Benjamin, R.A. and Cox, D.P., 2001, The Distribution of the Warm Ionized Medium in the Galaxy, AJ, 122, 908.

Gómez-Gonzàlez, J. and Guélin, M., 1974, Pulsar Hydrogen Line Absorption and the Electron Density in the Interstellar Medium, A&A, 32, 441.

Gordon, C.P., Gordon, K.J. and Shalloway, A.M., 1969, Estimates of Pulsar Distances from the Neutral Hydrogen Absorption, Nature, 222, 129.

Gordon, K.J. and Gordon, C.P., 1973, Measurements of Neutral-Hydrogen Absorption in the Spectra of Eight Pulsars, A&A, 27, 119.

Gordon, M.A. and Gottesman, S.T., 1971, Electron Density and Temperature in the Diffuse Interstellar Medium Determined from Recombination Lines, ApJ, 168, 361.

Gould, D.M. and Lyne, A.G., 1998, Multifrquency Polarimetry of 300 Radio Pulsars, MNRAS, 301, 235.

Gould, R.J., 1971, Pulsar Dispersion Measures and the Mean and Mean-Square Interstellar Electron Density, Ap&SS, 10, 265.

Gry, C., Lemonon, L., Vidal-Madjar, A., Lemoine, M. and Ferlet, R., 1995, GHRS Observations of Diffuse Clouds in the Local Bubble, A&A, 302, 497.

Guélin, M., 1973, Pulsars as Probes of the Interstellar Medium, Proc. IEEE, 6, 1298.

Guélin, M., Guilbert, J., Huchtmeier, W. and Weliachew, L., 1968, The Scale Height of the Galactic Free Electron Cloud, Nature, 221, 249.

Gunn, J.E. and Ostriker, J.P., 1970, On the Nature of Pulsars. III. Analysis of Observations, ApJ, 160, 979.

Habing, H.J. and Pottasch, S.R. 1968, Distances to the Pulsating Radio Sources, Nature, 219, 1137.

Han, J.L., Manchester, R.N., Lyne, A.G. and Qiao, G.J., 2002, Conterclockwise Magnetic Fields in the Norma Spiral Arm, ApJ, 570, 17.

Han, J.L., Manchester, R.N., Lyne, A.G., Qiao, G.J. and Van Straten, W., 2006, Pulsar Rotation Measures and the Large Scale Structure of the Galactic Magnetic Field, ApJ, 642, 868.

Heiles, C., 1998, Interstellar and Circumstellar Matter, ApJ, 498, 689.

Hewish, A., 1955, The Scattering of Radio Waves in the Solar Corona, Proc. RSA, 228, 238.

Hewish, A., Bell, S.J., Pilkington, J.D.H., Scott, P.F. and Collins, R.A., 1968, Observation of a Rapidly Pulsating Radio Source, Nature, 217, 709.

Hewish, A., Scott, P.F. and Wills, D., 1964, Interplanetary Scintillation of Small Diameter Radio Sources, Nature, 203, 1214.

Hey, J.S., Parsons, S.J. and Phillips, J.W., 1946, Fluctuations in Cosmic Radiation at Radio Frequencies, Nature, 158, 234.

Hill, A.S., Stinebring, D.R., Barnor, H.A., Berwick, D.E. and Webber, A.B., 2003, Interstellar Scintillation of PSR J0437-4715 on Two Scales, ApJ, 599, 457.

Hjellming, R.M., Gordon, C.P. and Gordon, K.J., 1969, Properties of Interstellar Clouds and the Inter-Cloud Medium, A&A, 2, 202.

Hobbs, G., Lyne, A.G. and Kramer, M., 2010, An Analysis of the Timing Irregularities for 366 Pulsars, MNRAS, 402, 1027.

Hobbs, G., Lyne, A.G., Kramer, M., Martin, C.E. and Jordan, C., 2004, Long-Term Timing Observations of 374 Pulsars, MNRAS, 353, 1311.

Holberg, J.B., Bruhweiler, F.C., Barstow., M.A. and Dobbie, P.D., 1999, Far - Ultraviolet Space Telescope Imaging Spectrometer Spectra of the White Dwarf REJ 1032+532, 1. Interstellar Line of Sight, ApJ, 517, 841.

Igoshev, A.P., 2012, Spin-Down Age: The Key to Magnetic Field Decay, MNRAS, arxiv:1204 ï 3445.

Joss, P.C. and Rappaport, S.A., 1984, 5 hr Pulse Period and Broadband Spectrum of the Symbiotic X-ray Binary 3A 1954-319, ARA&A, 24, 537.

Karttunen, H., Kroger, P., Oja, H., Poutanen, M. and Donner, K.J., 2006, Fundamental Astronomy, 5th ed. Springler Verlag, Berlin.

Kaspi, V.M., 1997, Observations of Millisecond Pulsars on Time Scales of 10 nanoseconds to 10 years, in Maoz, D., Sternberg, A. and Leibowitz, E.M., eds, Astronomical Time Series, Kluwer Academic Publishers, Dordrecht.

Kaspi, V.M. and Helfand, D.J., 2002, in: Neutron Stars in Supernova Remnants, eds, Slane, P.O. and Gaensler, B.M., ASP, San Francisco.

Kaspi, V.M., Taylor, J.H. and Ryba, M., 1994, Recycled Pulsars, ApJ, 428, 713.

Kiziltan, B., 2011, Reassessing the Fundamentals: On the Evolution, Ages and Masses of Neutron Stars, Universal Publishers.

Haensel, P., Potekhin, A.Y. and Yakovlev, D.G., 2007, Neutron Stars, Springer.

Komesaroff, M.M., 1970, Possible Mechanism for the Pulsar Radio Emission, Nature, 225, 612.

Komesaroff, M.M., Hamilton, P.A. and Ables, J.G., 1972, Analytical Solution to the Temporal Broadening of a Gaussian-Shaped Radio Pulse by Multipath Scattering from a Thin Screen in the Interstellar Medium, AJP, 25, 759.

Kramer, M., Lange, C., Lorimer, D.R., Backer, D.C., Xilouris, K.M., Jessner, A. and Wielebinski, R., 1999b, Emission Altitudes in Young and Old Radio Pulsars, ApJ, 526, 957.

Kramer, M., Xilouris, K.M., Jessner, A., Wielebinski, R. and Timofeev, M., 1996b, Observations of Pulsars at 9 Millimetres, A&A, 306, 867.

Kramer, M., Xilouris, K.M., Lorimer, D.R., Doroshenko, O., Jessner, A., Wielebinski, R., Wolszczan, A. and Camilo, F., 1998, Physics of Relativistic Objects in Compact Binaries, ApJ, 501, 270.

Lallement, R. and Ferlet, R., 1997, The Ionization of the Local Interstellar Medium, A&A, 324, 1105.

Lallement, R., Bertaux, J.L. and Clarke, J.T., 1993, Deceleration of Interstellar Hydrogen at the Heliospheric Interface, Science, 260,1095.

Lallement, R., Bertin, P., Ferlet, R., Vidal-Madjar, A. and Bertaux, J.L., 1994, Kinematics of the LISM, A&A, 286, 898.

Lallement, R., Grzedzielski, S., Ferlet, R. and Vidal-Madjar, A. 1996, in Science with the Hubble Space Telescope, eds, Benvenuti, P., Macchetto, F.D. and Schreier, E.J. (Baltimore: STScl), in press.

Lang, K.R., 1971, Interstellar Scintillation of Pulsar Radiation, ApJ, 164, 249.

Large, M.I., Vaughan, A.E. and Mills, B.Y., 1968, A Pulsar Supernova Association?, Nature, 220, 340.

Lehner, N., Jenkins, E.B., Gry, C., Moos, H.W., Chayer, P. and Lacour, S., 2003, Radiative Cooling of the Diffuse Gas, ApJ, 595, 858.

Lequeux, J., 2005, The Interstellar Medium, Springer.

Lorimer, D.R. and Kramer, M., 2005, Handbook of Pulsar Astronomy, Cambridge University Press.

Lyne, A.G, Anderson, B., Salter, M.J., 1982, The Proper Motions of 26 Pulsars, MNRAS, 201, 503.

Lyne, A.G. and Lorimer, D.R., 1994, High Birth Velocities of Radio Pulsars, Nature, 369, 127.

Lyne, A.G. and Rickett, B.J., 1968, The Second Cambridge Pulsar Survey at 81.5 MHz, Nature, 219, 1339.

Lyne, A.G. and Smith, F.G., 1989, Pulsar Studies and Magnetic Fields in Galaxies, MNRAS, 237, 533.

Lyne, A.G. and Smith, F.G., 1990, Pulsar Astronomy, Cambridge University Press.

Lyne, A.G. and Smith, F.G., 1998, Pulsar Astronomy, 2nd ed. Cambridge University Press.

Lyne, A.G. and Smith, F.G., 2012, Pulsar Astronomy, 4th ed. Cambridge University Press.

Lyne, A.G., Burgay, M., Kramer, M., Possenti, A., Manchester, R.N., Camilo, F., McLaughlin, M., Lorimer, D.R., Joshi, B.C., Reynolds, J.E. and Freire, P.C.C., 2004, A Double-Pulsar System ï A Rare Laboratory for Relativistic Gravity and Plasma Physics, Science, 303, 1153.

Lyne, A.G., Pritchard, R.S., Smith, F.G. and Camilo, F., 1996, Very Low Braking Index for the Vela Pulsar, Nature, 381, 497.

Malofeev, V.,1996, In Pulsars: Problems and Progress, eds, John, S., Walker, M.A. and Bailes, M., ASP, San Francisco.

Manchester, R.N. and Taylor, J.H., 1977, Pulsars, San Francisco.

Manchester, R.N., Durdin, J.M. and Newton, L.M., 1985, A Second Measurement of a Pulsar Braking Index, Nature, 313, 31.

Manchester, R.N., Hobbs, G.B., Teoh, A. and Hobbs, M., 2005, The Australia Telescope National Facility Pulsar Catalogue, ApJ, 129, 1993.

Manchester, R.N., Murray, J.D. and Radhakrishnan V., 1969, Pulsar H-line Absorption and Dispersion in the Interstellar Medium, Ap (Letters), 4, 229.

Maron, O., Kijak, J., Kramer, M. and Wielebinski, R., 2000, In Young Neutron Stars and Their Environment, A&AS, 147, 195.

Matsakis, D.N., Taylor, J.H. and Eubanks, T.M., 1997, A Statistic for Describing Pulsar and Clock Stabilities, A&A, 326, 924.

Matthews, H. E., Pedlar, A. and Davies, R. D., 1973, Radio Recombination Line Emission from the Galactic Plane, MNRAS, 165, 149.

Melatos, A., 2000, Radiative Precession of an Isolated Neutron Star, MNRAS, 313, 217.

McComas, D.J., Ebert, R.W., Elliott, H.A., Goldstein, B.E., Gosling, J.T., Schwadron, N.A. and Skoug, R.M., 2000, Solar Winds along Curved Magnetic Field Lines, JGR, 105, 10419.

Nice, D.J., Sayer, R.W. and Taylor, J.H., 1996, Timing Behavior of 96 Radio Pulsars,

ApJ, 466, 87.

Noutsos, A., Johnston, S., Kramer, M. and Karastergiou, A., 2008, New Pulsar Rotation Measures and the Galactic Magnetic Field, MNRAS, 386, 1881.

Oppenheimer, J.R., and Volkoff, G., 1939, On Massive Neutron Cores, Phys. Rev., 55, 374.

Ostriker, J.P. and Gunn, J.E., 1969, On the Nature of Pulsars. I. Theory, ApJ, 157, 1395.

Phillips, J.A. and Wolszczan, A., 1992, Probing Pulsar Dispersion Measures using the GMRT, ApJ, 385, 273.

Prentice, A.J.R. and Ter Haar, D., 1969, HII Regions and the Distances to Pulsars, Nature, 222, 964.

Radhakrishnan, V., Cooke, D.J., Komesaroff, M.M. and Morris, D., 1969, Evidence in Support of a Rotational Model for the Pulsar PSR 0833-45, Nature, 221, 443.

Rand, R.J. and Lyne, A.G., 1994, Relativistic Aspect of Nuclear Physics, MNRAS, 268, 497.

Rankin, J.M., Comella, J.M., Craft, H.D., Richards, D.W., Campbell, D.B. and Counselman, C.C., 1970, Disappearance of the Precursor Pulse at 606 MHz, ApJ, 162, 707.

Redfield, S. and Falcon, R.E., 2008, the Structure of the Local Interstellar Medium. V. Electron Densities, ApJ, 683, 207.

Rickett, B.J., 1990, Radio Propagation through the Turbulent Interstellar Plasma, ARA&A, 28, 561.

Rickett, B.J., Coles, W.A. and Bourgois, G., 1984, Diffractive and Refractive Timescales at 4.8 GHz in PSR B0329+54, A&A, 134, 390.

Rickett, B.J., Lyne, A.G. and Gupta, Y., 1997, Interstellar Fringes from Pulsar B0834+06, MNRAS, 287, 739.

Ruderman, M.A. and Sutherland, P.G., 1975, The Lives of the Neutron Stars, ApJ, 196, 51.

Ruderman, M.A., 1976, Global Static Electrospheres of Charged PulsarsApJ, 203, 213.

Saltpeter, E. E., 1969, High Energy Gamma-Ray, Nature, 221, 31.

Scheuer, P.A.G., 1968, Intensity Variations of the Pulsar CP 1919, Nature, 218, 920.

Schwenn, R., 2006, Space Weather: The Solar Perspective, LRSP, 3, 2.

Seiradakis, J.H. and Wielebinski, R., 2004, Morphology and Characteristics of radio pulsars, A&A, 12, 239.

Shabanova, T.W., 1995, Evidence for Planets around B0329+54, ApJ (letter), 453, 779.

Shapiro, S.L. and Teukolsky, S.A., 1983, Black Holes, White Dwarfs and Neutron Stars, The Physics of Compact Objects, Wiley ï Interscience, New York.

Shemar, S.L. and Lyne, A.G., 1996, Observations of Pulsar Glitches, MNRAS, 282, 677.

Shklovskii, I,S., 1966, Supernovae, Nauka, Mosco.

Shklovskii, I.S., 1970, Possible Causes of the Secular Increase in Pulsar Periods, SvA, 13,562.

Sieber, W., 1973, Pulsar Spectra ï A Summary, A&A, 28, 237.

Shutter, W. L. H., Venugopal, V.R. and Mahoney, M.J., 1968, Distances to Pulsars, Nature, 220, 356.

Sieber, W., 1982, Casual Relationship between Pulsar Long-Term Intensity Variations and the Interstellar Medium, A&A, 113, 311.

Smith, F.G., 1968, Faraday Rotation of Radio Waves from the Pulsars, Nature, 220, 891.

Spitzer, L., 1978, Physical Processes in the Interstellar Medium, Wiley.

Staelin, D.H. and Reifenstein, E.C., 1969, Faraday Rotation in Pulsars, ApJ, 156, I21.

Taylor, J.H. and Cordes, J.M., 1993, Pulsar Distances and the Galactic Distribution of Free Electrons, ApJ, 411, 674.

Taylor, J.H. and Weisberg, J.M., 1982, A New Test of General Relativity: Gravitational Radiation and the Binary Pulsar PSR B1913+16, ApJ, 253, 908.

Taylor, J.H. and Weisberg, J.M., 1989, The Relativistic Binary Pulsar B1913+16, ApJ, 345, 434.

Terzian, Y. and Davidson, K., 1976, Pulsars: Observational Parameters and a Discussion on Dispersion Measures, Ap&SS, 44, 479.

Terzian, Y., 1972b, in Lenchek, A., ed, The Physics of Pulsars, Gordon and Breach, N.Y., 85.

Thompson, C. and Duncan, R.C., 1996, Cosmic Gamma-Ray Sources, ApJ, 473, 322.

Thompson, D.J., 2008, Gamma-Ray Astrophysics: The EGRET Result, Rep. Prog. Phys., 71, 116901.

Thomson, R.C. and Nelson, A.H., 1980, Counterclockwise Magnetic Fields in the Norma Spiral Arm, MNRAS, 191, 863.

Thorndike, S.L., 1930, Interstellar Matter, ASP, 42, 246.

Toscano, M; Britton, M.C., Manchester, R.N., Bailes, M., Sandhu, J.S., Kulkarni, S.R. and Anderson, S.B., 1999, Parallax of PSR J1744 - 1134 and the Local Interstellar Medium, ApJ, 523, 171.

Trimble, V.L., 1968, Frequency of Events Producing Pulsars, AJ, 73, 535.

Urama, J.O., 2002, Glitch Monitoring in PSRs B1046-58 and B1737-30, MNRAS, 330, 58.

Urama, J.O. and Okeke, P.N., 1999, Glitch Observations in Slow Pulsars, MNRAS, 310, 313.

van Straten, W., Bailes, M., Britton, M., Kulkarni, S.R., Anderson, S.B., Manchester, R.N. and Sarkissian, J., 2001, PSR J0437-4715, Nature, 412, 158.

Verschuur, G.L., 1969a, Zeeman Effect Observations of HI Emission Profiles, ApJ, 156, 861.

Verschuur, G.L., 1969b, Observations of Possibly Expanding Neutral-Hydrogen Shell, ApJ (Letters), 155, 155.

Vitkevitch, V.V., 1955, Results of Observations of the Scattering of Radio Waves by the Electronic Inhomogeneities of the Solar Corona, DANUSSR, 101, 429.

Wang, N., Manchester, R.N., Pace, R.T., Bailes, M., Kaspi, V.M., Stappers, B.W. and Lyne, A.G., 2000, Glitches in Southern Pulsars, MNRAS, 317, 843.

Weisberg, J.M. and Taylor, J.H., 2003, In Radio Pulsars, eds, Bailes, M., Nice, D.J. and Thorsett, S.E., ASP, San Francisco.

Weiler, K.W. and Sramek, R.A., 1988, Supernovae and Supernova Remnants, ARA&A, 122, 18.

Weisberg, J.M. and Taylor, J.H., 2004, In Binary Pulsars in Press, eds, Rasio, F. and Stairs, I.H., ASP, San Francisco.

Will, C., 2001, Confrontation between General Relativity and Experiment, LRR, 4, 4.

Wiringa, R.B., Fiks, V. and Fabrocini, A., 1988, Secular Instability of G-Models in Rotating Neutron Stars, Phys. Rev., 38, 1007.

Wolleben, M. and Reich, W., 2003, Modeling Faraday Screens in the Interstellar Medium, eds, Uyaniker, B., Reich, W. and Wielebinski, R., Antalya, Turkey.

Wolszczan, A. and Frail, D.A., 1992, A Planetary System around the Millisecond Pulsar PSR1257+12, Nature, 355, 145.

Wolszczan, A., Doroshenko, O., Konacki, M., Kramer, M., Jessner, A., Wielebinski, R., Camilo, F., Nice, D.J. and Taylor, J.H., 2000, Timing Observations of Four Millisecond Pulsars with the Arecibo and Effelsberg Radio Telescopes, ApJ, 528, 907.

Wood, B.E. and Linsky, J.L., 1997, A New Measurement of the Electron Density in the Local Interstellar Medium, ApJ, 474, 39.

York, D. G., and Kinahan, B.F., 1979, Phosphorus in the Diffuse Interstellar Medium, ApJ, 228, 127.

You, X.P. Hobbs, G., Coles, W.A., Manchester, R.N. Edwards, R., Bailes, M., Sarkissian, J., Verbiest, J.P.W., Van Straten, W., Hotan, A., Ord, S., Jenet, F., Bhat, N.D.R. and Teoh, A., 2007, Dispersion Measure Variations and their effect on Precision Pulsar Timing, MNRAS, 378, 493.

Young, M.D., Manchester, R.N. and Johnston, S. 1999, A Radio Pulsar with an 8.5 Seconds Period that Challenges Emission Models, Nature, 400, 848.